Theranostic and Matched Pair Radionuclides as Radiopharmaceutical as for Imaging and Radiotherapy

---

A Dissertation presented to the Faculty of the Graduate School

At the University of Missouri-Columbia

In partial fulfillment of the requirements for the degree

Doctor of Philosophy

By

Firouzeh Najafi Khosroshahi

Professor Silvia S. Jurisson, Dissertation Supervisor

December 2020

The undersigned, appointed by the dean of the Graduate School, have examined the dissertation entitled

Theranostic and Matched Pair Radionuclides as Radiopharmaceutical as for Imaging and Radiotherapy

Presented by Firouzeh Najafi Khosroshahi, a candidate for the degree Doctor of Philosophy, and hereby certify that, in their opinion, it is worthy of acceptance.

Professor Silvia S. Jurisson

Professor Heather M. Hennkens

Professor Kent S. Gates

Professor Thomas P. Quinn

Professor Alan R. Ketring

Acknowledgments

Above all, I would like to express my deepest gratitude to my committee chair and graduate advisor Professor Silvia S. Jurisson. Without her encouragement, guidance and persistent help, this dissertation would not have been possible. I am honored to have her as my advisor.

I would not have had accomplishment in my graduate carrier without the support and encouragement of my family over the years. I would like to express my appreciation to my husband Amir Soheil Tolebeyan for his love and care. I am so fortunate to have him by my side. Many thanks to my wonderful parents, Samad and Mansoureh, and my beloved brothers, Reza and Behrouz for their selfless love and sacrifice especially after my immigration.

I also want to thank professor Heather Hennkens for her mentorship and my work at the MU Research Reactor. I am grateful to Dr. Timothy Hoffman for his mentorship during my pharmacokinetic studies at the Truman VA Hospital. I would like to thank my committee members, Professor Kent Gates, Professor Thomas Quinn and Professor Alan Ketring for their instructions and advice. I would like to express my thankfulness to Dr. Yutian Feng for his help and advice. He helped me to learn the fundamentals of radiochemistry research. His enthusiasm at the research was a great encouragement for me. I am thankful to Dr. Steven Kelley for his expertise in single crystal X-ray crystallography. I would like to thank Dr. Fabio Gallazzi and Dr. Brian Mooney at the University of Missouri for their assistance with solid-phase peptide, LC-MS facility and high-resolution mass spectrometry. I would like to thank undergraduate student Simon Manring and graduate students Li Ma and Chathurya Munindradasa. Working as their trainer taught me how to give advice and build positive working relationship.

Contents

List of Illustrations

List of Figures

List of Tables

List of Schemes

List of Abbreviations

α : alpha particle
β^+: positron
β^-: negatron
γ: gamma photon
ε: electron capture
IT: isomeric transition
LET: linear energy transfer
NCA (or nca): no carrier added
PET: positron emission tomography
SPECT: single photon emission computerized (computed) tomography
BFC: bifunctional chelator
BFCs: bifunctional chelators
BBN: bombesin peptide
BBN(7-14)NH_2: bombesin peptide residues (7-14)NH_2
BFCA: bifunctional chelating approach
BNL: Brookhaven national laboratory
ANL: Argonne national laboratory
ACN: acetonitrile
DIPEA: diisopropylethylamine
DMSO: dimethyl sulfoxide
DMSA:2,3-dimercaptosuccinic acid
BAL: 2,3-dimercaptopropanol (or British anti-lewisite)
NMR: nuclear magnetic resonance
TLC: thin layer chromatography
ESI-MS: electrospray ionization mass spectroscopy
LC-MS: liquid chromatography mass spectroscopy
HPLC: high performance liquid chromatography
RP-HPLC: reversed phase HPLC
CCDC: Cambridge crystallographic data centre
Fmoc: fluorenylmethyloxycarbonyl protecting group
HBTU: N,N,N',N'-tetramethyl-O-(1H-benzotriazo1-yl)uranium hexafluorophospate
HMOC: heteronuclear multiple quantum coherence
Tbu: *tert*-butanol protecting group
Trityl: triphenylmethane
GRP: receptors: gastrin releasing receptors
HEPES: 4-(2-hydroxyethyl)-1-piperazinethanesulfonic acid
BSA: bovine serum albumin
EDC: 1-ethyl-3-(3-dimethylaminopropyl)carbodiimide
DMAP: 4-dimethylaminopyridine
NHS: N-hydroxysuccinimide
TFA: trifluoroacetic acid

TES: triethyl silane
TCEP: tris(2-carboxyethyl)phosphine
NaI(Tl): sodium iodide gamma ray detector
HPGe: High purity germanium detector
IC50: The half maximal inhibitory concentration
mAb: monoclonal antibody
m/z: mass to charge

Academic Abstract

The main focus of this dissertation is on the development of arsenic and rhenium radiopharmaceuticals as potential theranostic candidates.

Chapter 2 focuses on ^{72,77}As radiopharmaceuticals for potential PET imaging and therapy: Synthesis, evaluation and biological studies of a linkable trithiol ligand with an improved hydrophilicity. Arsenic-72 and ^{77}As are a suitable radioisotope matched pair for development of theranostic radiopharmaceuticals. Bombesin (BBN) peptide analogues generally target gastrin-releasing peptide (GRP) receptors expressed in the pancreas of normal mice and human cancers of the prostate. Previous biodistribution studies with ^{77}As-trithiol(a)-BBN(7-14)NH_2 in normal mice showed high lipophilicity of ^{77}As-trithiol(a)-BBN(7-14)NH_2 followed by fast and high hepatobiliary excretion and no significant pancreatic uptake. A new trithiol bifunctional chelate with an improved hydrophilicity and flexibility in the structure for conjugation to targeting biomolecules was developed. This new trithiol chelate was conjugated to the RM2 peptide (a GRP receptor antagonist) through a two serine (Ser) spacer. The trithiol(b)-$(Ser)_2$-RM2 conjugate was radiolabeled with no carrier added ^{77}As and conditions were optimized to maximize radiolabeling yield. Biodistribution studies in normal mice were conducted and is herein reported.

Chapter 3 examines the development and synthesis of trithiol conjugated Herceptin and radiolabeling of the conjugate with arsenic radioisotopes. Radiolabeling monoclonal antibodies (mAbs) with a vast range of radionuclides are being utilized in clinical diagnosis and therapy. The idea of labeling monoclonal antibodies with radioactive arsenic isotopes for the purpose of molecular imaging have been examined in the past. Bifunctional chelating agents (BCAs) have

been developed to facilitate covalent bonding between a radiometal chelate to mAbs for the purpose of higher *in vivo* stability of the radiometal chelate followed by reducing the amount of free radiometal uptake in normal and non-targeted tissue. [1] Herceptin, known as Trastuzumab, is an IgG1 kappa-containing human framework region with the complementarity-determining regions of a murine anti-p185 Her2 antibody. Herceptin has anti-angiogenesis effect on Her2 positive breast cancer tumors. A method for conjugation of a new trithiol ligand with an improved hydrophilicity to Herceptin followed by radiolabeling with arsenic radioisotopes for diagnosis and treatment of Her2-positive breast cancer tumors was investigated. The method involved preparing amine-reactive esters of a carboxylate group on a trithiol ligand with *N*-hydroxysuccinimide (NHS) and 1-ethyl-3-(3-dimethylaminopropyl)carbodiimide (EDC) resulting in a stable trithiol-NHS active ester. [2, 3] A previously reported simple method for conjugation of monoclonal antibodies with NHS-trithiol active esters in aqueous solution was utilized for the conjugated trithiol-Herceptin compound. Radiolabeling attempts of the conjugated Herceptin with [^{77}As]AsSR are underway. [4-6]

Chapter 4 investigates the synthesis and evaluation of a monoamine monoamide dithiol (MAMA) ligand with an improved hydrophilicity for developing bifunctional chelators and their $^{186/188}$Re compounds. A series of N_xS_{4-x} tetradentate chelates are used to bind to oxo-rhenium core. Small peptides such as Bombesin are favorable biomolecules for delivering a radiophamaceutical to specifc target sites in the body. Various MAMA analogues including 222-MAMA, 222-MAMA (N-6-Ahx-OEt), and 222-MAMA (N-6-Ahx-BBN (7-14)NH_2 have been previously synthesized and radiolabeled with ^{186}Re (high and low specific activity). [7] Biological evaluation of ^{186}ReO 222-MAMA (N-6-Ahx BBN (7-14)NH_2) was previously studies in mouse models bearing PC-3 human prostate cancer cells, which showed high *in vivo* stability and

demonstrated high binding affinity to the GRP receptors on PC3 cells. However, ^{186}ReO(222-MAMA (N-6-Ahx-OEt)) showed lipophilicity and was excreted more through the hepatobiliary and GI system relative to the renal system. [7] The ongoing research presented in chapter 4 focuses on synthesis and evaluation of a 222-MAMA chelate with an improved hydrophilicity followed by radiolabeling with ^{99m}Tc and ^{186}Re. Conjugation of 222-MAMA-(N-6-Ahx-OEt) to RM2 peptide as the targeting vector is ongoing.

Chapter 1: Introduction

Nuclear Medicine

Nuclear chemistry could be classified into several categories of study, such as the chemical and physical aspects of radioactive elements, nuclear properties, macroscopic phenomena and measurement applications of nuclear phenomena. [8] Radiopharmaceutical studies are a branch of measurement applications. Radionuclides in radiopharmaceuticals are utilized for diagnosis and therapy of numerous diseases. Radionuclides are used in medicine mainly based on a very important characteristic: the tracer approach and was developed by George de Hevesy, the Nobel Prize winner of 1943. [9] Early use of radiotracers in medicine began in the early 1900s. In 1926, "Radium C", which is the generic name of ^{214}Bi, was injected to monitor blood flow, which was the first clinical use of radiotracer. In 1937, ^{32}P was used to treat leukemia, which is considered as the first use of artificial radioactivity to treat patients. Technetium was also discovered in the same year. In 1939, ^{131}I was used for diagnosis, and in 1946, it was used to totally cure all metastases associated with thyroid cancer.

Radioactive Decay of Radionuclides and their Application in Nuclear Medicine

Nuclear medicine works with the application of radioactive decay in diagnosis and treatment of diseases. However, these two fields of diagnosis and therapy contain distinctive methods for their use in nuclear medicine. As far as diagnosis or imaging goes, emitted radiation from an injected radioactive drug is detected by scanners to generate a specific image of an organ, bone or tissue. Most diagnostic radionuclides decay by either gamma ray (γ) or positron (β^+) emissions, although some of them decay by electron capture (EC), isomeric transition (IT) or a combination of two or more types of emission. Some of the most common radionuclides used in diagnosis are ^{11}C, ^{18}F, ^{64}Cu, ^{68}Ga, ^{85}Sr, ^{99m}Tc, ^{111}In, $^{123,125}I$, ^{99m}Tc, ^{111}In, ^{68}Ga,^{201}Tl [8] Approximately 95% of nuclear medicine procedures are diagnostic and 5% are therapeutic. Most favorable diagnostic radionuclides for SPECT imaging emit photons with an energy between 100 and 200 keV. Tc-99m is one of the most favorable diagnostic radionuclides given its 140 keV γ-ray, which is detectable by today's gamma cameras. In therapy, a radiopharmaceutical drug containing therapeutic radionuclide is injected into the body. Therapeutic radionuclides mostly decay by either alpha (α) or beta (β^-) particles and some of them decay by Auger electrons. Some of the FDA approved radionuclides are ^{131}I, ^{90}Y, ^{153}Sm and ^{177}Lu. [8]

Radiopharmaceuticals

Radiopharmaceuticals are radioactive compounds which are used for diagnostic or therapeutic purposes. To date, most radiopharmaceutical drugs (95%) are used for diagnosis and almost only 5%are served for therapy. [8]

Imaging

X-ray imaging is the oldest technique for providing images of the tissue and bones by utilizing an external radiation source. Computerized tomography (CT) is an improved X-ray imaging technique which shows slices of body or tissue with a common resolution of <1 mm. [8] As opposed to X-ray imaging, diagnostic radiopharmaceutical drugs are administered into a patient's body, which then further localize in a specific organ or tissue. There are two radiopharmaceutical imaging methods: single-photon process called single photon emission computerized tomography (SPECT) and a two-photon process called positron emission tomography (PET). In SPECT imaging, a radionuclide-containing drug, which is a γ-emitter, is administered into the body and the emitted radiation is detected by gamma cameras and finally a three-dimensional computer reconstructed image is obtained using multiple two-dimensional images from different alignments. Some of the most common single photon emitters are ^{99m}Tc, ^{67}Ga, ^{111}In, ^{201}Tl. Tc-99m is the most widely used SPECT imaging radionuclide worldwide. Its 6 h half-life and single 140 keV photon and,

most importantly, being readily available from a $^{99}Mo/^{99m}Tc$ generator make ^{99m}Tc the most favorable SPECT imaging radionuclide (**Figure 1.1**).

Figure 1.1: Single-photon emission computed tomography (SPECT). https://www.shutterstock.com/image-vector/spect-scan-radiologist-single-computed-image-1329727592

PET imaging is claimed to be the most powerful imaging method in nuclear medicine. PET imaging utilizes proton-rich radionuclides, which emit positrons. A positron interacts with an electron after being emitted from the nuclide followed by positron-electron annihilation resulting in two coincidental 0.511 MeV photons in almost opposite directions. In PET imaging, drugs are prepared by incorporating a relatively short-lived positron emitting radionuclide into a biomolecule. A drug with a specific positron-emitting radionuclide is injected into the body. The two 0.511 MeV photons outline a line from the point where the decay happened.

The two photons are detected by scintillation detectors surrounding the patient. Multiple images are obtained over numerous alignments. Finally, a high-resolution three-dimensional image is obtained after multiple scans. Some of the most common single photon emitters are ^{18}F, ^{11}C, ^{15}O, ^{13}N, ^{68}Ga. Among these radionuclides, ^{18}F, ^{11}C and ^{68}Ga have been incorporated into a drug among them (**Figure 1.2**).

Figure 1.2: Positron emission Tomography (PET)

https://www.nutaq.com/blog/pet-scanners-rapid-data-acquisition-daq-hardware

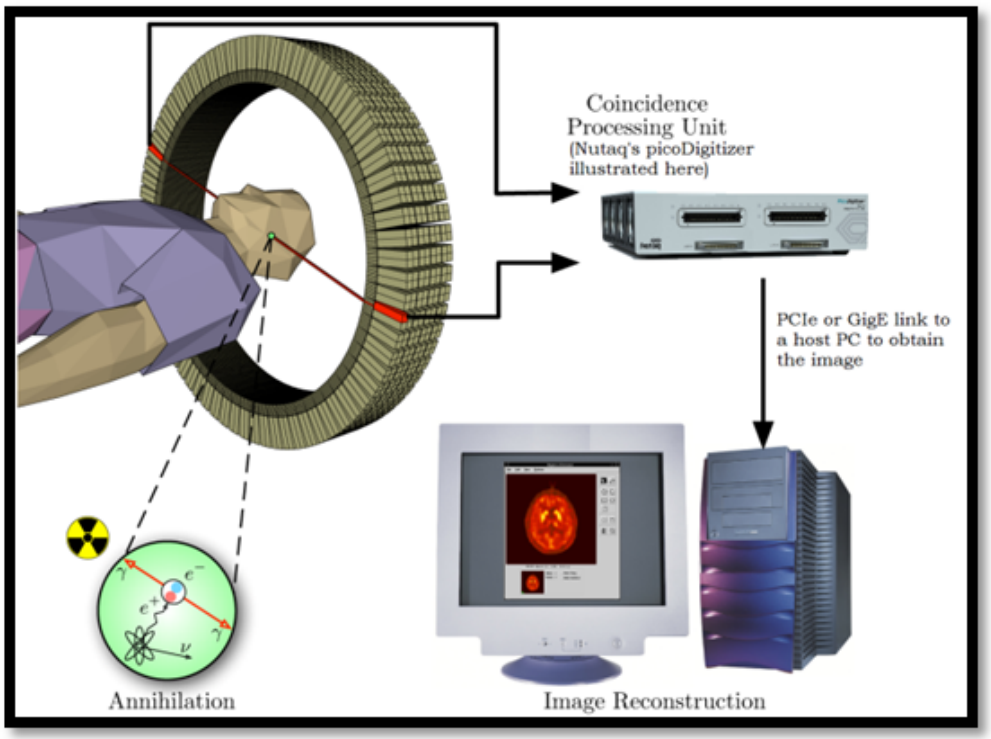

To date, nearly 90% of the applications of PET imaging are in oncology. 2-[^{18}F]fluoro-2-deoxy-glucose ([^{18}F]FDG) is one of the favorable PET imaging agents. [^{18}F]FDG is an analogue of glucose and is converted to

fluorodeoxyglucose-6-phosphate similar to its glucose analogue. However, unlike glucose-6-phosphate, fluorodeoxyglucose-6-phosphate cannot be metabolized further by glycolysis. Due to the high activity and metabolism of cancer cells, [^{18}F]FDG is used for detecting of high glucose use. (**Scheme 1.1**).

Scheme 1.1: Schematic figure of [^{18}F]FDG

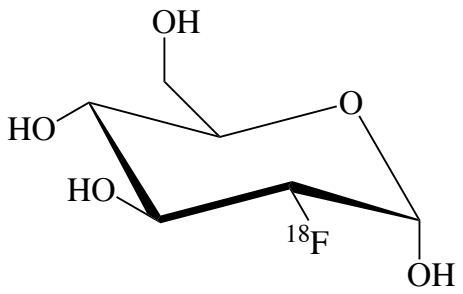

Therapy

Radiotherapy is utilized for treatment of approximately 50% of patients with localized contained tumors. The main challenge in radiotherapy is to prevent killing normal cells as much as possible. An important obstacle is that cancer cells have lower oxygen levels than normal cells and thus are more resilient to radiation. In 1946, ^{131}I was used to completely cure metastatic thyroid cancer by accumulating in the thyroid and decaying by β^- particles (90%) followed by irradiating the nearby tissue. The thyroid is located in the throat and far from other organs. I-131 treatment is proven to be highly successful and is considered as the first and only true magic bullet. [8] The most important criteria for a suitable therapeutic radionuclide

are favorable decay characteristics. The desired half-life is between 6 h and 7 d and the emitted radiation should have a favorable linear transfer energy (LET, the energy transferred to the medium per unit length) parameters in the targeted tissue with minimal uptake in normal tissue. The stability of a therapeutic agent at the nanomolar level is essential since it should stay for a longer period of time in the body compared to diagnostic radiopharmaceuticals. [10]

β^- Emitting Radionuclides

Most of the therapeutic radionuclides are β^- emitters. Their ranges of penetration in the tissues are dependent on their energies. Neutron-rich radionuclides are mostly β^- emitters and most of them are produced with by neutron activation in a nuclear reactor. Some radionuclides such as ^{186}Re and ^{67}Cu can be produced by either a reactor or accelerator. The commonly used β^- emitting therapeutic radionuclides are listed in Table 1.1. In addition to the commonly used β^- emitter radionuclides, some other β^- emitters such as ^{47}Ca, ^{47}Sc, ^{77}As, ^{105}Rh, ^{159}Gd, ^{161}Tb, ^{166}Dy and ^{169,171}Er have potential therapeutic application in nuclear medicine (**Table 1.1**). [10]

Table 1.1: Some commonly used or potential β^- emitting radionuclides

Radionuclide	$T_{1/2}$	$E_{\beta\text{-max}}$ (MeV)	E_γ (keV) (I_γ in %)
^{32}P	14.3 d	1.7	
^{67}Cu	2.6 d	0.6	185 (45)
^{89}Sr	50.5 d	1.5	
^{90}Y	2.7 d	2.3	
^{131}I	8.0 d	0.6	364 (81)
^{153}Sm	1.9 d	0.8	103 (28.3)

^{166}Ho	1.1 d	1.8	81 (6.2)
^{177}Lu	6.7 d	0.5	208 (11)
^{186}Re	3.8 d	1.1	137 (8.5)
^{188}Re	17.0 h	2.0	155 (14.9)

Auger Electron Emitter Radionuclides

Auger electron emission occurs when de-excitation of an atom creates an inner shell vacancy. Three important nuclear properties that create such a vacancy are: a) photoelectric effect, b) electron capture (EC) and c) internal conversion (IC). In photoelectric effect, an electron is ejected from an atom as a result of an interaction between a γ ray and the atom. The energy of the ejected electron equals to the energy of the γ ray minus the atomic binding energy of electron. Photoelectric event mostly happens for γ ray emissions with the energies lower than 1 MeV in high-Z absorbers. In EC, the excited nucleus, captures an inner shell electron. Electron capture decay produces Auger electrons and X rays as a result of atomic electron rearrangement. In IC, the excited nucleus deexcites and transfers its energy to an orbital electron followed by ejection of that electron from the atom. IC decay results in Auger electron emission because of the created vacancy in the atomic orbital. In Auger electron transitions, the initial vacancy in the lower major shell is filled by a higher major shell electron followed by another electron ejection from a higher major shell. Table 2 shows a comparison of Auger electron yields of some radionuclides that are considered as therapeutic radionuclides. [11, 12] Both

reactors and accelerators are used for production of Auger electron emitting radionuclides. Accelerators have a higher potential to produce Auger electron emitters given that they generally have neutron deficiency. Despite being Auger electron emitters, ^{67}Ga and ^{111}In are considered as diagnostic radionuclides because of suitable γ ray emissions. However, being Auger electron emitters, they are under study as therapeutic radionuclides. Among Auger electron-emitting radionuclides, ^{125}I is notable since it emits a 35 keV γ ray in low abundance and 100% Auger electrons and is readily attached to a DNA molecule. [10] Recent studies are mainly focused on developing Auger electron emitting radiopharmaceuticals, which are able to be internalized in cancer cells followed by damaging and destroying their DNA (**Table 1.2**).

Table 1.2: Comparison of Auger electron yields of some radionuclides. [10, 12, 13]

Nuclide	Half-life	Number of Auger electrons per event
^{67}Ga	3.26 d	4.96
^{111}In	2.80 d	7.43
^{123}I	13.2 h	13.7
^{125}I	59.4	20
^{201}Tl	3.04 d	20.9
^{195m}Pt	4.02 d	36.6

α Emitting radionuclides

Alpha emitting radionuclides are relatively large atoms. The atomic number of an element is generally higher than 83 in order to be able to undergo α decay. Alpha decay emits monoenergetic cationic alpha particles (He^{2+}). Alpha particles have relatively much shorter range than $ß^-$ and hence, high LET. They cause intense ionization in matter and consequently, have substantial cell death effects. [14] The commonly used α-emitters are listed in Table 3. One of the most promising α-emitting radionuclides is ^{225}Ac. The importance of ^{225}Ac is both in itself and its daughter isotope, ^{213}Bi. There is much research with α emitters and their potential therapeutic radiopharmaceuticals. However, their chemistry and radiochemistry are still under study. Although there is much research with α emitters and their potential therapeutic radiopharmaceuticals, the application of α-emitting radionuclides in nuclear medicine demands strong quality control studies and tests. For instance, most of the α-emitting radionuclides undergo multiple consecutive decays. Therefore, α-emitting radionuclide chelates conjugated to targeting vectors must have high *in vivo* stability to avoid toxicity of free radionuclides in normal and non-targeted organs and tissues. (**Table 1.3**). [9, 10, 12, 14]

Table 1.3: Some commonly used α-emitting radionuclides. [10]

Radionuclide	$T_{1/2}$	E_α (MeV)	E_γ (keV) (I_γ in %)
^{211}At	7.2 h	5.9	
^{213}Bi	46 min	5.9	440 (16.5)

^{225}Ac	10.0 d	5.8	100 (1.7)
^{223}Ra	11.4 d	5.54	270 (13.9)

Design and Development of Radiopharmaceuticals

Radiopharmaceutical drugs are agents which deliver the radionuclides to specific sites in the body. There are various delivery methods. In some cases, the radiopharmaceutical drug is a simple ion such as $[^{131}I]I^-$, which is used for treatment of thyroid-related diseases. Most often, radiopharmaceuticals generally contain two parts, the radionuclide and the pharmaceutical. The radionuclide determines if the drug serves as a diagnostic or therapeutic agent. The pharmaceutical component facilitates targeting a specific organ or tissue. Designing and development of radiopharmaceuticals require a vast knowledge, from the chemistry, radiochemistry and nuclear physics of the radionuclide to the biological aspects of the pharmaceutical. The radiotracer principal explains that the concentration of radiotracers should be low enough to minimize the side effects on human bodies. As such, concentrations of radionuclides for radiopharmaceutical utilization purposes are usually in the nanomolar range. In general, designing radiopharmaceuticals have three main approaches: the small molecule approach, the integrated approach, and the bifunctional chelate approach.

Small Molecule Approach

As far as science of pharmacology and biology go, a molecule which has a molecular weight lower than 900 daltons and the ability to control and

facilitate a biological process is considered as a small molecule. A small molecule approach is basically a radionuclide coordinated to a chelator. Small molecule approach is used for diagnosis or therapy of cancers that are not receptor specific. The type of donor atoms on the chelators and overall charge of chelate can be modified in order to change the functionality of the small molecule drug. [^{99m}Tc]Tc-sestamibi (Cardiolite®) and Tetrafosmin (Myoview) used as heart agents are the examples of the drugs made by small molecule approach.

Integrated Approach

In the integrated approach for synthesis of radiopharmaceutical drugs, the drug consists of a targeting vector and a radionuclide integrated into the targeting vector. The targeting vector is a molecule that participates in a specific metabolic process or binds to a specific site or receptor. A good example of a drug made by integrated approach is [^{18}F]FDG, which is a widely used PET imaging agent specially brain imaging purposes (**Scheme 1.2**).

Scheme 1.2: One of the approaches of [^{18}F]FDG synthesis as a PET imaging agent.

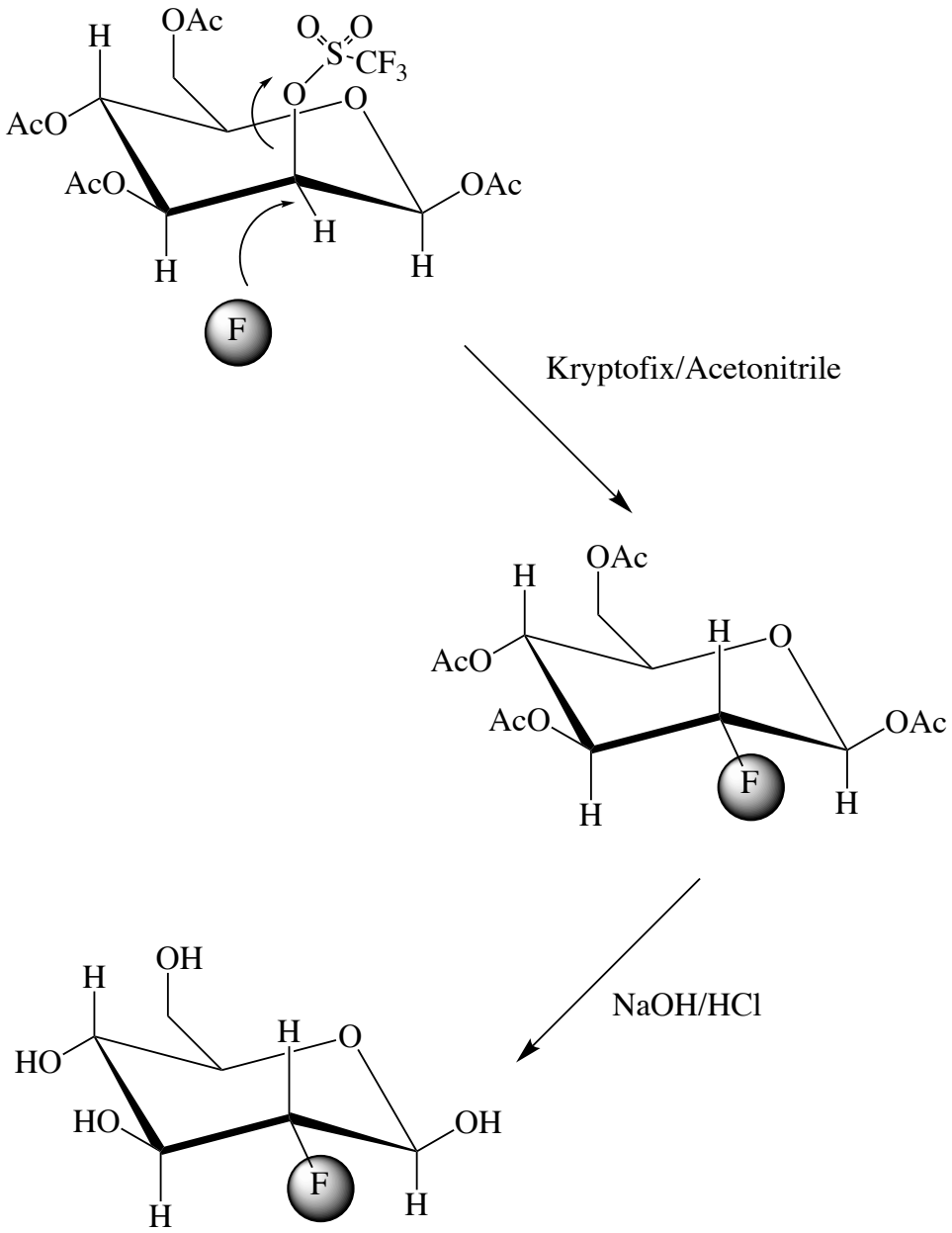

Bifunctional Chelate Approach

In the bifunctional chelate approach, a radionuclide binds or coordinates to a chelator that contains a linker which then connects to a biomolecule. [15] A suitable chelator is selected based on the binding stability between the radionuclide and the chelator throughout the administration process of the radiotracer, biodistribution of the radiotracer, its accumulation in the tissues and organs and final excretion. [16] In other words, the chelator component in the radiopharmaceutical drug must show *in vivo* stability in binding to the radionuclide as well as specific binding to the target site and quick excretion from the non-target organs and tissues. [^{177}Lu]Lu-DOTATATE (Lutathera®) is a drug made by bifunctional chelate approach. This drug is used for the treatment of adult patients with somatostatin receptor-positive gastroenteropancreatic neuroendocrine tumors**.**

Theranostic Radiotracers

Based on the type of radionuclide explained above, radiopharmaceutical drugs could be used for diagnosis or therapy. Diagnostic radionuclides decay by γ ray emissions or high-energy photons that are able to penetrate the body and have optimal energy to be detectable by a camera. Therapeutic radionuclides decay by a particle such as β^- or α that are ionizing radiation. Ionization could lead to breaking bonds followed by intended destruction. Theranostic is a term coined by combination of

therapeutic and diagnostic. The purpose of developing theranostic radiopharmaceutical drugs is expanding diagnostic tests of a disease along with therapeutic application to optimize effectiveness. Matched pair or theranostic radionuclides have advantages due to the identical chemical properties of the diagnostic and therapeutic counterparts such as ^{64,67}Cu, ^{44,47}Sc and^{125,131}I. The subject of "theranostic radionuclides" is indeed one of the oldest subdivisions of nuclear medicine. The oldest use of theranostic goes back to 1939 and the application of ^{131}I for imaging and treatment of thyroid disease. Iodine-131 was the only widely applicable example of a therapeutic and diagnostic radiotracer for years. By application of ^{123}I, ^{123}I/^{131}I became the first widely used matched pair for clinical purposes in nuclear medicine. [17] Nuclear medicine is experiencing a regeneration after ^{177}Lu-DOTATATE (Lutathera®) (**Scheme 1.3)** , ^{68}Ga-DOTATATE (NETSPOT™), and ^{131}I-MIBG (Azedra®) **(Scheme 1.4)** having been approved by the United States Food and Drug Administration (FDA). [17]

Scheme 1.3. Structure of [^{177}Lu]Lu-DOTATATE (Lutathera®) for treatment of adult patients with somatostatin receptor-positive gastroenteropancreatic neuroendocrine tumors**.**

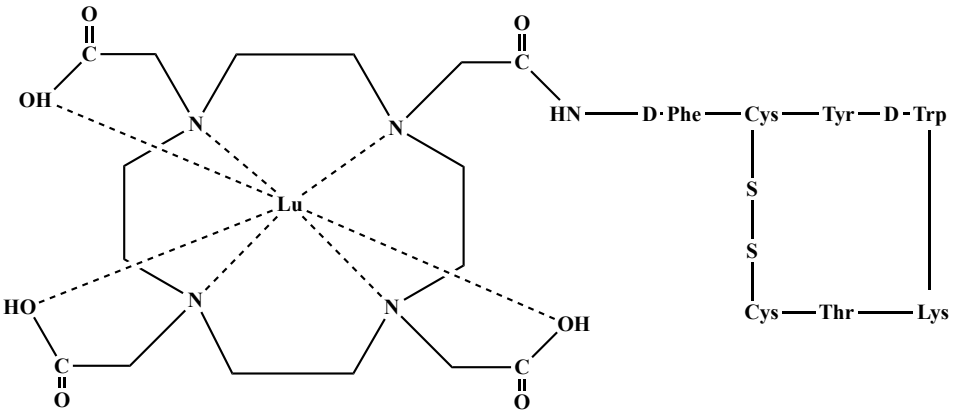

Scheme 1.4. Structure of ^{131}I-MIBG (Azedra®) for treatment of malignant pheochromocytoma and paraganglioma.

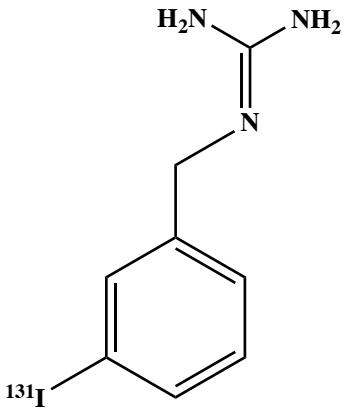

Technetium and Rhenium as a Theranostic Matched Pair

Technetium

Technetium (Tc) (Z=43) belongs to the group (VII) transition metals. The range of oxidation state for Tc is -1 to +7. The most common oxidation states of Tc are +7, +5 and +4. Metallic technetium is soluble in nitric acid and also aqua regia and not soluble in concentrated or dilute hydrochloric acid. Technetium will be present with its highest oxidation state (VII) in the form of $[TcO_4]^-$ under suitable oxidizing conditions. This metal has a rich coordination chemistry, which makes it a suitable candidate for development of various compounds including radiopharmaceutical complexes. Technetium-99m is the most commonly used radionuclide for SPECT imaging. It was discovered by Glenn T. Seaborg and Emilio Segre in 1938. As mentioned above, the 140 keV gamma energy and 6 h half-life is perfect for SPECT imaging. Also, ^{99m}Tc is available from ^{99}Mo/^{99m}Tc generator with a reasonable price, which makes it easily available in medical centers. There are different pathways for the production of ^{99}Mo. The conventional and one of the most efficient production methods for ^{99}Mo is neutron irradiation of highly enriched ^{235}U (HEU) targets in reactors. In this production route, ^{99}Mo is a fission by-product. [8] The United States is a main consumer of ^{99}Mo. In 2014, there was a ^{99m}Tc supply crisis because of the small number of ^{99}Mo-producing reactors. Also, these reactors are old at this time and there are safety concerns about their operations. Different solutions are being developed to increase

production of ^{99}Mo. Some of the solutions are utilizing low enriched uranium (LEU) in reactors, neutron activation-based and accelerator-based production methods. NorthStar Medical Radioisotopes has developed $^{99}Mo/^{99m}Tc$ generators based on the neutron activation of ^{98}Mo.

Mo-99 decays by β^- particles to ^{99m}Tc:

$$^{99}Mo \xrightarrow[86\%]{\beta^-} {}^{99m}Tc \xrightarrow[E\gamma=140\ keV]{IT} {}^{99}Tc$$

The $^{99}Mo/^{99m}Tc$ generator is prepared by loading anionic molybdate ($[^{99}MoO_4]^{2-}$) onto an acidic alumina column. Mo-99 decays by β^- particles (87%) to ^{99m}Tc to form a transient equilibrium (**Scheme 1.5**). Transient equilibrium occurs on the condition that the half-life of the parent is almost 3-10 times longer than the half-life of the daughter (**Scheme 1.5**). There is a transient equilibrium between ^{99}Mo (parent, $t_{1/2} = 65.9$ h) and ^{99m}Tc (daughter, $t_{1/2} = 6$ h). This column can be eluted with 0.9% saline (NaCl) to give pertechnetate ($[^{99m}TcO_4]^-$). $[^{99}MoO_4]^{2-}$ remains on the column for decay-growth of the $^{99}Mo/^{99m}Tc$ generator. The eluted $[^{99m}TcO_4]^-$ is converted to a suitable complex to be utilized in a medical radiopharmaceutical kit for diagnostic purposes. [8]

Scheme 1.5: The decay-growth of $^{99}Mo/^{99m}Tc$ generator

https://www.researchgate.net/profile/Indra_Saptiama2/publication/312235124/figure/fig2/AS:450871180959746@1484507474614/The-Decay-growth-of-the-99-Mo-99m-Tc-generator-system.png [18]

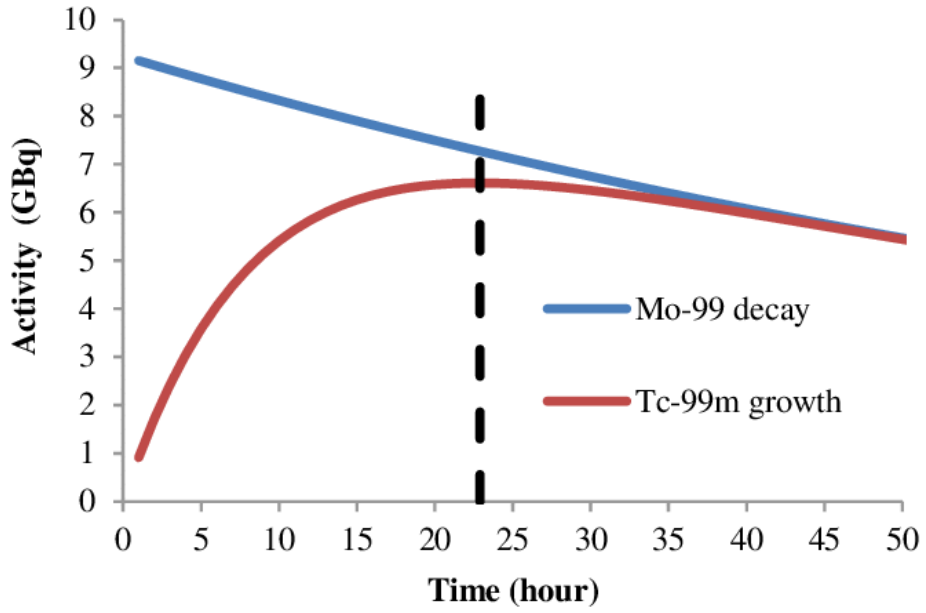

As mentioned before, ^{99m}Tc is an ideal SPECT radionuclide. Availability, half-life and detectable gamma energy are the main factors for making ^{99m}Tc a favorable SPECT agent. Technetium-99m DTPA (diethylenetriamine pentaacetate) was developed in the1970s, and is used in renal imaging. **(Scheme 1.6)** The common applications of ^{99m}Tc are whole body bone scans (**Scheme 1.7**), myocardial perfusion and cardiac ventriculography (**Scheme 1.8**). [8]

Scheme1.6: ^{99m}Tc-DTPA Draximage® DTPA used for renal SPECT imaging.

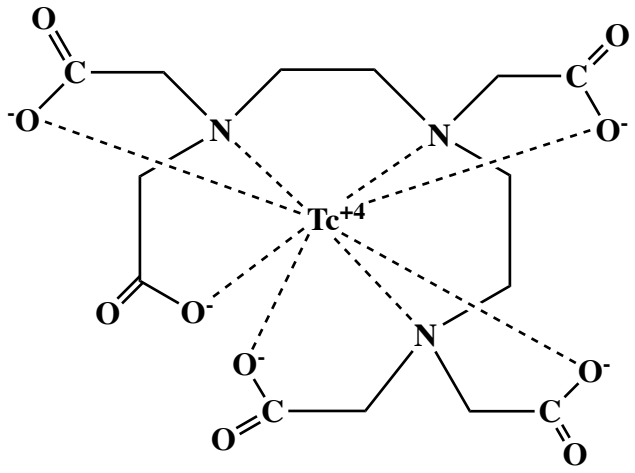

Scheme1.7: ^{99m}Tc-Methylene diphosphonate (^{99m}Tc-MDP), FDA approved bone agent for SPECT imaging.

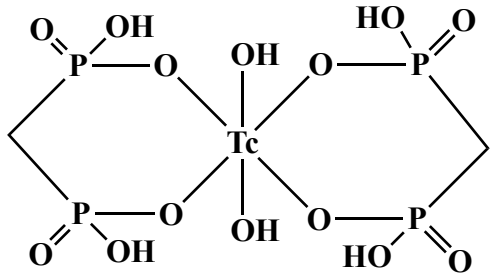

Scheme1.8: [^{99m}Tc]Tc-sestamibi Cardiolite® and Tetrafosmin Myoview used as heart agents in SPECT imaging.

Sestamibi

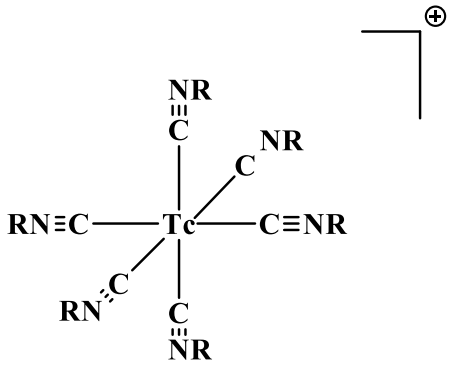

R: -$CH_2C(CH_3)_2OCH_3$

Tc: Tc-99m

Tertrafosmin

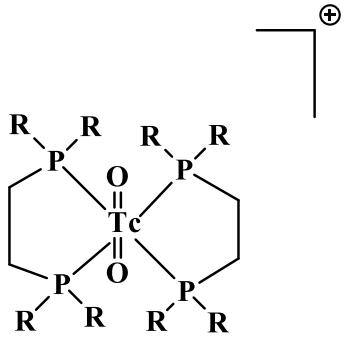

R: -$CH_2CH_2OCH_2CH_3$

Tc: Tc-99m

Most Tc(V) radiopharmaceuticals contain the mono oxo core. ^{99m}Tc-MAG3 is an oxotechnetium agent used as renal SPECT imaging agent (**Scheme 1.9**). [^{99m}Tc]Tc-$_{D,L}$-HMPAO (Ceretec®) and [^{99m}Tc]Tc-$_{L,L}$-ECD (Neurolite®) , which are oxotechnetium agents, are used for cerebral perfusion imaging. The lipophilic nature of these agents helps them to pass through the blood-brain-barrier and visualize cerebral blood flow (**Scheme 1.9**).

Scheme 1.9: Structures of ^{99m}Tc-MAG3, renal SPECT imaging, [^{99m}Tc]Tc-$_{D,L}$-HMPAO (Ceretec®) and [^{99m}Tc]Tc-$_{L,L}$-ECD (Neurolite®), brain SPECT imaging agents

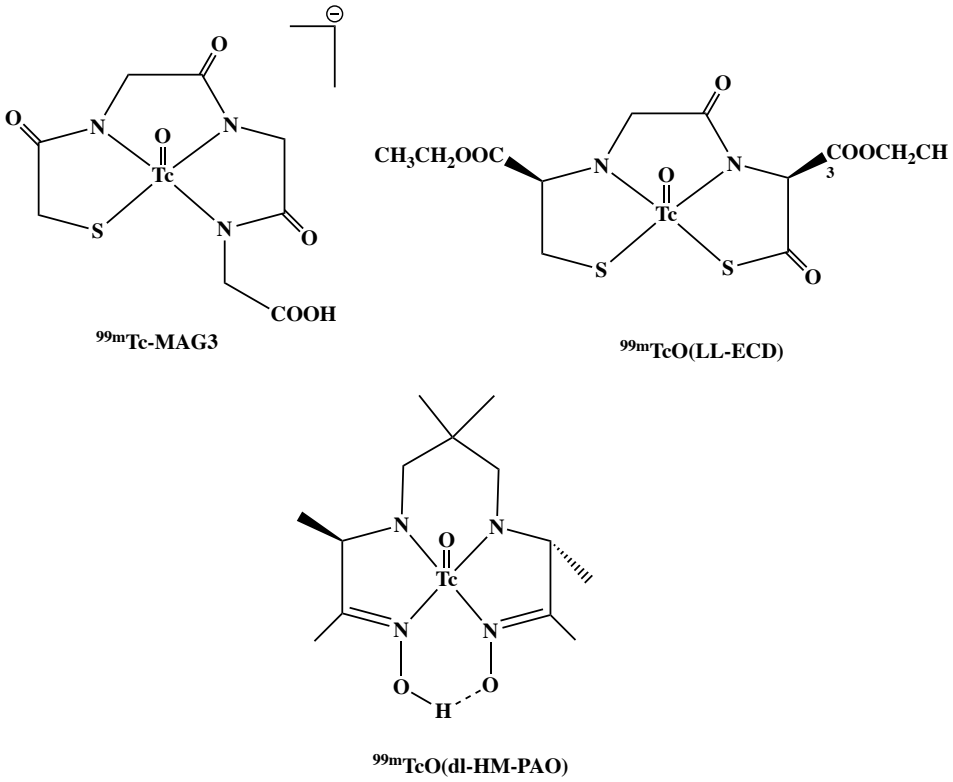

Rhenium

Rhenium is a group VII metal of transition elements, the same as technetium. It has atomic number 75 and seven valence electrons for bonding ([Xe] $4f^{14}5d^{5}6s^{2}$ configuration). Rhenium has 2 naturally occurring isotopes ^{185}Re 37.4%, ^{187}Re 62.6%) with typically metallic structure. Rhenium has nine known oxidation states ranging from -1 to +7. These properties make Re favorable for a vast variety of coordination chemistry and organometallic synthesis. Rhenium has similar chemical

properties as technetium. Technetium-99m is used as a diagnostic radionuclide in a vast area of SPECT imaging. Therefore, due to the similarity of Re and Tc, ^{99m}Tc chelating knowledge could be applicable for ^{186}Re and ^{188}Re, which could potentially be the therapeutic counterpart to ^{99m}Tc. However, there are some differences between ^{99m}Tc and $^{186/188}$Re complexes such as kinetics and redox chemistry that must be considered. For instance, Schiff base complexes of Re(V) and Tc(V) act differently as a result of slower substitution rates for Re. The ^{186}Re and ^{188}Re radionuclides have the advantage of being utilized as both diagnostic and therapeutic agents because they decay by β^- particle accompanied by γ emissions. (**Table 1.4**).

Table 1.4: Some commonly used rhenium radionuclides.

Radionuclide	$T_{1/2}$	Decay mode	E_x (I_γ in %)
^{186}Re	3.72 d	ß$^-$ (92.5%) ε (7.5%)	1.07 MeV (ß$^-$) 137 keV (9%) (γ)
^{188}Re	17 h	ß$^-$ (100%)	2.12 MeV (ß$^-$) 155 keV (16%) (γ)
^{189}Re	24.3 h	ß$^-$ (100%)	1.01 MeV (ß$^-$) 335 keV (62%) (γ)

The half-life of ^{188}Re is 17.0 h. It has 2.12 MeV β^- and 155 keV γ emissions. W-188 has 69.8 d half-life and decays by β^- (100%) to ^{188}Re. Considering parent and daughter suitable half-lives, ^{188}Re could be obtained from a ^{188}W/^{188}Re generator of which the parent isotope ^{188}W can be produced by double neutron capture on ^{186}W. The half-life of ^{186}Re is

3.72 d. It has 1.07 MeV ß$^-$ and 137 keV γ emissions and can be produced by either ^{nat}Re (n, γ) ^{186}Re (low specific activity) or ^{186}W (p, n) ^{186}Re (high specific activity). Specific activity indicates radioactivity per mass unit. Administration of higher specific activity radiopharmaceuticals into the body is more favorable since they have both higher radioactive atom numbers and dose compared to the administration of the same mass of a lower specific activity radiopharmaceutical. In the first pathway of ^{186}Re production, parent and daughter are Re isotopes resulting in having a lower amount of activity per mass unit compared to the second approach. Thus, the second production approach is more favorable because of producing ^{186}Re with relatively higher specific activity since parent and daughter (W and Re) have different chemical properties and are separable (**Scheme 1.10**).

Scheme 1.10: Some common production routes for ^{186}Re and ^{188}Re.

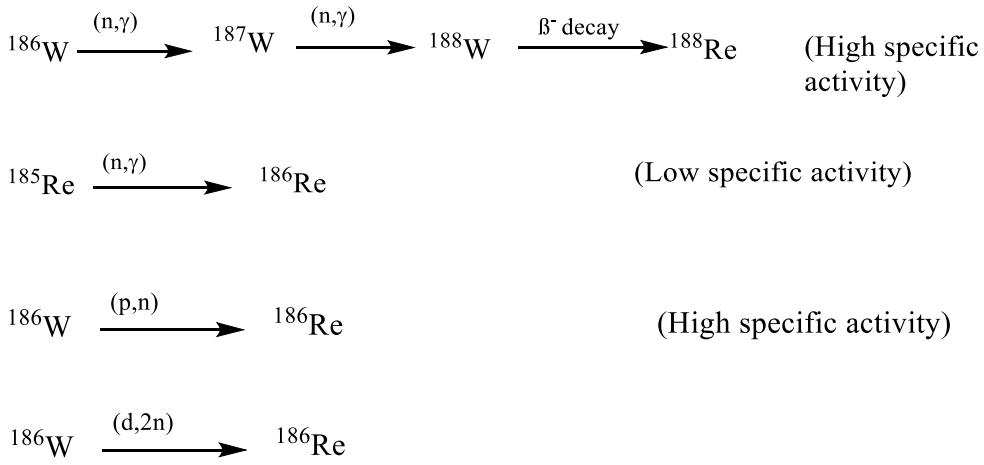

Radiochemistry of Arsenic

Arsenic belongs to the group 15 elements and has only one stable isotope with 100% abundance. [19] The ground-state electronic configuration of elements in this group is $ns^2\ np^3$ ([Ar]$3d^{10}\ 4s^2$ 4p3) with an unpaired electron in each p orbital. The most common oxidation states for As are +5 and +3. Arsenic usually has oxidation states of 1 and 3. The most common oxidation state of arsenic is 3. Arsenic is between metals and non-metals and is either a soft Lewis acid or base tied to the type of its bonding. Arsenic and its compounds have been considered poisons for centuries. The estimated fatal dose of arsenic in adults is 70-200 mg or 1 mg/kg per day. Nonetheless, the amount of administered radioarsenic drug into the body for PET imaging or therapy is approximately 100 MBq (~3 mCi), which contains ~70 ng- 0.007 ng (1 nmol- 1 pmol) and thus, is not considered to be toxic. [20] Arsenic has shown thiophilic properties and

forms complexes with mono, di and trithiols. This thiophilic nature has been utilized for the treatment of arsenic poisoning for years by using thiols such as 2,3-dimercaptopropanol (British Anti-lewisite, BAL) and 2,3-dimercaptosuccinic acid (DMSA) as arsenic chelators. Recently, the thiophilic nature of arsenic has been used for the development of arsenic-thiol radiotracers. The current popularity of ^{177}Lu in radiotherapeutic applications could not be achieved without having its Ga counterpart in PET imaging application, which has led to the vast interest in development of theranostic radionuclides. Interest in arsenic radioisotopes could be their potential for development of theranostic radiopharmaceuticals. [21] Arsenic-74 (β^+ 3.33 MeV, $t_{1/2}$=17.8 d) has been utilized in positrocephalography in the 1950s and 1960s, which is considered as the parent of PET imaging. [22] Arsenic-72 (β^+ 3.33 MeV, $t_{1/2}$=26 h) and ^{77}As (β^- 0.683 MeV, $t_{1/2}$=38.8 h) are a suitable radioisotope matched pair for development of theranostic radiopharmaceuticals. High specific activity As-77 is mainly produced by neutron activation of enriched ^{76}Ge targets. There are various pathways for production of ^{72}As, with an interesting pathway through the decay of ^{72}Se (EC, $t_{1/2}$= 8.5 d). Production of ^{72}Se can be achieved by mid-high-energy proton irradiation of monoisotopic natural arsenic through the ^{75}As(p,4n)^{72}Se reaction or alpha irradiation of enriched ^{70}Ge targets through the ^{70}Ge(α,2n)^{72}Se reaction. Selenium-72 and ^{72}As would be in transient equilibrium with t_{max}=88 h, which is a favorable timespan for development of a generator. The studies for

development of a $^{72}Se/^{72}As$ generator for radiopharmaceutical purposes are underway. [23-26]

Table 1.5: Some commonly used arsenic radionuclides

Radionuclide	$T_{1/2}$	Decay mode (%)	E_x (I_γ in %)
^{71}As	65.3 h	ε , β^+ (100%)	2.013 MeV (ε) 174 keV (82%) (γ)
^{72}As	26.0 h	β^+ (88) ε (12)	3.33 MeV (β^+) 834 keV (81%) (γ)
^{74}As	17.8 d	β^+ (66.2%) β^- (34%)	1.35 MeV (β^+) 596 keV (59%) (γ)
^{77}As	38.79 h	β^- (100%)	0.683 MeV (β^-) 239 keV (1.6%) (γ)

Arsenic is thiophilic and this quality has led to develop monodentate, bidentate (dithioaryls) and tridentate (trithiol) ligands for development of arsenic radiotracers. [27-30] *N*-succinimidyl *S*-acetylthioacetate-modified (SATA-modified) monoclonal antibodies have been directly radiolabeled with radioarsenic and shown high radiolabeling and *in vitro* and *in vivo* stability. [30, 31]

Conclusion and Outline of Dissertation

The main purpose of this dissertation is the development of arsenic and rhenium radiopharmaceuticals as potential theranostic candidates. Development of a new, second generation trithiol bifunctional chelate with an effort for development of a less hydrophobic BCA for $^{72,77}As$ is discussed in Chapter 2. A method for conjugation of a new more

hydrophilic trithiol ligand to a specific type of monoclonal antibodies (Herceptin) and radiolabeling with [^{77}As] radioarsenic is discussed in Chapter 3. Re(V) MAMA base compounds, the microwave-assisted synthesis and characterization of Re(V) and Tc(V) compounds with the N_2S_2 MAMA base ligand encompasses Chapter 4.

Chapter 2: A New, Second Generation Trithiol Bifunctional Chelator for ^{72,77}As: Trithiol(b)-$(Ser)_2$-RM2

Introduction

Matched pair radionuclides for imaging and for radiotherapy are of a great deal of interest to radiopharmaceutical development. Having a theranostic pair with the same element would be ideal because the chemistry and biological handling would be the same. Arsenic-72 and ^{77}As are such a matched pair of radioisotopes and are potentially beneficial for PET imaging and radiotherapy, respectively (^{72}As: 2.49 MeV β^+, 26 h; ^{77}As: 0.683 MeV β^-, 38.8 h). Arsenic-72 is a cyclotron produced radionuclide. Development of a ^{72}Se/^{72}As generator in which ^{72}Se (with a half-life of 8 days) decays by electron capture to ^{72}As would make ^{72}As more readily available [26, 32-36]. Arsenic-77 is mainly produced in a reactor by neutron activation of enriched $^{76}GeO_2$ targets [23]. Arsenic is thiophilic and this quality has led to the development of monodentate, bidentate (dithioaryls) and tridentate (trithiol) ligands for development of arsenic radiotracers. [27-30] *N*-succinimidyl *S*-acetylthioacetate-modified (SATA-modified) monoclonal antibodies have been directly radiolabeled with radioarsenic and shown high radiolabeling and *in vitro* and *in vivo* stability. [30] As far as dithioarylarsine complexes are concerned, it has been suggested that the

aryl-arsenic bond would increase stability to the compound, which is a vital quality for a radiotracer to reach to the target tissue. Several derivatives of dithioarylarsines have been developed and studied previously and has been translated into no carrier added radioarsenic at the tracer level (**Figures 2.1)**. [29]

Figure 2.1: Radiosynthesis of p-ethoxyphenylarsonic acid with nca ^{77}As. Using ammonium mercaptoacetate for reduction and complexation of *p*-ethoxyphenylarsonic acid followed by Substitution with 1,2-Ethane Dithiol. [29]

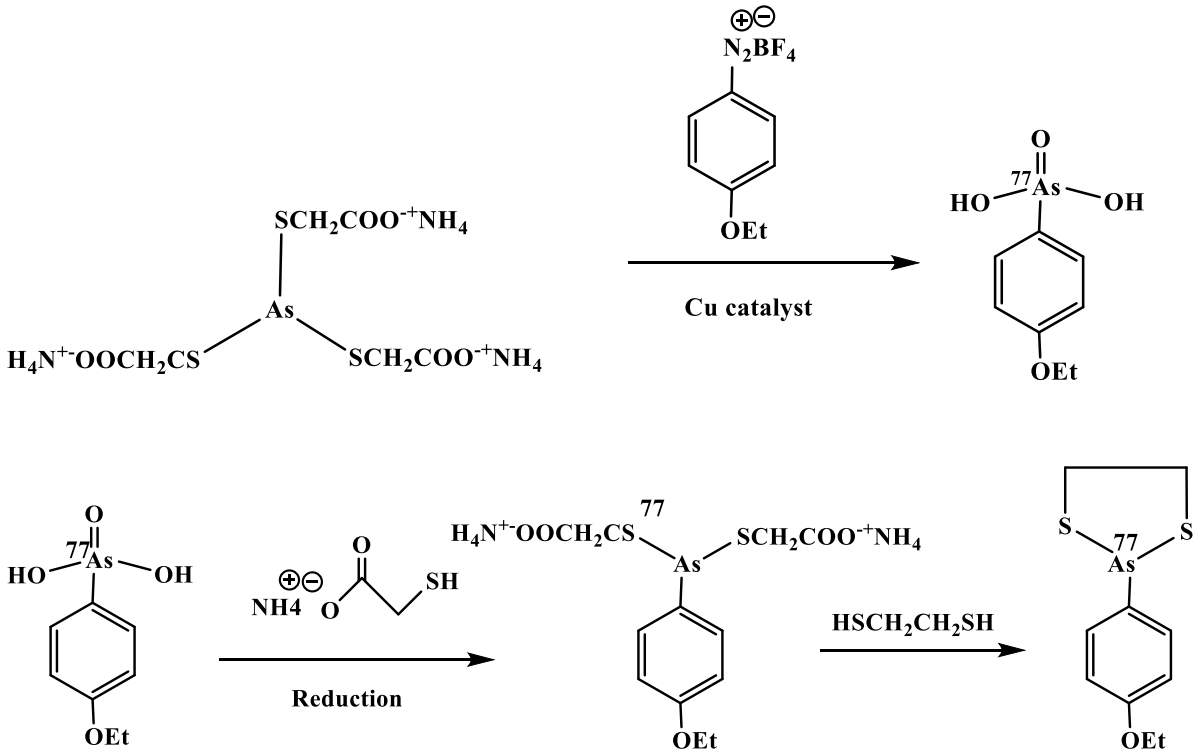

The trithiol ligand framework was focused on for development of bifunctional chelating agents. No carrier added radioarsenic needs to be in

the oxidation state of +3 for radiolabeling thiols, including SATA-modified antibodies and trithiol ligands (**Figure 2.2**). A simple [^{77}As]arsenic-trithiol [28] showed high *in vivo* stability but high lipophilicity, which led to attempts for development of more hydrophilic/less lipophilic bifunctional chelating trithiols followed by conjugation to a model peptide and *in vitro* and *in vivo* evaluation. [37]

Figure 2.2: Synthesis of 4-ethyl-2,6,7-trithia-1-arsabicyclo[2.2.2]octane, **5**

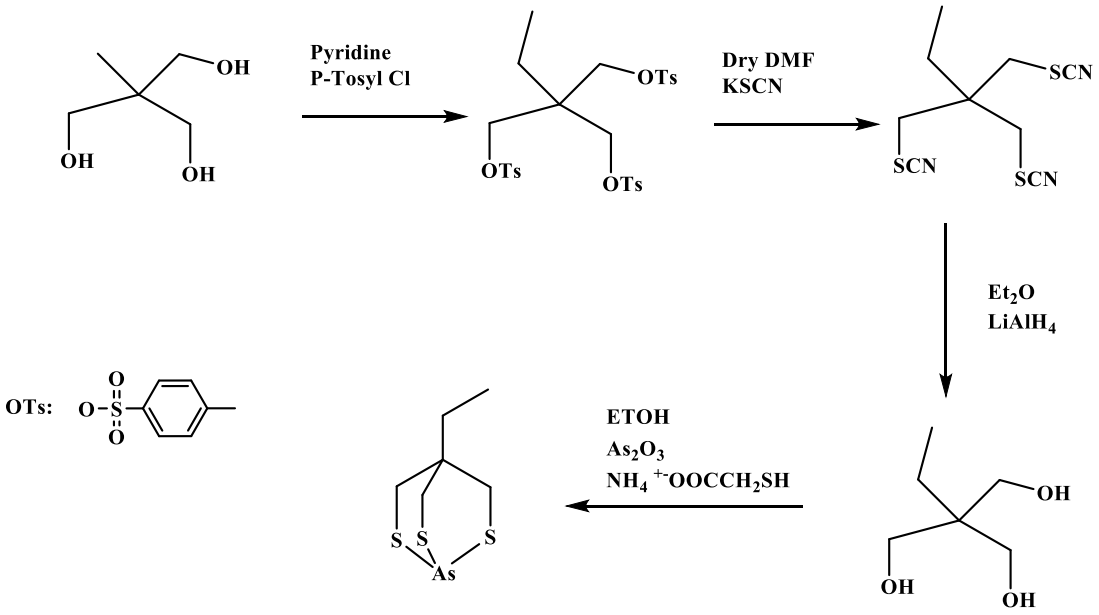

Figure 2.3. Structures of As(III) complexes of (a) aryl-dithiol, (b) ethyltrithiol, and (c) bifunctional trithiol-BBN(7-14)NH_2.

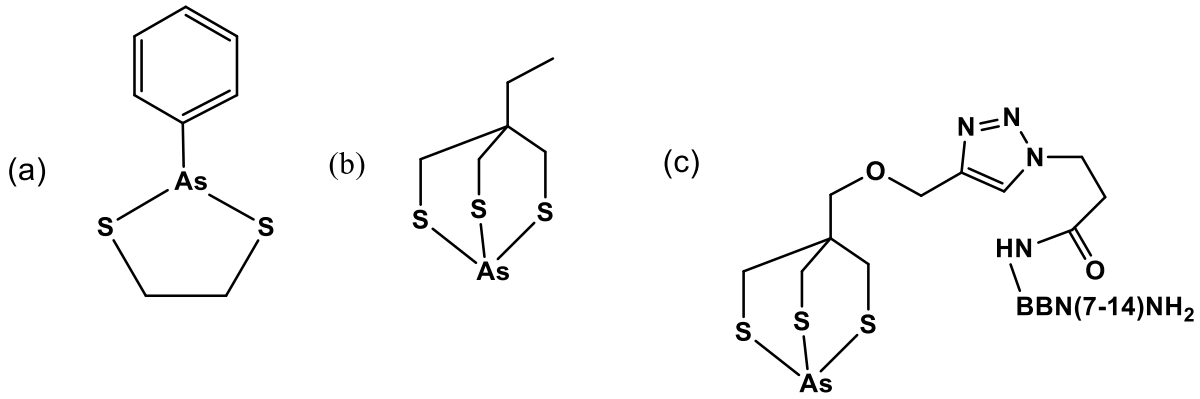

Bombesin (BBN) is a peptide consisting of 14 aminoacids and is an amphibian analogue of the mammalian counterpart gastrin-releasing peptide (GRP), which has 27 amino acids. Bombesin showed high binding affinity to the GRP receptors, which are normally found in pancreas, breast, prostate, lung and colon. GRP receptors are overexpressed in prostate cancer cells including PC-3 tumor cells, which make it a suitable targeting vector for prostate cancer cells. Bombesin (BBN) peptide analogues generally target gastrin-releasing peptide (GRP) receptors expressed in the pancreas of normal mice and human cancers of the prostate. Previous biodistribution studies with [^{77}As]As-trithiol(a)-BBN(7-14)NH_2 (**Figure 2.3, Scheme 2.1**) in normal mice showed high *in vivo* stability compared to free ^{77}As (arsenate). However, the high lipophilicity

of [^{77}As]As-trithiol(a)-BBN(7-14)NH_2 resulted in fast predominantly hepatobiliary excretion and no significant pancreatic uptake.

Scheme 2.1: Radiotracer synthesis of no carrier added ^{77}As-trithiol-BBN(7-14)NH_2 .

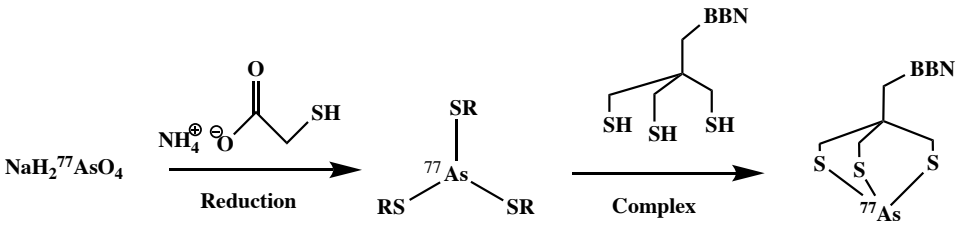

R: -$CH_2COO^-NH4^+$

The objective to develop a more hydrophilic trithiol ligand (**Figure 2.4**) led to the development of a potential bifunctional chelate for radioarsenic and other thiophilic radionuclides such as antimony. The trithiol has a carboxylic acid group for conjugation to peptides and other targeting moieties and the methyl-ester should increase hydrophilicity.

Figure 2.4: Trithiol(b) ligand with higher hydrophilicity.

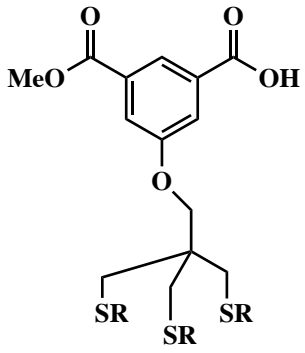

Figure 2.5: The structure of trithiol(b)-$(Ser)_2$-RM2 complex. (a) The structure of $(Ser)_2$-RM2 peptide. (b) The structure of trithiol(b)-$(Ser)_2$-RM2.

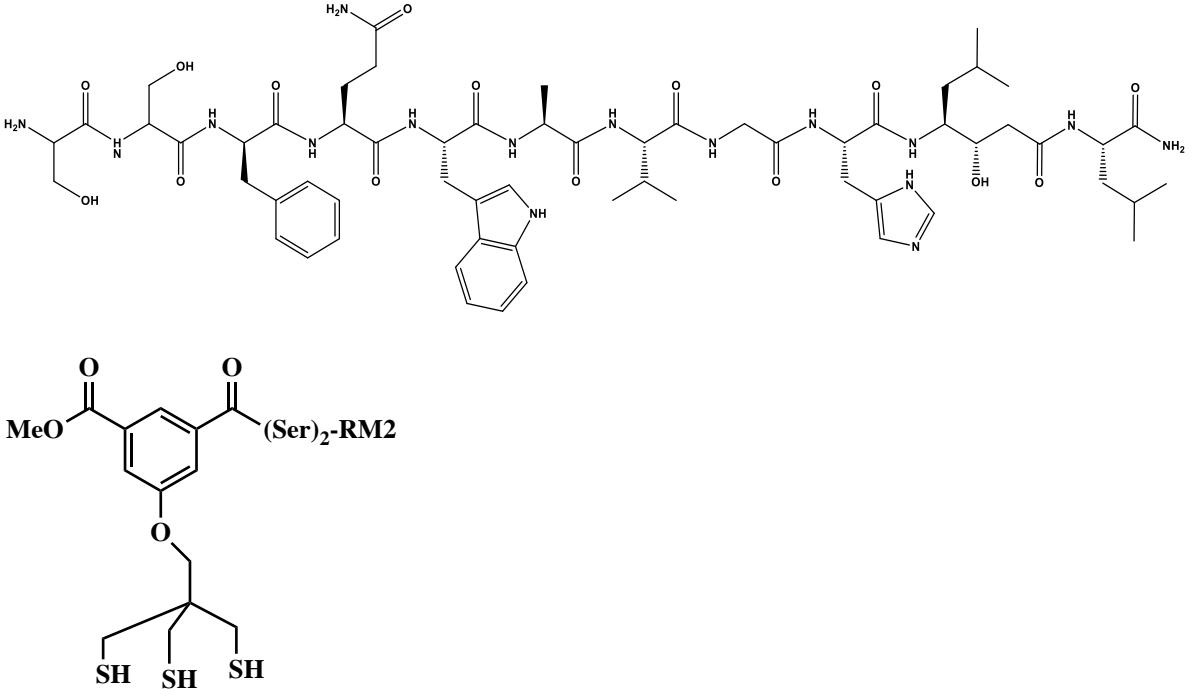

4

The new trithiol was conjugated to the RM2 peptide (*d*Phe-QWAVGH-Sta-L-$CONH_2$) (**Figure 2.5**) through solid phase peptide synthesis and a di-serine spacer was added for increasing hydrophilicity prior to the trithiol. The RM2 peptide is a well characterized antagonist for targeting gastrin-releasing peptide receptors (GRPr), which are over-expressed in human prostate cancer cells [38-42]. This chapter reports the synthesis and characterization of trithiol(b) and its arsenic complex, the trithiol(b)-$(Ser)_2$-RM2 bioconjugate molecule and its $^{nat}As(III)$ complex, the IC_{50} determination of the ^{nat}As-trithiol-$(Ser)_2$-RM2 in PC-3 cancer cells, the

evaluation and biodistribution of no carrier added (nca) ^{77}As radiolabeled trithiol-(Ser)$_2$-RM2 in PC3 tumor-bearing and normal mice.

Scheme 2.2 Synthesis of trithiol(b) (**2**).

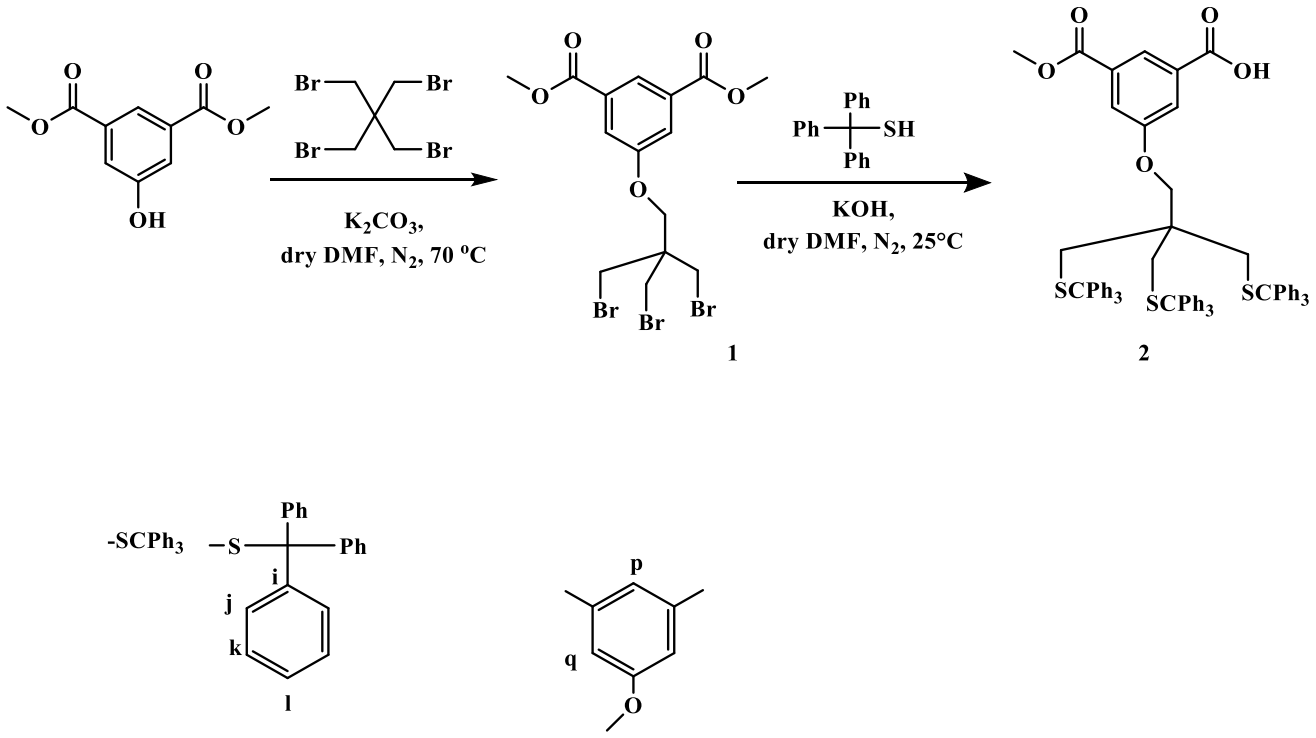

Experimental

Materials

Dimethyl 5-hydroxyisophthalate, pentaerythritol tetrabromide, tris(2-carboxyethyl)phosphine (TCEP), ammonium hydroxide solution (30% NH_3 in H_2O), thioglycolic acid, silica gel 60Å, triphenylmethane thiol, and potassium carbonate were purchased from Fisher Scientific or Sigma-Aldrich. Silica gel w/UV 254 TLC plates were purchased from Sorbtech Technologies. Iodine-125-(Tyr)$_4$-BBN was purchased from PerkinElmer.

L-Ascorbic acid (cell culture tested, γ-irradiated) was purchased from Sigma. Sodium chloride injection saline (0.9%) was purchased from Hospira, India. Hospira Tween-80 was purchased from Acros Organics. Bacteriostatic saline was purchased from Hospira Inc. Sep-Pak C18 Plus Light Cartridges were purchased from Waters. All solvents, and reagent grade acids and bases were purchased from Fisher Scientific or Sigma-Aldrich and used without further purification. Only 18 MΩ water was used during the experiments. Arsenic-77 was prepared by irradiation of 3-5 mg of enriched $^{76}GeO_2$ (98.6%; Trace Sciences International) in a thermal neutron flux of 2.4 x 10^{14} n/cm^2-s at the University of Missouri Research Reactor (MURR). [^{77}As]arsenate ([^{77}As]$H_2AsO_4^-$) was prepared as previously reported. [37, 23] *Caution!* Arsenic-77 and ^{77}Ge are radioactive and were handled in laboratories approved for working with radioactive materials and by trained personnel.

Physical Measurements

^{1}H and ^{13}C NMR spectra were obtained in $CDCl_2$, $CDCl_3$ or DMSO on a Bruker ARX-500 or 600 MHz spectrometer using TMS as an internal standard. An ORTEC HPGe detector equipped with Genie multichannel analysis software was used to evaluate ^{77}Ge and ^{77}As liquid samples. Reversed phase HPLC (RP-HPLC) was performed using a Shimadzu Prominence HPLC system equipped with a pump, controller, and Prominence UV-Vis detector (model SPD20-AV) and Phenomenex Jupiter C18 (5 μm, 150 mm x 4.6 mm) column. A linear gradient of

acetonitrile (MeCN) in water each containing 0.1% trifluoroacetic acid (TFA) was used as follows: 30 to 60% MeCN over 30 min, then from 60 to 90% MeCN over 3 min, followed by returning to 30% MeCN over 3 min, all at a flow rate of 1 mL/min. Peptide purification and analyses were performed on a Beckmann Coulter System Gold HPLC with a 168 diode array detector, a 507e autoinjector and the 32 KARAT software package (Beckmann Coulter, Fullerton, CA) using a C-18 XBridge BEH column (250 x 4.6 mm, 5 μm, 130 Å; Waters, Milford, MA). All LC-MS analyses and MS assisted preparative purifications were performed with an LCQ Fleet instrument (Thermo Fisher, Waltham, MA). Gamma spectroscopy was performed with an ORTEC HPGe detector equipped with Genie multichannel analysis software to evaluate ^{77}Ge and ^{77}As liquid samples. An Eppendorf ThermoMixer equipped with a 1.5 mL tube holder was used for radiochemical syntheses. An Eckert & Ziegler AR-2000 Bioscan was used for radio-TLC measurements. Elemental analyses were performed by Atlantic Microlabs, Inc. (Norcross, GA). High resolution mass spectral analyses were performed at the University of Missouri by the Charles W Gehrke Proteomics Center by direct infusion on a Bruker TIMS-TOF pro with an ESI positive ion source; data were acquired with TIMS off, a full spectrum scan of 200-2000 m/z for 2 min, and deconvolution using Brucker's DataAnalysis (v 5.3) software

Syntheses

***Dimethyl 5-(3-bromo-2,2-bis(bromomethyl)propoxy)isophthalate [$C_{15}H_{17}Br_3O_5$],* 1**. Compound **1** was synthesized using a modified literature procedure [43]. Pentaerythritol tetrabromide (13.8 g, 35.7 mmol) and dimethyl 5-hydroxyisophthalate (4.98 g, 23.7 mmol) were dissolved in 100 mL of anhydrous dimethyl formamide (DMF) under a N_2 atmosphere in a 500 mL round bottom flask. The reaction mixture was stirred at 70 °C in an oil bath for 24 h. DMF was removed under vacuum after bringing the reaction mixture to the room temperature. Deionized water (500 mL) was added to the reaction and the mixture was extracted with dichloromethane (DCM) (3 x 300 mL). The organic layers were collected and combined, dried over anhydrous sodium sulfate solid, filtered and taken to dryness to afford the crude product. The crude product was purified by silica gel column chromatography (5.06 cm X 29.5 cm, 320 mg) using hexanes: DCM (3:1) as the mobile phase based on silica gel TLC (dimethyl 5-hydroxyisophthalate, $R_f \approx 0$, pentaerythritol tetrabromide; $R_f \approx 0.5$; **2**, $R_f \approx 0.15$). The product was eluted with DCM and the fractions were collected, combined and taken to dryness to afford the pure product as a white solid. Yield: 67%, 8.2 g (**Scheme 2.2**). ^{1}H NMR ($CDCl_3$; 500 MHz) δ ppm: 3.680 (s, 6H, C**H$_2$**Br), 3.956 (s, 6H, OC**H$_3$**), 4.147 (s, 2H, OC**H$_2$**), 7.779 (d, 2H, **p**), 8.333 (t, 1H, **q**). ^{13}C NMR ($CDCl_3$; 125.8 MHz) δ ppm: 34.09 (**C**H_2Br), 43.71 (**C**$(CH_2)_4$), 52.54 (**C**H_3), 67.77 (**C**H_2O), 119.97 (OC=**C**), 123.93 (O=CC=**C**), 132.02

(O=C**C**), 158.11 (O**C**=C), 165.91 (**C**OO). ESI-MS (*m/z*): 516.87 (517.01 calc'd for $C_{15}H_{18}Br_3O_5$ $[M+H]^+$) (**Figures 9.2- 11.2**) [37]. Elem. Anal. found (calc'd for $C_{15}H_{17}Br_3O_5$): C 34.93 (34.84); H 3.26 (3.31).

3-(methoxycarbonyl)-5-(3-(tritylthio)-2,2-bis((tritylthio)methyl)propoxy)benzoic acid, [$C_{71}H_{60}O_5S_3$] 2. Compound **1** (1.3 g, 2.51 mmol) and triphenylmethanethiol (2.5 g, 9.05 mmol) were dissolved in anhydrous DMF (25 mL) under a N_2 atmosphere in a 100 mL round bottom flask and stirred at room temperature for 72 h. The reaction mixture was transferred into a separatory funnel and extracted with ethyl acetate (3 x 50 mL). The organic layer was washed with DI water (3 x 50 mL), saturated NaCl solution (1 x 50 mL) and dried over anhydrous sodium sulfate. The organic layer was then filtered and taken to dryness to yield the crude product. The crude product was purified with silica gel column chromatography (5.06 cm X 29.5 cm, 0.320 g) using 1:3 ethyl acetate:DCM as the mobile phase based on silica gel TLC (**1**, $R_f \approx 0.15$, **2**, $R_f \approx 0.1$). A pale-yellow band was observed in the column and eluted to give a pale-yellow foam. Yield: 73%, 2.01 g. (**Scheme 2.2**). ^{1}H NMR ($CDCl_3$; 600 MHz) δ ppm: 2.182 (s, 6H, C**H**$_2$SCPh$_3$), 3.550 (s, 2H, C**H**$_2$O), 3.987 (s, 3H, C**H**$_3$O), 7.157-7.210 (m, 9H, **l**), 7.260-7.480 (m, 18H, **j**), 7.482-7.501 (m, 21H, **k, p, q**), 8.333 (s, 1H, COO**H**). ^{13}C-NMR (500 MHz, $CDCl_3$, δ (ppm)): 36.44 (-**C**H$_2$-S-), 42.46 (**C**H$_3$-O-CO-), 52.62 (-**C**H$_2$-O-), 66.39 (**C**OOCH$_3$),123.67 (**l**), 126.76 (**j**), 127.94 (**k**), 131.79 (**i**),

144.69 (**C**OOH). ESI-MS (*m/z*): 1110.94 (1110.92 calc'd for $C_{71}H_{60}O_5S_3$ $[M+Na]^+$) (**Figures 2.12-2.14**).

Scheme 2.3: Synthesis of trithiol(b)-$(Ser)_2$-RM2 (**4**). Synthesis of the non-radioactive As-trithiol(b)-$(Ser)_2$-RM2 (**5**) by reducing compound **3** to **4**.

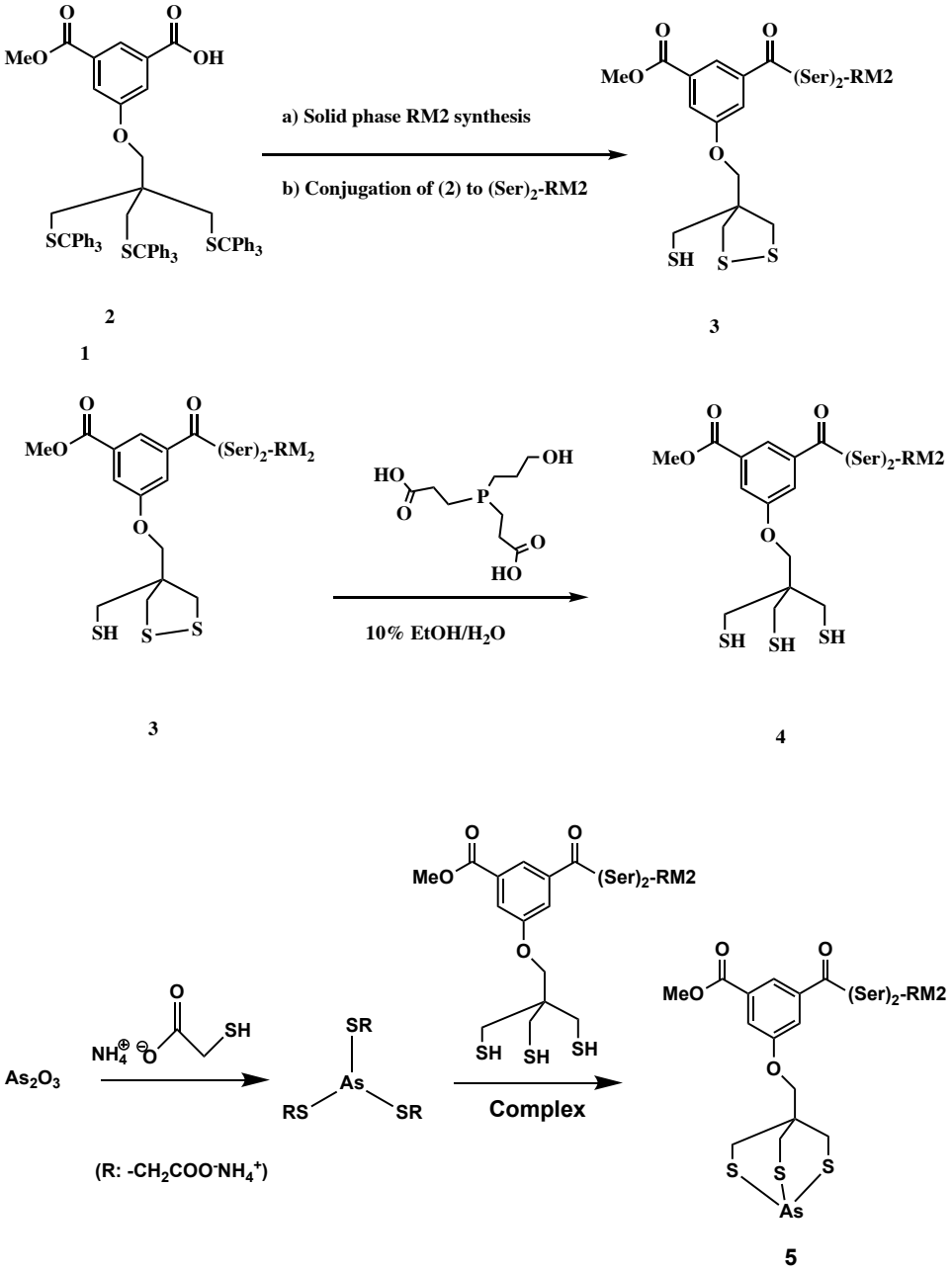

Synthesis of Trithiol(b)-(Ser)$_2$-RM2 3.

Trithiol(b)-(Ser)$_2$-RM2 (trithiol-SS-*d*Phe-QWAVGH-Sta-L-CONH$_2$) **3** was synthesized by solid phase peptide synthesis (model AAPPTEC 396 Omega, Louisville, KY) using Fmoc chemistry on Sieber Resin (300 μmoles, 480 mg). The protecting groups used for the amino acid side chains were: trityl (Gln, His); *tert*-butyloxycarbonyl (Boc) (Trp). The fluorenylmethoxycarbonyl (Fmoc) protecting groups were removed at each subsequent cycle by treatment with 20% piperidine for 10 min. The peptide chain was assembled by sequential acylation (20 min for coupling) with "*in situ*" activated Fmoc-amino acids. Re-coupling was automatically performed at every cycle. The "*in situ*" activation of Fmoc-amino acids (3 equiv. compared to the resin amount) was carried out using uronium salts (HBTU, 2.7 equiv., HOBt 3 equiv.) and diisopropylethylamine (DIEA) (6 equiv.). Compound **2** (1.05 g, 0.945 mmol) was conjugated to the *N*-terminus of the (Ser)$_2$-RM2 peptide on the resin in a single coupling reaction for 2 hours, after being converted to the activated ester by reaction with DIEA, HBTU and HOBt. The peptidyl resin was cleaved and deprotected in a single reaction (2 h, room temperature) with the following mixture: TFA, phenol, water and triisopropylsilane (TIS) (85:5:5:5). Precipitation and multiple washings with diethyl ether gave the final crude product. The product was HPLC purified as the deprotected trithiol(b)-(Ser)$_2$-RM2 containing one disulfide and one free thiolate, characterized by LC-ESI-MS (1631.37; 1631.70 calc'd for

$C_{75}H_{107}O_{19}N_{16}S_3$ [$M+H^+$]), lyophilized and stored in the freezer (-20 °C) until further use. Yield: 300 μmol, 47 mg, > 90 % purity. **(Scheme 2.3, Figure 2.6, Figure 2.15).**

Synthesis of ^{nat}As-trithiol(b)-$(Ser)_2$-RM2 5.

Caution! Arsenic is toxic and should be handled with care. Compound **4** was prepared by reducing compound **3** using tris(2-carboxyethyl) phosphine (TCEP) as follows: Compound **3** (2.24 mg, 0.00137 mmol) was dissolved in 10% EtOH in water (2 mL) and TCEP (2 mg, 0.0070 mmol) was added. The reaction mixture was placed in a 55 °C thermomixer and stirred for 30 min (**Scheme 2.3**) to generate **4**. Arsenic trioxide (5.5 mg, 0.027 mmol) was suspended in 1 mL of 10% EtOH in water and ammonium mercaptoacetate (0.5 mL, 5.5 M, 2.76 mmol, 28 eq.) was added. Compound **4** (2 mL, 1.47 mg, 0.00137 mmol) was added to the arsenic reaction mixture and placed in a 55 °C thermomixer and stirred for 1 h. The reaction was cooled to room temperature and diluted with 15 mL of water. A Sep-Pak C18 Plus Light cartridge was preconditioned with ethanol and rinsed with water, and then the diluted reaction mixture was loaded on the cartridge and washed with 10 mL of water. ^{nat}As-trithiol(b)-$(Ser)_2$-RM2 **5** was eluted from the cartridge with 3 mL of ethanol and characterized by LC-ESI-MS (1703.30 (1703.60 calc'd for $C_{75}H_{104}O_{19}N_{16}S_3As$))), high resolution ESI-MS (1704.8372 [$M+H^+$]; (**Figure 2.16**) and HPLC (**Figure 2.17**).

Scheme 2.4: Radiotracer synthesis of Trithiol(b)-$(Ser)_2$-RM2 with nca ^{77}As.

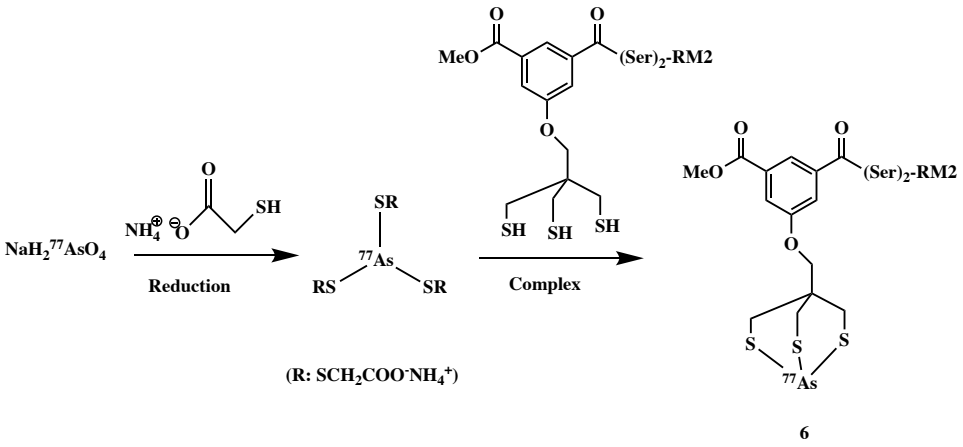

Radiotracer synthesis of [^{77}As]As-trithiol(b)-$(Ser)_2$-RM2 6.

No carried added [^{77}As]$H_2AsO_4^-$ (222 MBq/mL (6 mCi/mL)) in aqueous solution was obtained from the University of Missouri Research Reactor (MURR). [^{77}As]$H_2AsO_4^-$ (200 µL, 44 MBq (1.2 mCi)) was added to a 2 mL Eppendorf tube containing 581 µL of DI water. Ammonium acetate (18.2 µL, 5.5 M, 100 µmol) was added to the reaction mixture and placed in a 55 °C thermomixer and stirred for 45 min. Compound **4** (200 µL, 0.0139 mmol; as prepared above) in 10% EtOH in DI water was added to the reaction mixture with heating and stirring continued for 45 min. The reaction was cooled to room temperature and purified using RP-HPLC. A Phenomenex Jupiter C18 column was eluted with a linear gradient as follows: 30 to 60% MeCN/H_2O w/ 0.1% TFA over 30 min, then from 60 to 90% MeN/H_2O over 3 min, followed by returning to 30% MeCN/H_2O

over 3 min (flow rate 1 mL/min). The fractions containing [^{77}As]As-trithiol(b)-(Ser)$_2$-RM2 were collected and the solvent was removed under a stream of N_2(g) at 55 °C and then reconstituted with sterile and non-pyrogenic saline. The purified product was monitored by RP HPLC and radio-TLC (silica gel; 50% MeCN/H_2O as the mobile phase, $R_f \approx 0.86$ determined by Bioscan). *L*-ascorbic acid (30 μg) and 0.1% (v/v) Tween-80 were added to the solution to prevent radiolysis and sticking to the vessel wall, respectively. The radiochemical yield after purification was determined to be 27.5 MBq (700 μCi; 58.3%) (**Scheme 2.4**, **Figures 2.6**).

Figure 2.6: RP HPLC of ^{77}As-trithiol(b)-(Ser)$_2$-RM2 (gamma detector) before HPLC purification (**top**) and after HPLC purification (**bottom**).

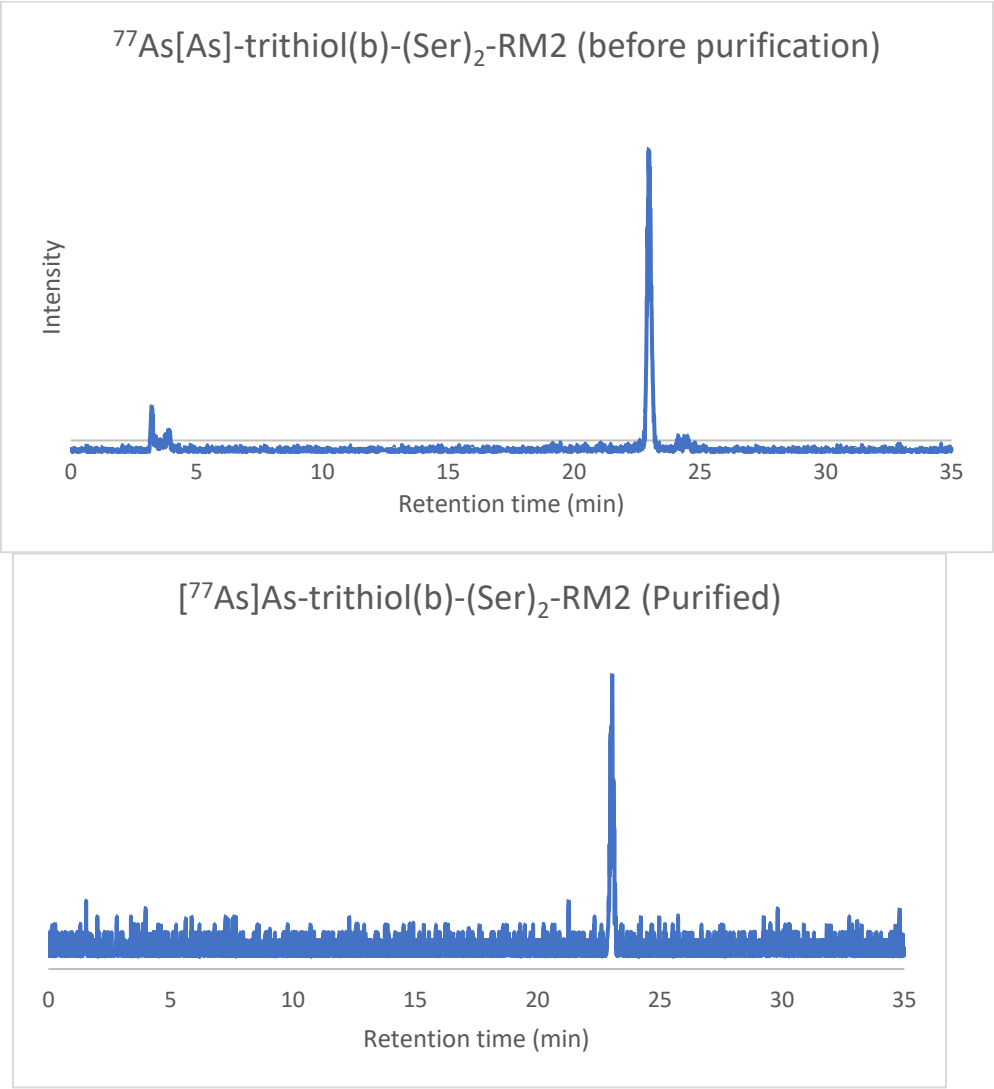

Scheme 2.5: Synthesis of non-radioactive As-Trithiol(b) complex (**5**)

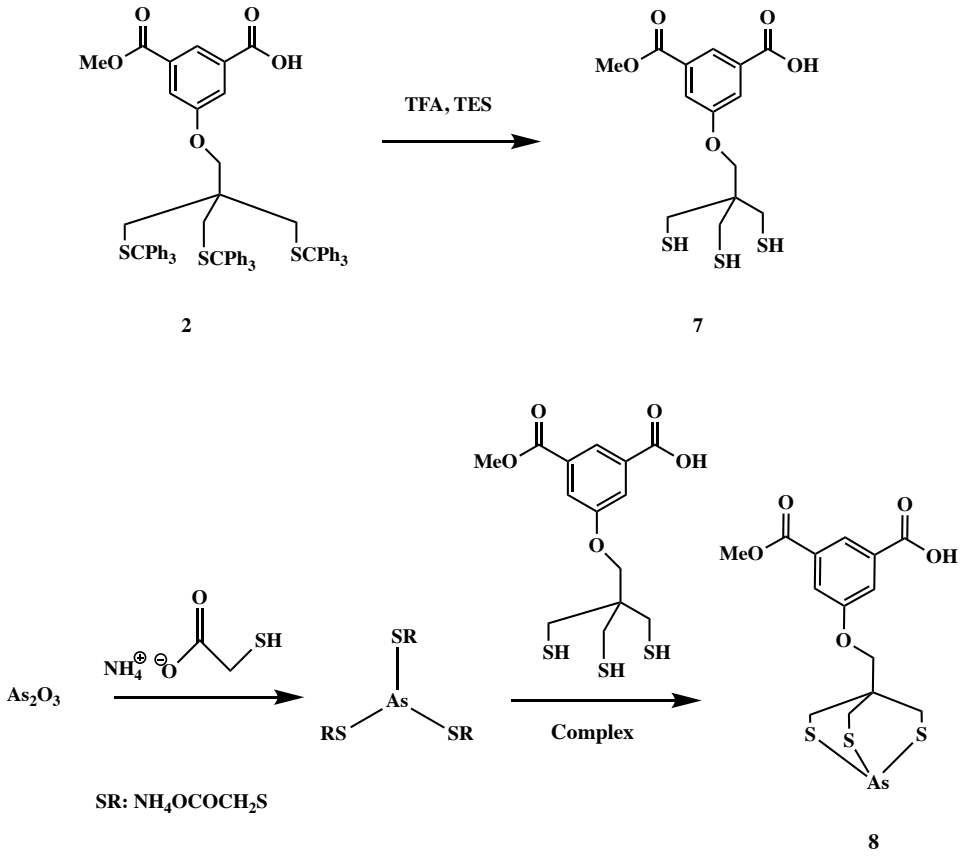

Non-radioactive As-trithiol(b) ***3-((2,6,7-trithia-1-arsabicyclo[2.2.2]octan-4-yl)methoxy)-5-(methoxycarbonyl)benzoic acid, [$C_{14}H_{15}AsO_5S_3$] 8.***

Arsenic trioxide (11.27 mg, 0.057 mmol) was partially dissolved in 5 mL of 90% ethanol in water solution. Ammonium mercaptoacetate (238 µL, 5.5 M, 0.512 mmol, 9 eq.) was added to the mixture and placed in 55 °C oil bath and stirred for 40 min. Compound **2** (30 mg, 0.028 mmol) was deprotected with trifluoroacetic acid (2.13 mL, 27 mmol) in the presence of triethylsilane (0.112 mL, 0.70 mmol) to yield compound **3**. Compound **7** was added to the reaction mixture and placed in a 55 °C oil bath and

stirred for 40 min. The reaction mixture was then placed in a freezer overnight. A precipitate was formed, filtered, washed with ice water (around 5 °C) and ethyl ether and dried in vacuum to afford compound **8** as a white solid (**Scheme 2.5, Figure 2.18)**. ^{1}H NMR (DMSO; 500 MHz) δ ppm: 3.150 (s, 3H, C**H**$_2$S), 3.350 (s, 5H, OC**H**$_2$, C**H**$_2$S). 3.850 (s, 3H, OC**H**$_3$), 7.750 (d, 2H, C**H**), 8.120 (t, 1H, C**H**), 12.500 (s, 1H, COO**H**).

Scheme 2.6: Synthesis of ^{77}As-Trithiol(b) complex (**9**).

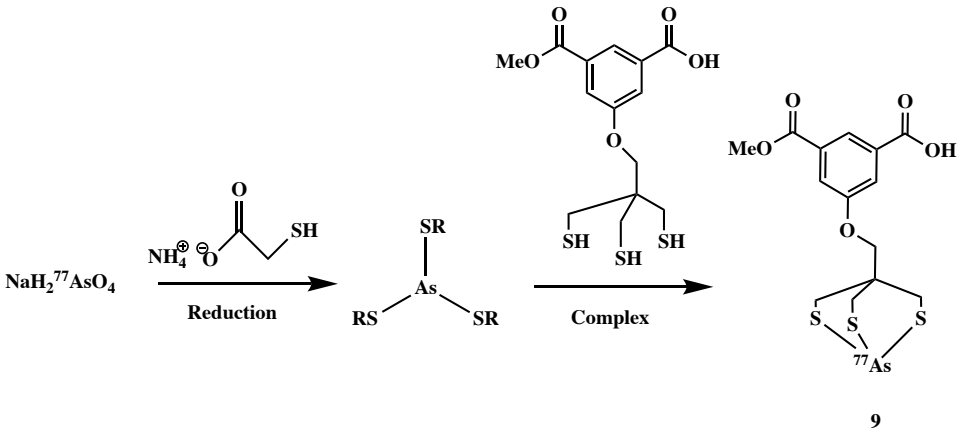

9

Radiotracer synthesis of [^{77}As]As-trithiol(b) 9. No carried added ^{77}As[^{77}As]$H_2AsO_4^-$, (222 MBq/mL (6 mCi/mL)) in aqueous solution was prepared at the University of Missouri Research Reactor (MURR) as previously reported [23]. 200 µL, 44 MBq (1.2 mCi) of [^{77}As]$H_2AsO_4^-$ solution in water was added to a 2 mL Eppendorf tube containing 581 µL of 10% EtOH in DI water. Ammonium acetate (18.2 µL, 5.5 M, 100 µmol) was added to the reaction mixture and placed in a 55 °C thermomixer and stirred for 45 min. Compound **7** (200bµL, 0.4 mg, 0.0139 mmol) in 10% EtOH in DI water was added to the reaction mixture

and continued heating and stirring for 45 min. The reaction was cooled to the room temperature, filtered through a 0.2 μm core size syringe filter, and injected on to the RP HPLC. The Phenomenex Jupiter C18 column was eluted. A linear gradient as follows: 30 to 60% MeCN/H_2O w/ 0.1% TFA over 30 min, then from 60 to 90% MeCN/H_2O over 3 min, followed by returning to 30% MeCN/H_2O over 3 min (flow rate 1 mL/min). The product was compared with the non-radioactive As-trithiol(b) standard ([^{77}As] **8,** retention time=29.6 min; [^{nat}As] **6**, retention time 30 min). The results showed the 99% radiolabeling yield and no further purification was required. (**Scheme 2.6**).

Distribution coefficient (log$D_{7.4}$) studies of [^{77}As] As-trithiol(b)-$(Ser)_2$-RM2 6.

Phosphate-buffered saline (PBS) buffer solution (2 mL, pH 7.4, 15 mM) was added to a centrifuge tube along with 2 mL of *n*-octanol. [^{77}As]As-trithiol(b)-$(Ser)_2$-RM2 in DI water (200 μL, 3.7 MBq (100 μCi)) was added to the centrifuge tube and the resultant mixture stirred on a vortex mixer for 5 min, and then centrifuged (3200 rpm) for 2 min. The aqueous (1.5 mL) and the organic layers (1.5 mL) were separated and each counted on an HPGe detector. The experiment was carried out in triplicate.

Stability of [^{77}As] As-trithiol(b)-(Ser)$_2$-RM2

The stability of [^{77}As]As-trithiol(b)-(Ser)$_2$-RM2 in saline solution, and containing ascorbic acid as prepared above, was assessed over 72 h by RP-HPLC and radio-TLC (^{77}As-colloid, $R_f \approx 0$; [^{77}As]As-trithiol(b)-(Ser)$_2$-RM2, $R_f \approx 0.86$; free ^{77}As, $R_f \approx 1$). [^{77}As]As-trithiol(b)-(Ser)$_2$-RM2 (11.6 MBq (300 μCi)) in sterile saline was set aside at room temperature and monitored at 24, 48 and 72 h.

***In vitro* Cell Binding Studies**

In vitro cell binding studies of ^{nat}As-trithiol(b)-(Ser)$_2$-RM2, **5**, with human PC-3 prostate cancer cells were performed following the procedure previously reported. [7, 44] [^{125}I]-Tyr$_4$-BBN(NH$_2$) (PerkinElmer, Waltham, MA) was used as the competitor peptide. Briefly, RPMI 1640 cell media (Invitrogen, Carlsbad, CA) was supplemented with approximately 30 mM bovine serum albumin (BSA, 1 g, 15 mmol) and 20.6 mM 2-[4-(2-hydroxyethyl)piperazin-1-yl]ethanesulfonic acid (HEPES, 2.46 g, 10.3 mmol), filtered through a 0.22 mm sterile filter, and adjusted to pH 7.4. Approximately 30,000 PC-3 cells, 20,000 cpm of [^{125}I]-Tyr$_4$-BBN(NH$_2$), and varying concentrations of ^{nat}As-trithiol(b)-(Ser)$_2$-RM2 (9.6×10^{-13} to 9.6×10^{-6} M) were incubated at 37 ^{o}C, 95% humidity, and 5% CO_2 for 45 min in the modified growth media. The cells were washed with cold modified media (3X) to remove any unbound radioactivity. An LTi Multi-Wiper was used to count the activity bound to the cells. The entire process

was performed three times in duplicate (n=6). The IC_{50} value was calculated using GraphPad Prism, Version 8.0.1 (145).

Biodistribution studies of no carried added [^{77}As] As-trithiol(b)-(Ser)$_2$-RM2 on PC-3 Bearing SCID mice

All animal experiments were carried out according to protocols approved by the Harry S. Truman Memorial Veterans' Administration Hospital Subcommittee for Animal Studies. Male SCID mice (4-5 weeks of age; Taconic Biosciences, Germantown, NY) were housed in autoclaved ventilated caging system with ad libitum access to irradiated food (Lab Diet 5053, St. Louis, MO) and autoclaved acidified water in a 12 h light/12 h dark environment. Mice were subcutaneously administered 5 million cultured PC-3 cells suspended in RPMI 1640 in both rear flanks. Tumors were allowed to develop for 4 weeks prior to the pharmacokinetic studies. Animals were administered [^{77}As]As-trithiol(b)-(Ser)$_2$-RM2 (0.19 MBq (~5 μCi)) in 100 μL of sterile saline through the lateral tail vein. Mice were sacrificed at 15 min, 1 h, 4 h, and 24 h post-injection with 3-4 animals per time point. An additional 4 animals were administered 20 nM ^{nat}As-trithiol(b)-(Ser)$_2$-RM2 in sterile saline at 5 minutes prior to administration of [^{77}As]As-trithiol(b)-(Ser)$_2$-RM2. These animals were sacrificed at 4 h post-injection of the radiotracer (4 h Blocked). Tissues and organs were collected, weighed and counted using a *Perkin Elmer Wizard2 Automatic Gamma Counter* (Waltham, MA). Data were analyzed and the percent injected dose (%ID) and percent injected dose per gram

(%ID/g) of selected organs and tissues were calculated. The total mass of the blood was estimated to be 6.5% of the total body weight (**Table 2.1**).

Biodistribution studies of no carried added [^{77}As] As-trithiol(b)-(Ser)$_2$-RM2 on CF-1 mice models

Male CF-1 mice were purchased at 4-5 weeks of age (from Charles River Laboratories; Wilmington, MA) and were used for pharmacokinetic studies at 5-7 weeks of age. Mice were fed *ad libitium* rodent chow and acidified wate*r* on a 12-h light/12-h dark light cycle in an AAALAC certified facility. All experiments were approved by the "HS Truman Memorial Veterans' Hospital subcommittee for animal studies (SAS)". Biodistribution studies of nca [^{77}As]As-trithiol(b)-(Ser)$_2$-RM2 were performed in CF-1 mice. Animals were administered 100 µL (0.37 MBq (~ 10µCi)) of [^{77}As] As-trithiol(b)-(Ser)$_2$-RM2 through the lateral tail vein. Mice were sacrificed at 15 min and 1 h post-injection with 3 animals per time point. Tissues and organs were collected, weighed and counted using a Perkin Elmer Wizard Automatic Gamma Counter. Data were analyzed and the percent injected dose (%ID) and percent injected dose per gram (%ID/g) of the organs and tissues were calculated (**Table 2.2. 2.3**).

Single crystal X-ray diffraction analysis

Single-crystal X-ray diffraction (XRS) data were collected on a Bruker X8 Prospector diffractometer (Bruker-AXS, Inc., Madison, WI, USA) using Cu-Kα radiation (λ = 1.54178) from a microfocus source. The crystal was

cooled to 100 K during collection using a Cryostream 700 cryostat (Oxford Cryosystems, Oxford, UK). A hemisphere of data was collected out to a resolution of at least 0.81 Å using strategies of scans about the phi and omega axes. Unit cell determination, data reduction, absorption correction, and scaling were performed using the Bruker Apex3 software suite.[59] The crystal structure was solved by direct methods using SHELXS [60] and refined by full-matrix least squares refinement using SHELXL [45] implemented via Olex2 [46]. Non-hydrogen atoms were located from the difference map and refined anisotropically. Hydrogen atoms were placed in calculated positions, and their coordinates and thermal parameters were constrained to ride on the carrier atoms (**Figure 2.8**, **Tables 2.4-2.9**).

Results and Discussion

Previous trithiol chelates synthesized for the purpose of theranostic $^{72/77}$As radiopharmaceuticals showed high *in vivo* stability but were too lipophilic for in vivo applications based on biodistribution results [28, 29, 37]. A more hydrophilic linkable trithiol ligand (trityl protected) was synthesized and then conjugated to the RM2 peptide with a two serines spacer using solid phase peptide synthesis to prepare trithiol(b)-$(Ser)_2$-RM2. This precursor required TCEP reduction prior to radiolabeling with ^{77}As for *in vitro* and *in vivo* evaluation. One thiol and a disulfide were formed on deprotection following peptide synthesis.

Synthesis of trithiol ligand

Synthesis of dimethyl 5-(3-bromo-2,2-bis(bromomethyl)propoxy)isophthalate, **1**, and 3-(methoxycarbonyl)-5-(3-(tritylthio)-2,2-bis((tritylthio)methyl)propoxy)benzoic acid, **2**, yielded 75% and 73%, respectively (**Scheme 2.2**) [7, 43]. Dimethyl 5-(3-bromo-2,2-bis(bromomethyl)propoxy)isophthalate, **1**, was synthesized by the reaction of pentaerythritol tetrabromide and dimethyl 5-hydroxyisophthalate in anhydrous DMF under a N_2 atmosphere at 70 °C for 24 h. This compound was purified by silica gel column chromatography using hexanes:DCM (3:1) as the mobile phase [47]. The protected trithiol ligand, 3-(methoxycarbonyl)-5-(3-(tritylthio)-2,2-bis((tritylthio)methyl)propoxy)benzoic acid, **2** , was synthesized by the reaction of **1,** and triphenylmethanethiol in anhydrous DMF under a N_2 atmosphere at room temperature for 72 h. The purification was performed with silica gel column chromatography using 1:3 ethyl acetate:DCM as the mobile phase. Compounds **1** and **2** were characterized by ^{1}H and ^{13}C NMR spectroscopy and LC-ESI-MS. The molecular ions for compounds **1** and **2** were observed in the LC-ESI-MS spectra at their calculated *m/z* values.

Trithiol(b)-$(Ser)_2$-RM2 synthesis

The gastrin-releasing peptide receptor (GRPR) is an attractive target for imaging and therapy since it is overexpressed in several human tumors such as prostate cancer, breast cancer (BC), and peritumoral vessels in ovarian cancer. RM2 targets gastrin-releasing peptide receptors as a

synthetic bombesin receptor antagonist [48]. A trithiol-$(Ser)_2$-RM2 peptide was synthesized for developing an [^{77}As]As radiolabeled RM2 peptide (**Scheme 2.4**). The synthesis of trithiol(b)-RM2 peptide was performed by coupling the trityl protected trithiol ligand as the last step of solid phase peptide synthesis to two serine amino acids that had been coupled to the RM2 peptide on resin (compound **3**, **Scheme 2.4**) using Fmoc chemistry on Sieber Resin. Re-coupling was automatically performed at every cycle. The "*in situ*" activation of Fmoc-amino acids (3 eq. compared to the resin amount) was carried out using HBTU, HOBt and DIEA. Trithiol ligand **2** was conjugated to the *N* terminus of the $(Ser)_2$-RM2 peptide on the resin in a single coupling reaction after being converted to the activated ester by reaction with DIEA, HBTU and HOBt. The peptidyl-resin was cleaved and deprotected in a single reaction with TFA, phenol, water and triisopropylsilane (TIS) (85:5:5:5). The product was HPLC purified as the deprotected trithiol-$(Ser)_2$-RM2 containing one disulfide and one free thiolate, characterized by LC-MS (1629.4 (1630.1 calc'd for $C_{57}H_{79}O_{11}N_{19}S_4$ [M+H+])). The trithiol-$(Ser)_2$-RM2 **3** required reduction to **4** with TCEP prior to radiolabeling (Scheme **2.4**). The yield of compound **4** was determined to be >95% with compound **3** as the impurity. No further purification was performed.

Trithiol(b)-$(Ser)_2$-RM2 radiolabeling

The nca ^{77}As radiolabeling of trithiol(b)-$(Ser)_2$-RM2 (compound **4**) was performed in 2 hours with over 95% radiochemical yield (**Scheme 2.4**) [28,

[37]. ^{77}[As]arsenate was isolated in the +5 oxidation state from the irradiated $^{76}GeO_2$ target and reduced to ^{77}[As]As(SR)$_3$ with As in the +3 oxidation state using mercaptoacetate (SR). Trithiol(b)-(Ser)$_2$-RM2 (compound **4**) was added and replaced the monothiols (SR groups). The radiolabeled complex was analyzed and purified by RP-HPLC (**Figure 2.15**). The peaks observed at 3.5 min, 3.93 min and 21.7 min by UV analysis were associated with the excess mercaptaacetate, TCEP and unreacted trithiol(b)-(Ser)$_2$-RM2, respectively. The monothiol (mercaptoacetate) and trithiol(b)-(Ser)$_2$-RM2 are in excess relative to nca ^{77}As. A Phenomenex Jupiter C18 (5 μm, 150 mm x 4.6 mm) column was used to purify the [^{77}As] As-trithiol(b)-(Ser)$_2$-RM2. The RP-HPLC purified [^{77}As] As-trithiol(b)-(Ser)$_2$-RM2 solution was brought to near dryness under a N_2 (g) atmosphere and gentle heating, and then reconstituted with sterile and non-pyrogenic saline. To prevent radiolysis, ascorbic acid was added to the [^{77}As]As-trithiol(b)-(Ser)$_2$-RM2 solution. [^{77}As]As-trithiol(b)-(Ser)$_2$-RM2 solution was evaluated by RP-HPLC and its retention time was consistent with [^{nat}As]As-trithiol(b)-(Ser)$_2$-RM2 and no free ^{77}As was observed (**Figures 2.6**).

In vitro lipophilicity (log $D_{7.4}$) studies

The octanol-water distribution coefficient was determined at pH 7.4 as an indicator of lipophilicity under biological pH. HPLC purified [^{77}As]As-trithiol(b)-(Ser)$_2$-RM2, which had been reconstituted in pH 7.4 PBS and contained ascorbic acid as a radioprotectant, was used for this

determination. The log $D_{7.4}$ value was calculated from the following equation:

$$\log D = log \frac{Radioactivity\ in\ octanol}{Radioactivity\ in\ water}$$

The log $D_{7.4}$ value determined for this complex was = 0.7 ± 0.1. The log $D_{7.4}$ value determined for this complex was determined to be 0.7 ± 0.1. [^{77}As]As-trithiol(b)-$(Ser)_2$-RM2 is more lipophilic than the NOTA-/NODAGA RM2 bioconjugates radiolabeled with the *fac*-$M(CO)_3^+$ core (M = ^{99m}Tc, ^{186}Re) recently reported (log $D_{7.4}$ -1.35 to -2.31). [49] The two or three dangling carboxylates of NOTA or NODAGA, respectively, make these ligands more hydrophilic than trithiol(b).

Stability of [^{77}As]As-trithiol(b)-$(Ser)_2$-RM2

The *in vitro* stability of HPLC purified [^{77}As]As-trithiol(b)-$(Ser)_2$-RM2 in saline solution with ascorbic acid added was assessed over 72 h by HPLC and radio-TLC. The formation of free ^{77}As was not observed by HPLC, which was consistent with the data previously reported [28, 37]. The formation of 5% ^{77}As colloid was observed by radio-TLC at 24 h. The colloid presumably formed from thiol oxidation of the excess trithiol(b)-$(Ser)_2$-RM2 present, which was not completely removed on HPLC purification (retention times of 21.76 min and 22.58 min for trithiol(b)-$(Ser)_2$-RM2 and [^{77}As]As-trithiol(b)-$(Ser)_2$-RM2, respectively). The HPLC solvent removal and reconstitution in saline would have accelerated

the thiol oxidation. The amount of ^{77}As colloid remained unchanged at 48 h and 72 h, indicating its stability under these conditions. When the [^{77}As]As-trithiol(b)-$(Ser)_2$-RM2 was not HPLC purified to remove the excess trithiol(b)-$(Ser)_2$-RM2 present prior to solvent removal and reconstitution in saline, much more (>90%) colloid formed, likely from oxidation of the thiols to form bridged disulfide oligomers.

In vitro cell binding studies

Competitive *in vitro* cell binding studies of HPLC purified ^{nat}As-trithiol(b)-$(Ser)_2$-RM2 were performed against [^{125}I]I-Tyr^4-BBN(NH_2) using PC-3 prostate cancer cells, which are known to express GRP receptors. A calculated IC_{50} value of 10 ± 2 nM (n = 6) was determined (**Figure 2.7**), which is comparable with previously reported results with other GRPR targeting radiolabeled compounds. [7, 50]

Figure 2.7: Plot showing the IC_{50} results for ^{nat}As-trithiol(b)-$(Ser)_2$-RM2 performed against [^{125}I]iodo-Tyr^4-BBN(NH_2) in PC-3 prostate cancer cells.

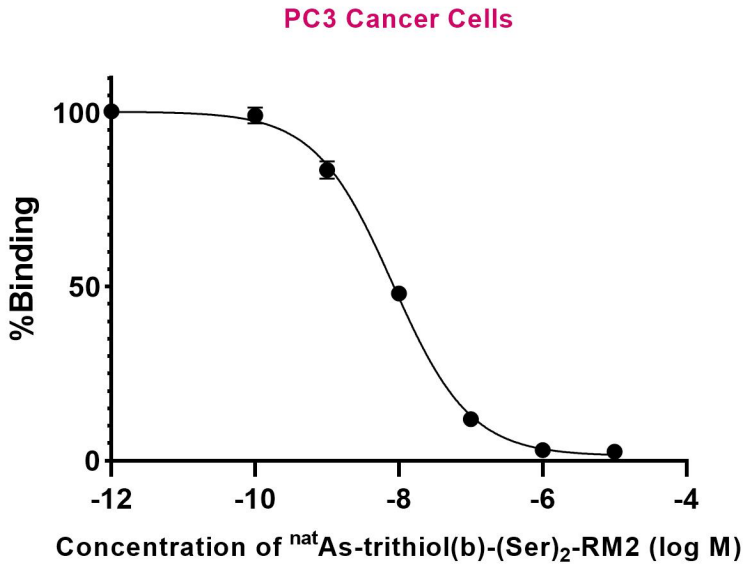

Biodistribution studies of no carrier added [^{77}As] As-trithiol(b)-$(Ser)_2$-RM2 in PC-3 tumor-bearing mice

Pharmacokinetic studies in PC-3 bearing SCID mice is shown in **Table 2.1** By 15 min, the lung uptake of [^{77}As]As-trithiol(b)-$(Ser)_2$-RM2 was 12.6 ± 1.56 %ID/g. Also, excretion of [^{77}As]As-trithiol(b)-$(Ser)_2$-RM2 through the kidneys was only 9.54 ± 0.95 %ID/g with its clearance mainly through the hepatobiliary system (38.9 ± 1.27% ID/g) and the activities in the small intestine and large intestine were 7.61 ± 2.85 and 0.27 ± 0.06 %ID/g, respectively. By 1 h, the liver excretion dropped to 29.8 ± 4.33 %ID and the clearance through the small and large intestines increased to 28.0 ± 3.79 %ID and 0.47 ± 0.39 %ID/g, respectively. The pancreas, tumor#1 and tumor#2 uptake of [^{77}As]As-trithiol(b)-$(Ser)_2$-RM2 were 1.91

± 0.13 %ID/gm, 0.58 ± 0.21 %ID and 0.52 ± 0.05 %ID at 15 min, and 1.86 ± 0.90 %ID /gm 0.87 ± 0.11 and 0.75 ± 0.17 at 1 h. By 4 h, the lung uptake of [^{77}As]As-trithiol(b)-$(Ser)_2$-RM2 decreased to 1.86±0.17%ID/g. Also, excretion of [^{77}As]As-trithiol(b)-$(Ser)_2$-RM2 through the kidneys was 2.18 ± 0.90 %ID/g, with its clearance mainly through liver, small intestine and large intestine by 10.3 ± 0.38, 9.98 ± 2.94 and 52.3 ± 7.37 %ID/g. The pancreas, tumor#1 and tumor#2 uptake of [^{77}As]As-trithiol(b)-$(Ser)_2$-RM2 were 1.91 ± 0.13 %ID/g, 0.58 ± 0.21 and 0.52 ± 0.05 at 4 h versus 0.69 ± 0.09% ID/gm, 0.39 ± 0.10 and 0.41 ± 0.07 at 4 h blocked. Unusual large amount of lung uptake was suggested to be as a result of colloid formation due to the oxidation of excess trithiol and oligomerization of trithiol(b)-$(Ser)_2$-RM2, which is also eluted along with [^{77}As]As-trithiol(b)-$(Ser)_2$-RM2. In some occasions, the colloid was formed during the process of Sep-pack purification. Thus, HPLC purification was suggested to be a better option to reduce the amount of excess trithiol(b)-$(Ser)_2$-RM2 and thus, the formation of colloid (**Table 2.1**).

Table 2.1: Biodistribution studies of no carried added [^{77}As] As-trithiol(b)-(Ser)$_2$-RM2 in PC-3 bearing SCID mice

Organ/Tissue	15 min	1 h	4 h	4 h Blocked	24 h
Heart	2.50±0.38	1.74±0.43	0.39±0.55	1.42±0.17	0.12±0.03
Lung	12.6±1.56	5.07±0.09	1.86±0.17	8.82±4.70	0.16±0.02
Liver	38.9±1.27	29.8±4.33	10.3±0.38	33.0±0.97	2.55±0.25
Kidneys	9.54±0.95	6.26±1.06	2.18±0.90	1.80±1.11	0.16±0.42
Spleen	6.81±1.29	5.59±0.86	4.61±1.57	18.0±6.48	0.73±0.38
Stomach	1.51±0.65	2.38±1.06	0.24±0.06	0.63±0.57	1.93±0.42
S. Intestine	7.61±2.85	28.0±3.79	9.98±2.94	4.18±1.07	0.42±0.14
L. Intestine	0.27±0.06	0.47±0.39	52.3±7.37	25.4±2.87	1.41±0.44
Muscle	0.39±0.02	0.24±0.04	0.22±0.11	0.20±0.11	0.03±0.01
Bone	1.01±0.11	0.71±0.06	0.55±0.05	1.31±0.17	0.26±0.02
Brain	0.24±0.09	0.09±0.02	0.11±0.01	0.11±0.02	0.01±0.01
Pancreas	1.91±0.13	1.86±0.90	0.91±0.32	0.69±0.09	0.02±0.00
Tumor#1	0.58±0.21	0.87±0.11	0.69±0.21	0.39±0.10	0.24±0.04
Tumor#2	0.52±0.05	0.75±0.17	0.69±0.07	0.41±0.07	0.20±0.03
Blood	3.96±2.57	3.86±2.36	0.18±0.08	0.21±0.04	0.02±0.01
Carcass	0.76±0.15	0.47±0.07	0.24±0.05	0.28±0.06	0.04±0.00
Feces					67.9±22.1

Biodistribution studies of nca [^{77}As]As-trithiol(b)-(Ser)$_2$-RM2 in normal mice

Limited biodistribution studies with HPLC purified [^{77}As]As-trithiol(b)-(Ser)$_2$-RM2 were performed in CF-1 mice, with three mice injected at each of two time points (15 min and 1 h). The mice were injected with 0.37 MBq (10 μCi) of [^{77}As]As-trithiol(b)-(Ser)$_2$-RM2; the biodistribution results are tabulated in **Table 2.2**. This somewhat lipophilic compound (log D_7 of 0.7) warranted a limited evaluation in mice for pancreatic uptake and clearance. Excretion was primarily via the hepatobiliary system with liver, small intestine and large intestine activities of 34.6 ± 0.92, 5.28 ± 1.87, and 0.59 ± 0.02% ID/g, respectively, at 15 min and 22.2 ± 0.7, 17.0 ± 3.66, and 5.12 ± 0.15% ID/g, respectively, at 1 h. Pancreatic uptake at 15 min and 1 h were 7.00 ± 0.44 and 7.30 ± 1.4% ID/g, respectively, and are consistent with GRP receptor binding, although no blocking studies were performed. A comparison of selected biodistribution results of [^{77}As]As-trithiol(b)-(Ser)$_2$-RM2 antagonist, our first generation [^{77}As]As-trithiol-BBN(7-14)NH_2 agonist and free [^{77}As]arsenate are shown in **Table 2.3**. Our second generation [^{77}As]As-trithiol(b)-(Ser)$_2$-RM2 exhibits markedly higher pancreatic uptake than our first generation [^{77}As]As-trithiol-BBN(7-14)NH_2 (7.30 ± 1.4 vs. 1.51 ± 0.52% ID/g, respectively, at 1 h) and higher blood uptake (1.80 ± 0.15 vs 0.58 ± 0.21% ID/g, respectively, at 1 h). [^{77}As]As-trithiol(b)-(Ser)$_2$-RM2 showed markedly slower hepatobiliary clearance than our first generation

[^{77}As]As-trithiol-BBN(7-14)NH_2. At the 1 h time point, [^{77}As]As-trithiol(b)-$(Ser)_2$-RM2 showed higher liver uptake than [^{77}As]As-trithiol-BBN(7-14)NH_2 (22.20 ± 0.77 vs. 8.03 ± 1.39% ID/g, respectively) while [^{77}As]As-trithiol-BBN(7-14)NH_2 showed much higher large intestinal uptake (27.12 ± 13.76 vs. 5.12 ± 0.15% ID/g, respectively) and somewhat lower uptake in the small intestines (13.77 ± 8.24% vs. 17.00 ± 3.66% ID/g, respectively) than [^{77}As]As-trithiol(b)-$(Ser)_2$-RM2. The faster hepatobiliary clearance of our first generation [^{77}As]As-trithiol-BBN(7-14)NH_2 may explain its very low pancreatic uptake. Both compounds exhibit very different biodistributions than that of free [^{77}As]arsenate, indicative of *in vivo* stability.

Table 2.2: Biodistribution of [^{77}As] As-trithiol(b)-$(Ser)_2$-RM2 in CF-1 normal mice at 15 min and 1 h post injection. N=3. Data are presented as %ID/g ± SD.

Organ/Tissue	15 min	1 h
Heart	**1.69±0.12**	**1.38±0.12**
Lung	**2.13±0.09**	**1.86±0.11**
Liver	**34.6±0.92**	**22.2±0.77**
Kidneys	**6.02±0.68**	**5.41±0.70**
Spleen	**2.57±0.56**	**1.79±0.16**
Stomach	**2.48±0.11**	**1.75±1.55**

S. Intestine	**5.28±1.87**	**17.0±3.66**
L. Intestine	**0.59±0.02**	**5.12±0.15**
Muscle	**0.73±0.07**	**0.70±0.09**
Bone	**1.58±0.04**	**1.44±0.19**
Pancreas	**7.00±0.44**	**7.30±1.4**
Blood	**4.95±0.33**	**1.80±0.15**

Table 2.3: Biodistribution of [^{77}As] As-trithiol(b)-$(Ser)_2$-RM2 vs. [^{77}As]As-trithiol-BBN(7-14)NH_2 in liver, S. intestine and L. intestine in CF-1 normal mice at 1 h post injection. Data are presented as %ID/g±SD.

	[^{77}As]As-trithiol(b)-$(Ser)_2$-RM2	**[^{77}As]As-trithiol-BBN(7-14)NH_2**	**free [^{77}As]arsenate**
Liver	**22.20 ±0.77**	**8.03 ±1.39**	**3.31 ±0.42**
Small intestine	**17.00 ±3.66**	**13.77 ±8.24**	**1.59 ±0.17**
Large intestine	**5.12 ±0.15**	**27.12 ±13.76**	**1.31 ±0.51**
Pancreas	**7.30 ±1.4**	**1.51 ±0.52**	**1.30 ±0.82**
Blood	**1.80 ±0.15**	**0.58 ±0.21**	**0.52 ±0.19**

Single crystal X-Ray structure

Compound **1** was characterized by single crystal X-ray diffraction analysis (by Dr. Steven Kelley at the university of Missouri-Columbia). The data regarding the crystal structure of the compound are presented in Tables **4.2-9.2**. The molecule crystallized in the monoclinic space group $P2_1/c$ with one unique molecule per asymmetric unit. The molecules were arranged approximately parallel to each other in the crystal lattice and formed layers parallel to the (-3,0,3) family of planes through weak hydrogen bonds between C-H groups and bromine or oxygen atoms. The molecules stacked perpendicular to these planes through electrostatic interactions, typically O or phenyl C atoms stacking above electropositive carbonyl C atoms. The three C-Br distances are (1.9592(19), 1.9538(19) and 1.956(2)) similar to reported C-Br bond distances [51, 52]. The C-C-Br bond angles are (112.59(13), 111.72(13) and 113.92(13)) within the range from reported for similar C-C-Br bond angles. [53]

Figure 2.8: X-Seed representation of (**1**). The molecule crystallizes in the monoclinic space group $P2_1/c$ with one unique molecule per asymmetric unit. The molecules are arranged roughly parallel to each other in the crystal and form layers parallel to the (-3,0,3) family of planes through weak hydrogen bonds between C-H groups and bromine or oxygen atoms. The molecules stack perpendicular to these planes through electrostatic interactions, typically O or phenyl C atoms stacking above electropositive carbonyl C atoms.

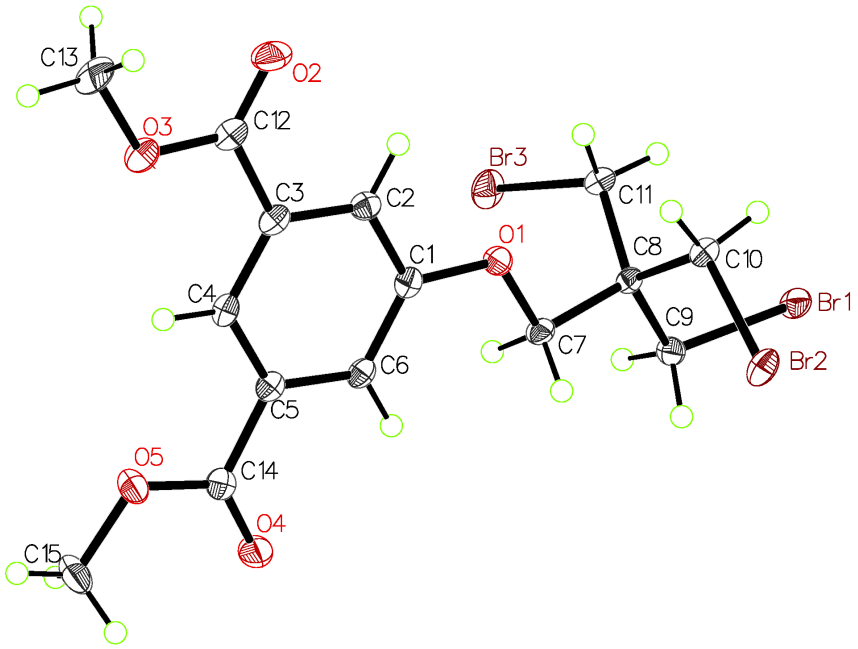

Conclusion and Future Studies

A second generation nca ^{77}As trithiol bioconjugate, namely [^{77}As]As-trithiol(b)-$(Ser)_2$-RM2, was synthesized, characterized and compared to our previously reported [^{77}As]As-trithiol-BBN(7-14)NH_2 complex. [37] [^{77}As]As-trithiol(b)-$(Ser)_2$-RM2 was found to be stable *in vivo* and *in vitro*, and is more hydrophilic than our first generation complex based on HPLC retention time. [^{77}As]As-trithiol(b)-$(Ser)_2$-RM2 was synthesized

with >95% radiochemical yield and purified by RP-HPLC. The 10 ± 2 nM IC_{50} value and limited normal mouse biodistribution studies of [^{77}As]As-trithiol(b)-$(Ser)_2$-RM2 showing markedly higher pancreatic uptake compared to our previously reported complex (7.30 ± 1.4 vs 1.51 ± 0.52 %ID/g) are very positive. Although these results are promising, development of a hydrophilic trithiol ligand with decreased hepatobiliary excretion is underway.

Chapter 3: Development and Synthesis of Trithiolated Herceptin and Radiolabeling with Arsenic Radioisotopes for Diagnosis and Treatment of Her2-positive Breast Cancer Tumors

Introduction

Tumor-targeted antibody therapy is one of the approaches for cancer therapy. Antibody-drug conjugates (ADCs), which are the drugs made by combining monoclonal antibodies with high cytotoxicity chemotherapeutic drugs, have been successfully utilized in clinical cancer therapy. [54] Human epidermal growth factor receptor 2 (Her2) is overexpressed in some tumor types including 20-25% of invasive breast cancers. Her2 has turned out to be an important target in breast cancer treatment since Her2 levels associate strongly with the pathogenesis and prognosis of breast cancer. Also, Her2 level in human cancer cells with gene intensification is a lot higher than normal tissues, which theoretically reduces the toxicity of Her2-targeting therapeutic agents. In addition, Her2 is present in a very high percentage of tumor cells. Since Her2 overexpression is found both in the primary and metastatic tumors, it would suggest that Her2 therapy might be effective in all diseases sites. [55] Herceptin, as known as Trastuzumab, is an IgG1 kappa-containing human framework region with the complementarity-determining regions of a

murine anti-p185 Her2 antibody. This antibody consists of 1,328 amino acids and has a molecular weight of ~148 kDa. Treatment with Herceptin has anti-angiogenesis effects on the Her2 positive breast cancer tumors regardless of their size and reduces the diameter and volume of tumor blood vessels compared with the diameter and volume of tumors that are treated with a control antibody. [56] Her2 initiates multiple cellular signaling pathways. Trastuzumab diminishes signaling from these signaling pathways by Herceptin-mediated internalization and degradation of Her2 receptors, which leads to stimulating cell cycle arrest and apoptosis. [55] Radiolabeling monoclonal antibodies with a vast range of radionuclides (mAbs) have being studied for the purpose of clinical diagnosis and therapy. The idea of labeling monoclonal antibodies with radioactive arsenic isotopes for the purpose of molecular imaging have been processed and examined in the past. As mentioned above, arsenic is thiophilic. Therefore, to increase the sulfur sites for binding, the mAbs that are subject for labeling with radioarsenic isotopes are usually modified with *N*-succinimidyl S-acetylthioacetate (SATA) [3, 30, 31] **Figure 3.1** shows the radiolabeling process of a SATA-modified antibody with $[^{74/77}As]AsI_3$.The results showed the feasibility of using arsenic radioisotopes for labeling monoclonal antibodies.

Figure 3.1 Radiolabeling SATA modified antibodies with radioarsenics. [30]

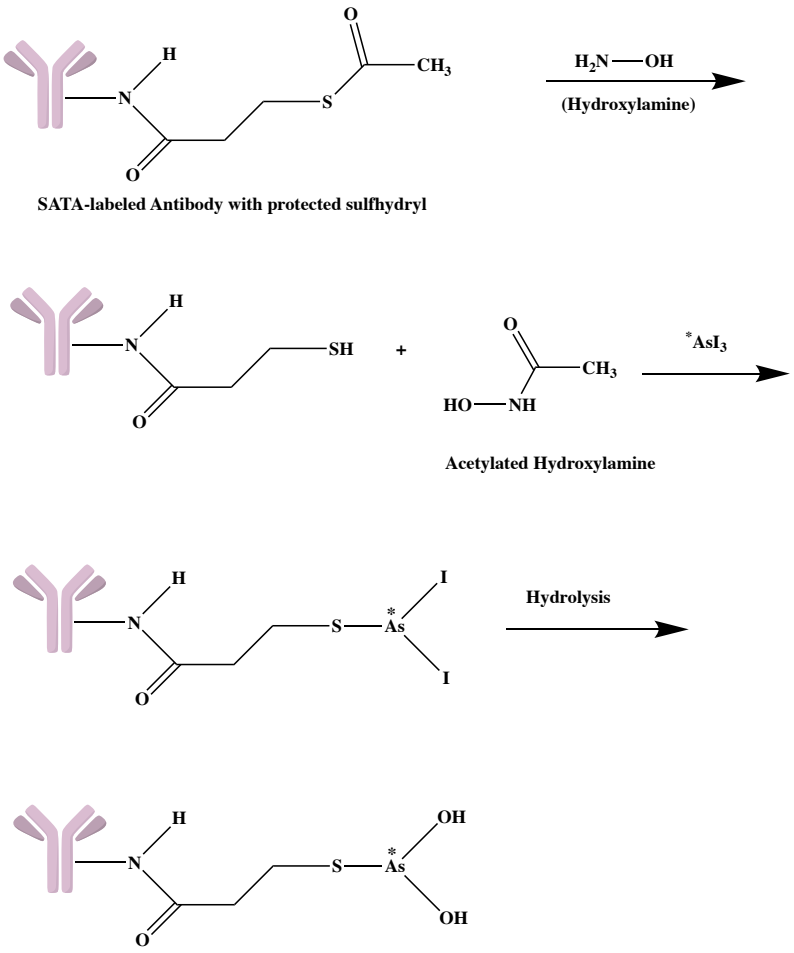

Bifunctional chelating agents (BFCAs) have been developed to facilitate a covalent bond between a radiometal chelate to mAbs for the purpose of higher *in vivo* stability of the radiometal chelate followed by reducing the amount of free radiometal uptake in normal and non-targeted tissue. [1] Using thiol-based chelators to develop BFCAs is prevalent in radioarsenic studies. Therefore, herein, we report a method for conjugation of a new trithiol ligand to Herceptin. The method included preparing amine-reactive esters of a carboxylate group on a trithiol ligand with *N*-hydroxysuccinimide (NHS) and 1-ethyl-3-(3-

dimethylaminopropyl)carbodiimide (EDC) resulting in a NHS-active ester trithiol. A previously reported simple method for conjugation of monoclonal antibodies with NHS-active ester trithiols in aqueous solution [2, 3, 57] was utilized to achieve a conjugated trithiol-Herceptin compound. [4-6] [31] Radiolabeling of a conjugated Herceptin with [^{77}As]As(SR)$_3$ is reported.

Experimental

Materials

N-hydroxysuccinimide (NHS), 4-dimethylaminopyridine (DMAP), 1-ethyl-3-(3-dimethylaminopropyl)carbodiimide (EDC), tris(2-carboxyethyl)phosphine (TCEP), sodium sulfate, sodium azide, sodium phosphate dibasic heptahydrate, sodium phosphate monobasic anhydrous, ammonium acetate, ammonium hydroxide solution (30% NH_3 in H_2O), thioglycolic acid, silica gel 60Å, Standard Protein Mix 15-600 kDa, and PBS pH 7.4 (1X) were purchased from Fisher Scientific or Sigma-Aldrich. Herceptin was obtained from the Siteman Cancer Center pharmacy. Silica gel w/UV 254 TLC plates were purchased from Sorbent Technologies. Zeba Spin Desalting columns 7k MWCO were purchased from Thermo Scientific. Amicon Ultra-0.5 mL Centrifugal Filters were purchased from Millipore Sigma. All solvents and reagent grade acids and bases were purchased from Fisher Scientific or Sigma-Aldrich and used without further purification. DI water and18 MΩ were used during the

experiments. Arsenic-77 was prepared by irradiation of 3-5 mg of enriched $^{76}GeO_2$ (98.6%; Trace Sciences International) in a thermal neutron flux of 2.4 x 10^{14} n/cm^2-s at the University of Missouri Research Reactor (MURR). [^{77}As]arsenate ([^{77}As]$H_2AsO_4^-$) was prepared as previously reported [37] [23].

Physical Measurements

^{1}H and ^{13}C NMR spectra were obtained in $CDCl_2$, $CDCl_3$ or DMSO on a Bruker ARX-500 or 600 MHz spectrometer using TMS as an internal standard. An ORTEC HPGe detector equipped with Genie multichannel analysis software was used to evaluate ^{77}Ge and ^{77}As liquid samples. Reversed phase HPLC (RP-HPLC) was performed using a Shimadzu Prominence HPLC system equipped with a pump, controller, and Prominence UV-Vis detector (model SPD20-AV) and Phenomenex Jupiter C18 (5 μm, 150 mm x 4.6 mm) column. The linear gradient was as follows: 30 to 60% ACN/H_2O w/ 0.1% TFA over 30 min, then from 60 to 90% ACN/H_2O over 3 min, followed by returning to 30% ACN/H_2O over 3 min (flow rate 1 mL/min). Size exclusion HPLC was performed using a size-exclusion TSKgel (model SuperSW3000) column (4 μm, 4.6 mm ID x 30cm) and guard column for monitoring trithiol-antibody conjugation and the radiolabeling process. The conditions were as follows: 0.35 mL/min isocratic flow; Eluent: 0.1 M Na_2SO_4 and 0.05% NaN_3 in 0.1 M phosphate buffer (pH 6.7). An Eppendorf Thermomixer equipped with 1.5

mL tube holder was used for mixing. An Eckert & Ziegler AR-2000 Bioscan was used for radio-TLC measurements.

Synthesis

Scheme 3.1: 5-(3-(tritylthio)-2,2-bis((tritylthio)methyl)propoxy)isophthalic acid, $C_{70}H_{58}O_5S_3$ (2-3).

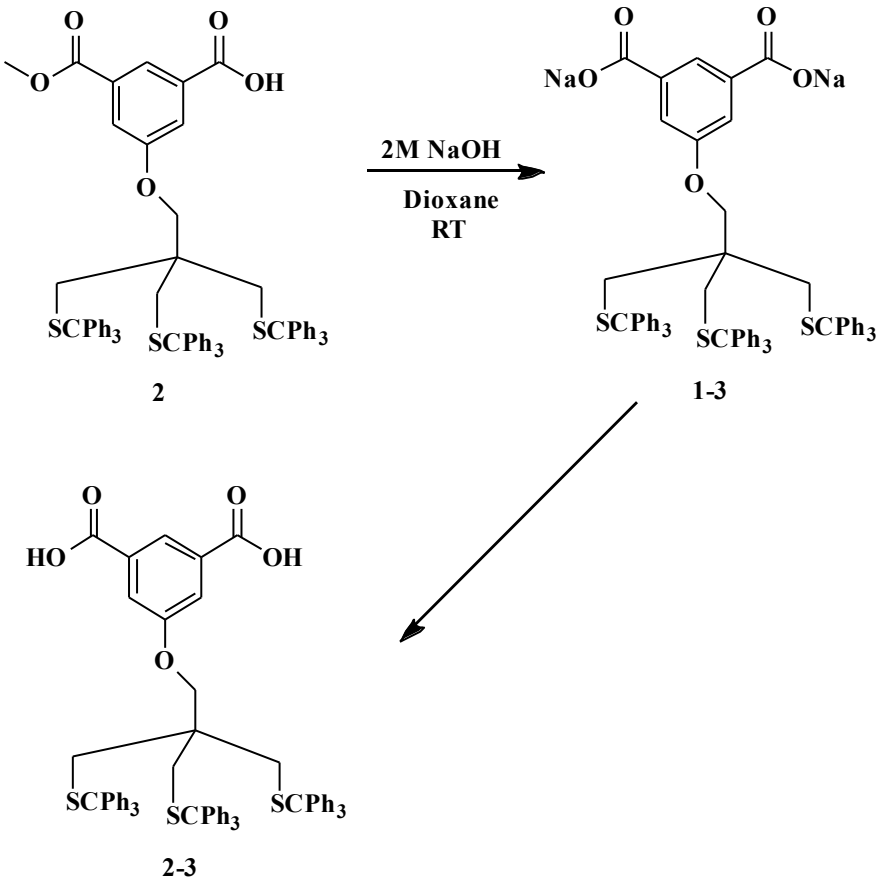

5-(3-(tritylthio)-2,2-bis((tritylthio)methyl)propoxy)isophthalic acid, $C_{70}H_{58}O_5S_3$ (2-3).

Compound **2** (200 mg, 0.184 mmol) was dissolved in dioxane (10 mL) under a N_2 atmosphere in a 100 mL round bottom flask. NaOH solution (2M, 5 mL) was added into the reaction mixture and stirred at room temperature for 24 h. The reaction mixture was taken to dryness to yield the white product **(1-3)**. The product was dissolved in 15 mL ethyl acetate and transferred into a separatory funnel. The product then washed with 15 mL of DI water and adding 0.1 M HCl until achieving a pH of 7 to yield the product **(2-3)**. The organic layer was washed with DI water (3 x 10 mL) and dried over anhydrous sodium sulfate. The organic layer was then filtered and taken to dryness to bear a white solid **(2-3).**Yield: 85%, 168 g. ^{1}H NMR (CD_2Cl_2; 600 MHz) δ ppm: 2.194 (s, 6H, C**H**$_2$SCPh$_3$), 3.550 (s, 2H, C**H**$_2$O), 7.177-7.215 (m, 9H, **l**), 7.218-7.320 (m, 18H, **j**), 7.382-7.526 (m, 21H, **k, p, q**), 8.337 (s, 2H, COO**H**). ^{13}C-NMR (600 MHz, CD_2Cl_2, δ (ppm)): 30.99 (-**C**-CH$_2$-S-), 36.71 (-**C**H$_2$-S-), 66.71 (-O**C**H$_2$-C-CH$_2$-S-),127.04 (**l**), 127.61 (**j**), 128.21 (**k**), 130.01 (**i**), 144.95 (**C**OOH). ESI-MS (*m/z*): 1119.94 (1119.31 calc'd for $[C_{70}H_{57}Na_2O_5S_3]^+$ $[M+H]^+$+2 Na^+) (**Figures 3.2, 3.3**).

Scheme 3.2: Synthesis of 5-(3-mercapto-2,2-bis(mercaptomethyl)propoxy)isophthalic acid ,$C_{13}H_{16}O_5S_3$ (3-3).

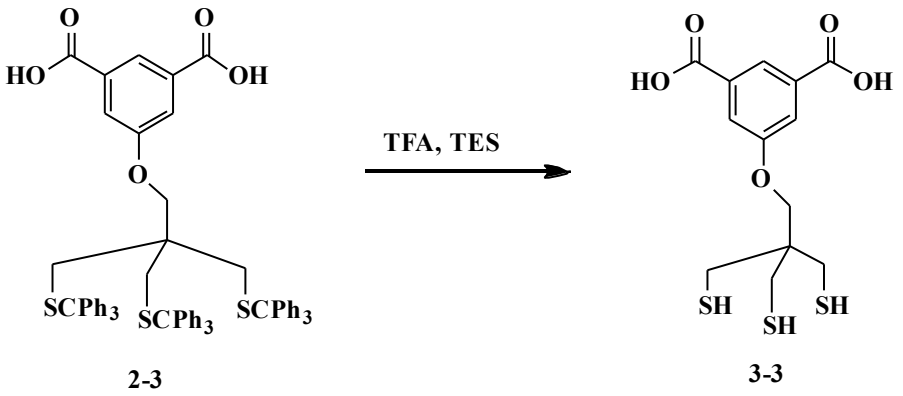

2-3 3-3

Synthesis of 5-(3-mercapto-2,2-bis(mercaptomethyl)propoxy)isophthalic acid ,$C_{13}H_{16}O_5S_3$ (3-3).

Compound **2-3** (200 mg, 0.186 mmol) was deprotected with trifluoroacetic acid (14.1 mL, 179.5 mmol) in the presence of triethylsilane (0.74 mL, 4.6 mmol). The product was washed with hexane (3×20 mL) to extract impurities into hexane. The product was dried in vacuum and under N_2 flow to yield compound **3-3**. ESI-MS (*m/z*): 349.45 (349.03 calc'd for $[C_{13}H_{17}NO_5S_3]^+$ $[M+H]^+$).

Single crystal X-ray diffraction analysis of compound 3-3

Single-crystal X-ray diffraction (XRS) data for compound **3-3** were collected on a Bruker X8 Prospector diffractometer (Bruker-AXS, Inc., Madison, WI, USA) using Cu-Kα radiation (λ = 1.54178) from a microfocus source (by Dr. Steven Kelley at the university of Missouri-

columbia). The crystal was cooled to 100 K during collection using a Cryostream 700 cryostat (Oxford Cryosystems, Oxford, UK). A hemisphere of data was collected out to a resolution of at least 0.81 Å using strategies of scans about the phi and omega axes. Unit cell determination, data reduction, absorption correction, and scaling were performed using the Bruker Apex3 software suite. [59] The crystal structure was solved by direct methods [60] and refined by full-matrix least squares refinement using SHELXL [45] implemented via Olex2 [46]. Non-hydrogen atoms were located from the difference map and refined anisotropically. Hydrogen atoms were placed in calculated positions, and their coordinates and thermal parameters were constrained to ride on the carrier atoms (**Figure 3.12**, **Table 3.1-3.6**).

Figure 3.12: X-Seed representation of 5-(3-mercapto-2,2-bis(mercaptomethyl)propoxy)isophthalic acid (**3-3**). 50% probability ellipsoid plot of formula unit. Unlabeled atoms are symmetry equivalents of labeled ones for compound **3-3**.

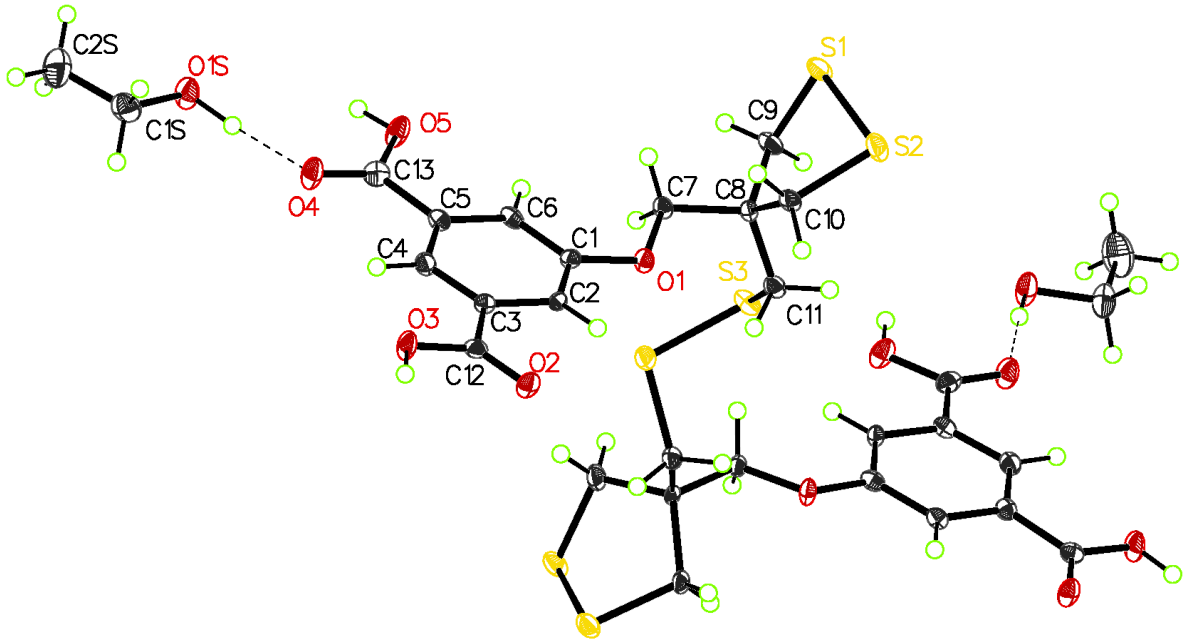

Scheme 3.3: 3-(((2,5-dioxopyrrolidin-1-yl)oxy)carbonyl)-5-(3-(tritylthio)-2,2-bis((tritylthio)methyl)propoxy)benzoic acid, $C_{74}H_{61}NO_7S_3$ (4-3).

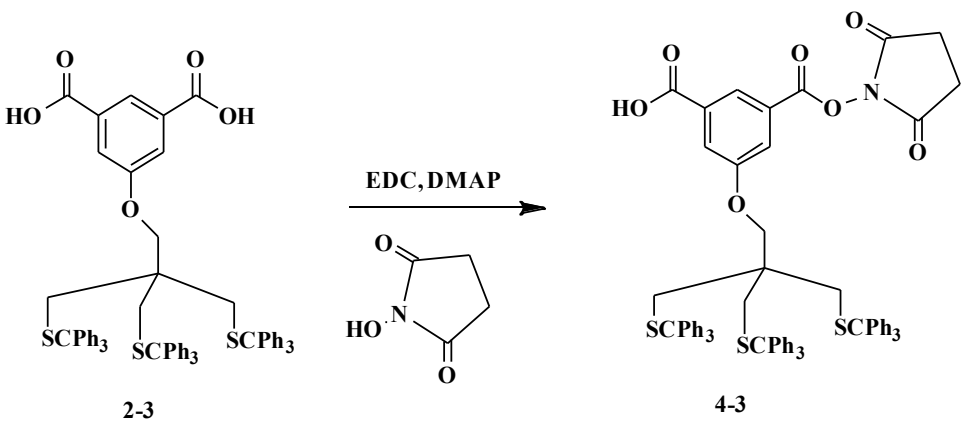

2-3 **4-3**

3-(((2,5-dioxopyrrolidin-1-yl)oxy)carbonyl)-5-(3-(tritylthio)-2,2-bis((tritylthio)methyl)propoxy)benzoic acid, $C_{74}H_{61}NO_7S_3$ (4-3).

Compound **2-3** (1.5 eq., 150 mg, 0.140 mmol) was dissolved in ethyl acetate (14 mL) under a N_2 atmosphere in a 100 mL round bottom flask. 1-ethyl-3-(3-dimethylaminopropyl)carbodiimide (EDC) (1 eq., 0.093 mmol, 17.8 mg) and 4-dimethylaminopyridine (DMAP) (1 eq., 0.093 mmol, 11.4 mg) were added into the reaction mixture and stirred at room temperature for 30 min. *N*-Hydroxysuccinimide (NHS) (1 eq., 0.093 mmol, 10.7 mg) was added to the reaction mixture and stirred at room temperature for 24 h. The reaction mixture was taken to dryness to yield the crude product. The crude product was purified with silica gel column chromatography (1 cm X 30 cm, 10 mg) using DCM as the mobile phase and then increased the polarity from 1:10 to 1:1 ethyl acetate: DCM based on silica gel TLC (1:10 ethyl acetate: DCM, **3-3**, $R_f \approx 0.3$). The column was eluted, and the product was collected based on the silica gel TLC to give a white solid. Yield: 46%, 50 mg. ^{1}H NMR (CD_2Cl_2; 600 MHz) δ

ppm: 1.217-1.263 (m, 4H, N-CO-C**H**$_2$-), 2.185 (s, 6H, C**H**$_2$SCPh$_3$), 3.531 (s, 2H, C**H**$_2$O), 7.177-7.215 (m, 9H, **l**), 7.171-7.321 (m, 18H, **j**), 7.374-7.564 (m, 21H, **k, p, q**), 8.366 (s, 2H, COO**H**). ^{13}C-NMR (600 MHz, CD_2Cl_2, δ (ppm)): 25.76 (**C**-CH$_2$-S), 36.21 (N-CO-**C**H$_2$), 42.44 (-**C**H$_2$S), 66.71 (**C**H$_2$-C-**C**H$_2$-S-), 126.63 (**l**), 127.80 (**j**), 128.21 (**k**), 129.58 (**i**), 144.92 (**C**OOH). ESI-MS (*m/z*): 1194.48 (1193.34 calc'd for $[C_{74}H_{60}NNaO_7S_3]^+$ $[M+H]^{+}$+ Na^+) (**Figures 3.4-3.6**).

Scheme 3.4: 3-(((2,5-dioxopyrrolidin-1-yl)oxy)carbonyl)-5-(3-mercapto-2,2-bis(mercaptomethyl)propoxy)benzoic acid, $C_{17}H_{19}NO_7S_3$ (**5-3**).

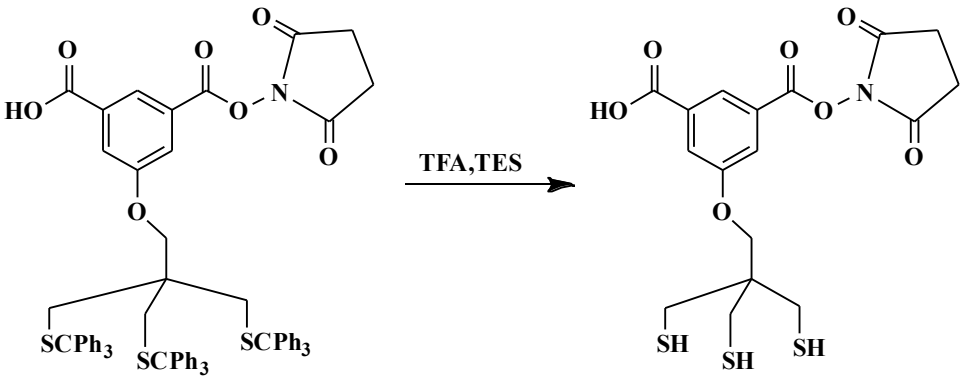

4-3 **5-3**

3-(((2,5-dioxopyrrolidin-1-yl)oxy)carbonyl)-5-(3-mercapto-2,2-bis(mercaptomethyl)propoxy)benzoic acid, $C_{17}H_{19}NO_7S_3$ (5-3)

(deprotection of trityl-protected active ester, 4-3).

Compound **4-3** (30 mg, 0.0256 mmol) was deprotected with trifluoroacetic acid (1.95 mL, 24.7 mmol) in the presence of triethylsilane (0.102 mL, 0.64 mmol). The product was washed with hexane (3×5 mL) to extract

impurities into hexane. The product was dried in vacuum and under N_2 flow to yield compound **5-3.** An aliquot of the mixture (10 μL) was was injected into the HPLC and eluted with phosphate buffer solution (eluent: 0.1 M Na_2SO_4 and 0.05% NaN_3 in 0.1 M phosphate buffer (pH 6.7); 0.35 mL/min isocratic flow) to determine the retention time of compound **5-3** on a size exclusion Tosoh column (**Scheme 3.4**, **Figure 3.11a**). Compound **5-3** was then stored under N_2 flow until performing the following step. ESI-MS (*m/z*): 443.71 (444.03 calc'd for $\mathbf{C_{17}H_{19}NO_7S_3}$ $[M+H]^+$) (**Figure 3.7**).

Quality control of Herceptin

Protein standard

A commercial "Standard Protein Mix 15-600 kDa" containing thyroglobulin (0.5 g/L), γ-globulin (1 g/L), Ovalbumin (1 g/L), ribonuclease A (1.5 g/L), *p*-aminobenzoic acid (0.01 g/L) was dissolved in 20 μL of ultra-pure water and was vortexed. The mixture (10 μL) was was injected into the HPLC and eluted with phosphate buffer solution (eluent: 0.1 M Na_2SO_4 and 0.05% NaN_3 in 0.1 M phosphate buffer (pH 6.7); 0.35 mL/min isocratic flow) to determine the retention time of Herceptin on a size exclusion Tosoh column (**Figure 3.8**).

Native Trastuzumab (Herceptin)

Herceptin solution (10 μL, 0.0146 μmol) was injected into the HPLC to determine the retention time of Herceptin with size exclusion Tosoh

column and eluted with phosphate buffer solution (eluent: 0.1 M Na_2SO_4 and 0.05% NaN_3 in 0.1 M phosphate buffer (pH 6.7); 0.35 mL/min isocratic flow) to determine the retention time of Herceptin with size exclusion Tosoh column and compare it with the retention time of protein (**Figure 3.9**).

Scheme 3.5: Synthesis of Compound 6-3 by conjugation of Herceptin to purified NHS-Trithiol.

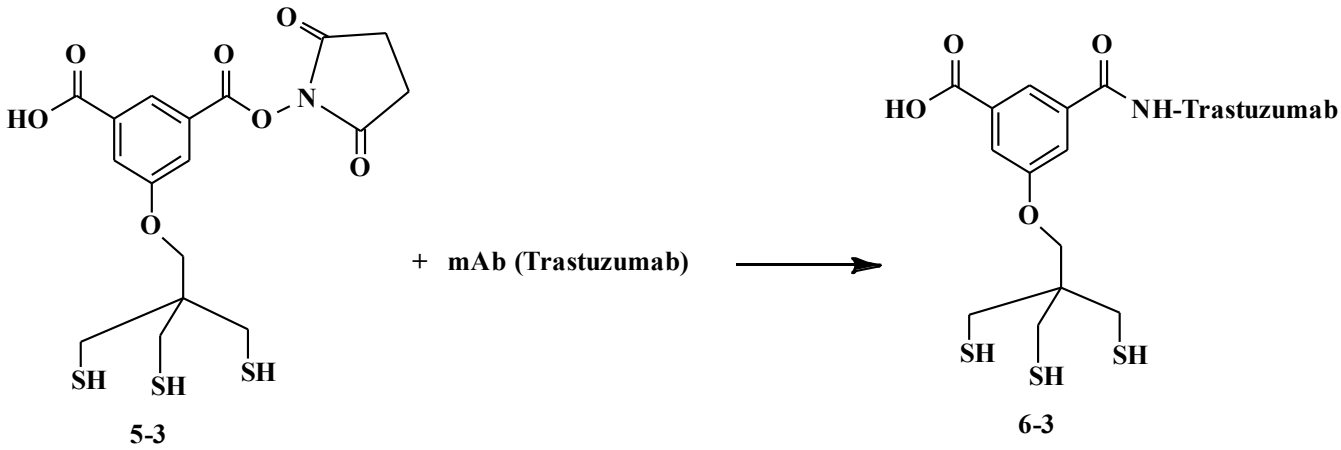

Conjugation of Herceptin to purified NHS-Trithiol

A solution of compound **5-3** (2 mg, 4×10^{-3} mmol) in 1 mL of PBS was prepared. TCEP (0.285 mg, 1 mmol) was added to the solution to reach 1 mM TCEP concentration. The pH of solution was adjusted to 6. 100 µL of the solution containing 0.4 µmol of compound **5-3** were transferred into an Eppendorf vial and 10 µL (0.00142 µmol) of an original Herceptin solution in PBS (24 µL, 0.0035 µmol) was added into the same Eppendorf vial. The reaction was incubateded at 37 ºC in the thermomixer for 45 min.

The reaction was later cooled down to the room temperature. 5 µL of the reaction mixture was injected to the HPLC to monitor the retention time and quality compared to the native Herceptin with Tosch size exclusion column (**Figures 3.9, 3.10**). The remaining reaction was purified with a Zeba Spin 7k column and concentrated down to 40 µL with na Amicon Ultra Centifuge filter. An aliquoat (20 µL) of the final concentrated reaction mixture was submitted for high resolution mass spectroscopy analysis (**Figure 3.11**).

High resolution mass spectroscopy analysis of conjugated Herceptin-Trithiol

A high resolution mass spectroscopy run on a C8 protein column with the following parameters was used: acquired mass range 295-3200 m/z; 0.63 spectra/second; fragmentor at 350V. The gradient was as follows: initial conditions (for trap load) was 3% B for 4 min (A: 0.1% formic acid in water; B: 99.9% acetonitrile, 0.1% formic acid); A rapid ramp to 90% B over 6 min; hold at 90% B for 15 min; ramp back to initial conditions over 1 min and hold at 3% B for 4 min prior to loading the next sample. A total run time was 30 min. A 1200 series LC is attached to an Agilent Technologies 6520A Quadrupole Time-of-Flight (Q-TOF). Samples (1µL) were loaded in sequence as follows: blank (5% acetonitrile 0.1% formic acid), sample; blank. Data were then examined using the qualitative analysis software provided with the instrument. The maximum entropy algorithm was used to deconvolute multi-charge-state peaks to intact

protein mass using the following parameters: mass: 5000 to 100000 Da or 135000 to 155000Da; mass step: 1Da; m/z range restricted: 1000-3000; baseline subtraction factor: 7; peak s:n of 30; 25% peak height for mass averaging; minimum charge state required for averaging: 5; iterations: 30 (**Figure 3.11**).

Radiolabeling Herceptin-Trithiol conjugated with ^{77}As

No carried added (nca) $^{77}As[^{77}As]H_2AsO_4^-$, (222 MBq/mL (6 mCi/mL)) in aqueous solution was isolated using a previously reported method. $^{77}As[^{77}As]H_2AsO_4^-$ (200 µL, 44 MBq (1.2 mCi)) was added to a 2 mL Eppendorf tube containing 100 µL of PBS. Ammonium acetate (18.2 µL, 5.5 M, 100 µmol) was added to the reaction mixture and placed in a 55 °C thermomixer and stirred for 45 min. A sample of conjugate (**5-3**) (20 µL, 0.00175 µmol) was disolved in 50 µL 1 M ammonium acetate (NH_4OAc) and added to the arsenic reaction mixture. The pH of the final reaction mixture was ≈6. The reaction was placed in a 37 °C thermomixer and stirred for 1 h. The reaction was then cooled down to the room temperature and centrifuged. 10 µL of the reaction mixture was injected into the HPLC filled with a Tosch size exclusiom column (**Figure 3.13**).

Results and Discussion

Previous trithiol chelates synthesized for the purpose of theranostic $^{72/77}$As radiopharmaceuticals showed high *in vivo* stability but were too lipophilic for *in vivo* applications based on biodistribution results. A second

generation linkable trithiol ligand (trityl protected) was synthesized and conjugated to Herceptin. Treatment with Herceptin has anti-angiogenesis effects on the Her2 positive breast cancer tumors regardless of their size and reduces the diameter and volume of tumor blood vessels compared with diameter and volume of tumors which are treated with a control antibody. [4-6] The Herceptin and trithiol ligand conjugation method included preparing amine-reactive esters of the carboxylate group on the trithiol ligand with NHS resulting in a NHS-active ester trithiol with high stability. A previously reported simple method for conjugation of monoclonal antibodies with NHS-trithiol active esters in aqueous solution was utilized to achieve conjugated trithiol-Herceptin compound. [2, 3, 57] Radiolabeling attempts of a conjugated Herceptin with [^{77}As]AsSR are performed.

Ligand and bifunctional chelator synthesis

Synthesis of 3-(methoxycarbonyl)-5-(3-(tritylthio)-2,2-bis((tritylthio)methyl)propoxy)benzoic acid, **2**, was reported in Chapter **2**. Compound **1-3** was dissolved in dioxane under a N_2 atmosphere. Aqueous NaOH solution (2 M) was added into the reaction mixture and stirred at room temperature for 24 h and brought to dryness to yield the white product **(1-3)**. The product was dissolved in ethyl acetate and neutralized with a 0.1 M HCl to yield a white solid (compound **2-3)** in 85% yield. Compounds **1-3** and **2-3** were characterized by ^{1}H and ^{13}C NMR

spectroscopy and LC-MS-MS. The molecular ions for compounds **1-3** and **2-3** were observed in the LC-ESI--MS spectra at the calculated *m/z* values. Compound **2-3** was deprotected with TFA in the presence of TES. The product was washed with hexane to extract impurities including deprotection by-products such as $CHPh_3$. The product was dried in vacuum and under N_2 flow to yield compound **3-3**. Compounds **3-3** was characterized LC-ESI-MS. The molecular ion for compound **3-3** was observed in the LC-ESI-MS spectra at the calculated *m/z* value. Compound **3-3** was also characterized by single crystal X-ray diffraction analysis. Its X-Seed representation is shown in **Figure 3.12.** The data regarding the crystal structure of the compound are presented in **Tables 3.1-3.6**. The crystal structure contained a molecule composed of two of the expected molecules linked by a single disulfide bond. The molecule crystallized in the monoclinic space group *C*2/*c* with half of a formula unit per asymmetric unit. The molecule also crystallized with two ethanol molecules per formula unit. The molecule resided on a crystallographic inversion center and packed by forming infinite layers parallel to the *ab* plane that are held together in one direction by strong hydrogen bonds between the carboxylic acid and ethanol molecules and in the other direction by interdigitation of the disulfide portions of the molecule.

EDC/NHS crosslinking of carboxylates with primary amines

NHS and EDC were used to prepare an amine-reactive ester with preferential activation of one carboxy group of trithiol ligand (**Scheme**

3.3). An excess amount of the trithiol ligand (compound **2-3**) compared with NHS and EDC was used to prevent activating both carboxylic acids on the ligand and converting them to the NHS esters. Compound **2-3** was dissolved in ethyl acetate under a N_2 atmosphere followed by adding EDC, DMAP and NHS into the reaction mixture and stirring at room temperature for 24 h. The reaction mixture was taken to dryness to yield a white solid. The crude product was purified with silica gel column chromatography and compound **4-3** was isolated in 46% yield and characterized by LC-ESI-MS, HPLC, ^{1}H NMR and ^{13}C NMR (**Figures 3.4-3.6**). Unlike previously reported NHS esters, [2, 57, 58] compound **4-3** showed high stability at room temperature for approximately a year.

Quality control of Herceptin

A "Standard Protein Mix 15-600 kDa" containing thyroglobulin, γ-globulin, ovalbumin, ribonuclease A, and *p*-aminobenzoic acid was injected into the HPLC and eluted with phosphate buffer solution to determine the retention time of Herceptin with a size exclusion Tosoh column. The closest molecular weight in this protein standard is γ-globulin with 155 kDa (8.9 min). The chromatogram was consistent with the Tosoh Bioscience's TSKgel inspection data (**Figure 3.8).** The Herceptin solution was also injected into the HPLC to determine its retention time of Herceptin on the size exclusion column and eluted with phosphate buffer solution.The chromatogram of γ-globulin from protein standard (**Figure 3.8**) and Herceptin were very close (9 min and 8.950 min, respectively)

(**Figure 3.9**), which could be considered as a reliable characterization method for conjugation and radiolabeling experiments.

Deprotection of trityl protected active ester (4-3)

Trityl groups of compound **4-3** were removed by TFA in the presence of TES (as the scavenger for trityl groups) to afford compound **5-3**. An aliquot of the mixture (10 μL) was injected into the HPLC and eluted with phosphate buffer solution. The retention time of compound **5-3** was determined to be 14.2 min. (**Scheme 3.4**, **Figure 3.13a).**

Conjugation of Herceptin to purified NHS-Trithiol and LC-MS analysis of conjugated Herceptin-Trithiol

A solution of compound **5-3** in PBS with TCEP was prepared and the pH of solution was adjusted to 6. Herceptin solution in PBS was added into the reaction mixture. The reaction was incubated at 37 ºC for 45 min. The reaction mixture was then injected in the HPLC to monitor the retention time and quality compated to the native Herceptin using Tosch size exclusion column (**Figure 3.10**). The remaining reaction was purified with Zeba Spin 7k column and concentrated with na Amicon Ultra Centifuge filter. An aliquoat of the final concentrated reaction mixture was submitted for mass spectroscopy analysis. Mass spectroscopy results showed that the

most abundant proteins identified were 148066.3, 148226.7 and 148388Da, with ~161 Da mass differences, which are different from the mass of Herceptin (145531.5), which indicates the conjugation of 7-8 trithiol ligands to the antibody and formation of compound **6-3** (**Figures 3.9-3.11**).

Radiolabeling Herceptin-Trithiol conjugated with ^{77}As

No carrier added ^{77}As was isolated in oxidation state +5 as arsenate during the separation from the neutron irradiated $^{76}GeO_2$ target. The first step of radiolabeling involves simultaneous reduction of ^{77}[As]arsenate to the +3 oxidation state and complexation with mercaptoacetate (SR) to generate ^{77}[As]As(SR)$_3$. Ammonium acetate (NH_4OAc) and added to the ^{77}[As]As(SR)$_3$ mixture. The pH of the final reaction mixture was ≈6. The Herceptin-trithiol conjugate (**6-3**) was then added to ^{77}[As]As(SR)$_3$. The reaction was placed in a 37 °C thermomixer and stirred for 1 h. The reaction mixture was then centrifuged and an aliquot of the supernatant was injected into the HPLC with Tosch size exclusiom column and eluted with the PBS buffer mixture (see experimental). According to the chromatogram (**Figure 3.13b**), The Herceptin-trithiol has been denatured and broke down showing a peak that has the same retention time as compound **5-3** (**Figure 3.13a**), which showed the radiolabeling of the free trithiol ligand after dissociation from Herceptin. This could be due to the presence of excess mercaptoacetate in the ^{77}[As]As(SR)$_3$ solution. Since the retention time of ^{77}[As]As(SR)$_3$ and mercaptoacetate in the RP-HPLC

are very close, it is not possible to separate them by HPLC purification. Also, other purification techniques such as Sep-pack columns are not applicable in this case since the polarity of ^{77}[As]As(SR)$_3$ and mercaptoacetate are very similar.

Conclusion and Future Work

The trithiol-NHS active ester (compound **5-3**) was successfully synthesized using a crosslinking method and characterized by NMR and LC-MS. This active ester showed high stability at the room temperature and -12 °C for a approximately three months and over a year, respectively. The conjugation of the new trithiol ligand to Herceptin in aqueous solution was successful. High-resolution LC-mass spectroscopy indicated the conjugation of at least 7 trithiol chelators to one Herceptin molecule. Herceptin-trithiol (**6-3**) radiolabeling attempts with ^{77}[As]As(SR)$_3$ were performed *in situ* reaction after simultaneous reduction of ^{77}[As]arsenate to the +3 oxidation state and complexation with mercaptoacetate (SR) to generate ^{77}[As]As(SR)$_3$, which led to the denaturing of the antibody. We are assuming that the presence of excess mercaptoacetate may have caused the dissociation of antibody (Herceptin) through the reduction of disulfide bonds in the antibody. The future work will focus on utilizing other reduction techniques such as using cysteine instead of mercaptoacetate followed by radiolabeling of the Herceptin-trithiol conjugate using ^{77}[As]As(III).

Chapter 4: Synthesis and Evaluation of Monoamine Monoamide Dithiol (MAMA) Based Bifunctional Chelators and Their ^{186}Re Radiolabeled Compounds

Introduction

Rhenium is a group (VII) transition metal and is in the same group as Tc. Rhenium has various oxidation states ranging from -1 to +7. Preparation of the +5 oxidation state of Re is relatively easy since Re(V) complexes are normally prepared by the reduction of $^{186}ReO_4^-$. As mentioned in the Introduction, technetium-99m is widely used as a diagnostic radionuclide in SPECT imaging. Due to the chemical behavior similarity of Re and Tc, ^{99}Tc chelating knowledge could be applicable for ^{186}Re and ^{188}Re which could potentially be the therapeutic counterpart of ^{99m}Tc. However, there are some differences in the substitution kinetics and redox chemistry, thus Re and Tc complexes can show different coordination geometries as a result of difference in the substitution kinetics. [15] Re(V) complexes are commonly square pyramidal. Tetradentate N_4S_{4-x} ligands and their Tc(V) and Re(V) complexes have been broadly developed and studies. N_XS_{4-X}

chelators contains bis(aminethiols) (BAT), diamid- edithiols, monoamine-monoamide dithiols (MAMA), and mercaptoacetyltriglycines (MAG3). MAMA ligands and Tc(V) and Re(V) oxo cores ($[Tc=O]^{3+}$ and $[Re=O]^{3+}$) form stable, lipophilic and neutral complexes. [21] Some recent research has focused on studying and developing N_2S_2 MAMA ligand-based bifunctional chelating agents with $^{186/188}Re$ and their conjugation to a targeting vector through amine functionalization. Bombesin (BBN) is a peptide containing 14 amino acids and an amphibian analogue of the mammalian counterpart gastrin-releasing peptide (GRP) containing 27 amino acids. Bombesin shows high binding affinity to the GRP receptors, which are expressed in pancreas, breast, prostate, lung, breast and colorectal. GPR receptors are also overexpressed in prostate cancer cells including PC-3 tumor cells, which makes it a suitable targeting vector for prostate cancer cells. [40] A BBN peptide derivative was conjugated to 222-MAMA through an alkane (Ahx) linker. The radiolabeling procedure was performed separately with no-carrier-added ^{99m}Tc and carrier-added ^{186}Re. Initially, [^{99m}Tc]technetium and [^{186}Re]rhenium glucoheptonate intermediates were prepared in which the radionuclides are present in the oxidation state of +5 followed by the ligand exchange reaction between the 222-MAMA-Ahx-BBN(7-14)NH_2 conjugate and [^{99m}Tc]tecnethium and [^{186}Re]rhenium glucoheptonate intermediates to form $^{99m}Tc/^{186}Re$-222-MAMA-Ahx-BBN(7-14)NH_2 . [7] *In vitro* competitive cell binding studies of $1^{86}Reo$-222-MAMA-Ahx-BBN(7-14)NH_2 in PC-3 prostate

cancer cells overexpressing GRP receptors showed that the complex binds to PC3-tumor cell surface receptors with high affinity. The gastrin-releasing peptide receptor (GRPR) is an attractive target for imaging and therapy since it is overexpressed in several human tumors such as prostate cancer, breast cancer (BC), and peritumoral vessels in ovarian cancer. However, the complex showed high lipophilicity and was excreted more through the hepatobiliary and GI system relative to the renal system. [7] The ongoing goal presented herein is to synthesize less hydrophobic 222 MAMA chelate with Re radionuclides for conjugation to the RM2 peptide, a GRPR antagonist, as the targeting vector and further biological evaluation.

Experimental

Materials

2-Chloroethylamine hydrochloride, triphenylmethanethiol, tris(2-carboxyethyl)phosphine (TCEP), silica gel 60Å, triphenylmethane thiol, sodium citrate dihydrate, tin(II) tartrate, ethyl 3-bromopropionate and bromoacetyl bromide were purchased from Fisher Scientific or Sigma-Aldrich. Silica gel w/UV 254 TLC plates were purchased from Sorbtech Technologies. Bacteriostatic saline was purchased from Hospira Inc. All solvents, and reagent grade acids and bases were purchased from Fisher Scientific or Sigma-Aldrich and used without further purification. Only 18 MΩ water was used during the experiments. Technetium-99m

pertechnetate was obtained from saline elution of a $^{99}Mo/^{99m}Tc$ generator (Mid-America Isotopes Inc, Ashland, MO). Rhenium-186 was obtained from acid dissolved 94.6% enriched $Al(^{185}ReO_4)_3$ targets (Isotech) with the $^{185}Re(n,\gamma)^{186}Re$ neutron activation reaction at the University of Missouri Research Reactor (MURR, Columbia, MO) with a specific activity of 3.6–6.4 GBq/mg (0.098–0.172 Ci/mg).

Physical Measurements

^{1}H and ^{13}C NMR spectra were obtained in $CDCl_2$, $CDCl_3$ or DMSO on a Bruker ARX-500 or 600 MHz spectrometer using TMS as an internal standard. An ORTEC HPGe detector equipped with Genie multichannel analysis software was used to evaluate ^{186}Re liquid samples. Reversed phase HPLC (RP-HPLC) was performed using a Shimadzu Prominence HPLC system equipped with a pump, controller, and Prominence UV-Vis detector (model SPD20-AV) and Phenomenex Jupiter C18 (5 μm, 150 mm x 4.6 mm) column. The Phenomenex Jupiter C18 column was eluted with a liner gradient of acetonitrile (ACN) in water each containing 0.1% trifluoroacetic acid (TFA) was used as follows: Three methods were used as the linear gradient: Method 1) 30 to 80% ACN over 20 min, then from 30 to 80% ACN over 5 min, followed by returning to 30% ACN over 3 min (flow rate 1 mL/min). Method 2) 40 to 80% ACN over 20 min, then from 80 to 90% ACN over 3 min, followed by returning to 40% ACN over 2 min (flow rate 1 mL/min). Method 3) 10 to 50% ACN over 30 min, then from 50 to 90% ACN over 5 min, followed by returning to 10% ACN over

5 min (flow rate 1 mL/min). All LC-MS analyses and MS assisted preparative purifications were performed with an LCQ Fleet from Thermo Fisher, Waltham, MA (by Dr. Fabio Gallazzi). An Eppendorf ThermoMixer equipped with a 1.5 mL tube holder was used for mixing. An Eckert & Ziegler AR-2000 Bioscan was used for radio-TLC measurements. Microwave reactions were performed using a CEM Discover® SP microwave reactor (CEM Corporation, Matthews, NC).

Synthesis

Compounds **1** and **2** (**Figure 4.1**) were previously synthesized and reported by Demoin et al. [7] Compound **3**, **4**, and **5** were synthesized following a preparation similar to Demoin et al. [7]

Scheme 4.1: Synthesis of 222-MAMA(*N*-3-Ahx-OEt)].

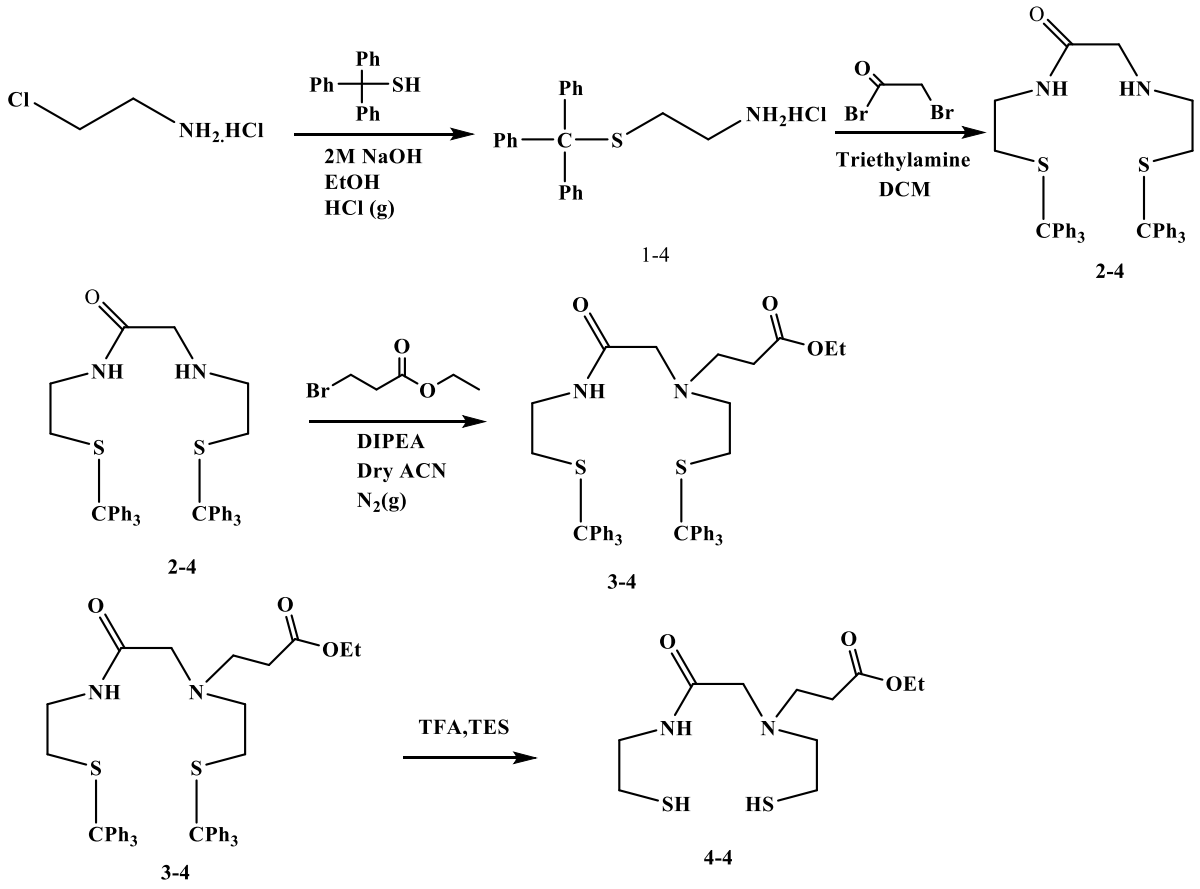

Synthesis of 2-(tritylthio)ethan-1-amine hydrochloride (1).

Triphenylmethanethiol) (12.5 g, 45.2 mmol) was added to a 500 mL round bottom flask along with a 1:1 mixture of ethanol and 2 M NaOH (60 mL each). After stirring and dissolving, 2-chloroethan-1-amine hydrochloride (4.7020 g, 36.2 mmol) was slowly added into the reaction. The reaction was fitted with a septum and stirred for approximately 48 hours. The reaction was monitored by silica gel TLC using 1:1 hexane and ethyl acetate as the mobile phase and visualized using UV and $KMnO_4$ (product R_f=4.5). The yellow milky reaction mixture was vacuum distilled to

remove ethanol. Then, the product was extracted with dichloromethane (DCM) (3 × 30 mL) and saturated sodium chloride (3 ×15 mL). Organic layers were combined, dried over anhydrous Na_2SO_4 and filtered. HCl gas was bubbled slowly into the filtrate while stirring in a 500 mL round bottom flask to obtain a white precipitate. The mixture was vacuum filtered and washed with copious amount of cold diethylether. Yield: 7.7948 g, 60%. ^{1}H-NMR (600 MHz, $CDCl_3$, δ (ppm)): 1.90 (2H, N**H₂**), 2.40-2.42 (2H, t, S-C**H₂**), 2.50-2.52 (2H, t, N-C**H₂**), 7.193-7.197 (6H, m, *o*-**H**), 7.205-7.265 (3H, t, *p*-**H**), 7.27, 7.29 (6H, m, *m*-**H**). ESI-MS (*m/z*): 356.40 (356.92 calc'd for $[C_{21}H_{23}ClNS]^+$ $[M+H]^+$) (**Figure 4.1**).

Synthesis of N-(2-(tritylthio)ethyl)-2-(((tritylthio)ethyl)amino)acetamide (2).

To a 500 mL round bottom flask while stirring in an acetone/water/dry ice bath (around -10 °C), compound **1-4** (7.795 g, 21.9 mmol) dissolved in dry DCM (30 mL) was added. Then triethylamine (4.85 mL, 3.5325 g, and 34.84 mmol) was added to the reaction. After approximately 10 min, bromoacetyl bromide (0.87 mL, 2.010 g, 9.954 mmol) was dissolved in chloroform (30 mL) and added dropwise over 30 min using an addition funnel. The reaction was brought to room temperature and was stirred for approximately 48 h. The reaction was monitored by silica gel TLC using 1:4 hexane:ethyl acetate and visualized using UV, I_2 and $KMnO_4$ (product R_f =0.35). DCM, chloroform and excess triethylamine was removed by vacuum distillation. The crude product (white foam) was dissolved in

ethyl acetate (50 mL) and washed with 2 M HCl (2 × 30 mL) and saturated sodium chloride (1 × 10 mL), once with water (1 x 30 mL) and 1 M NaOH (1 × 30 mL) to give a light yellow oil. Ethyl acetate was removed by vacuum filtration and further purification was performed by silica gel column chromatography (200 g silica gel) using 36:1:64% hexanes/triethylamine/ethyl acetate to give a white organic foam. Yield: 3.21 g, 70%. The product was characterized by LC-ESI-MS $[M+H]^+$ 779.75 $C_{49}H_{50}N_2O_3S_2$. ^{1}H-NMR (500 MHz, $CDCl_3$, δ (ppm)): 2.37 (4H, m, S-C**H₂**), 2.47 (2H, m, NH-C**H₂**), 3.04 (2**H**, s, CO-C**H₂**), 3.09 (2H, q, CO-NH-C**H₂**), 7.19-7.20 (2H, m, N**H**), 7.19-7.21 (6H, t, *p*-**H**), 7.25-7.39 (12H, m, *o*-**H**), 7.40-7.42 (12H, m, *m*-**H**). ^{13}C-NMR (500 MHz, $CDCl_3$, δ (ppm)): 32.3 (S-**C**H_2), 37.6 (CO-NH-**C**H_2), 48 (CH_2-NH-**C**H_2), 51.3 (HN-CO-**C**H_2), 66.7 (S-**C**-(C_6H_5)$_3$), 126.7 (*p*-**C**), 127.9 (*O*-**C**), 129.5 (*m*-**C**), 144.7 (S-C-(**C**$_6H_5$)$_3$), 171.26 (**C**O). ESI-MS (*m/z*): 679.3 (679.27 calc'd for $[C_{44}H_{44}N_2OS_2]^+$ $[M+H]^+$) (**Figures 4.2 and 4.3**).

Ethyl 3-((2-oxo-2-((2-(tritylthio)ethyl)amino)ethyl)(2-(tritylthio)ethyl)amino)propionate (3-4) [trityl protected 222-MAMA(N-3-Ahx-OEt)] (3-4).

Compound **2-4** (1.0054 g, 1.48 mmol) was dissolved in dry ccetonitrile (10 mL) in a 500 mL dry round bottom flask. The reaction was equipped with a condenser, purged with N_2 gas and heated to 85 ˚C. Then ethyl 3-bromopropionate (0.283 mL, 2.21 mmol) and diisopropylethylamine (DIPEA) (0.291 mL, 1.67 mmol) were added to the reaction while stirring.

The reaction was stirred for approximately 48 h and was monitored with silica gel TLC using 5%:95% ethyl acetate:DCM (**2-4** R_f=0; product, **3-4** R_f = 0.1). The volatile components of the reaction were removed by vacuum distillation and purified with silica gel column chromatography (4 cm × 33.5 cm column, 70 g silica gel) using 1:9 ethyl acetate:DCM as the mobile phase. A pale-yellow band was observed in the column and eluted to give a pale yellow foam. Yield: 460 mg, 70%. ^{1}H-NMR (600 MHz, CD_2Cl_2, δ (ppm)): 1.67 (3H, t, C**H₃**), 2.20-2.40 (8H, m, N-C**H₂**C**H₂**, S-CH-C**H₂**, S-CH-C**H₂**), 2.81 (2H, s, NH-CO-C**H₂**), 2.60 (2H, m, N-C**H₂**), 3.10 (2H, q, NH-C**H₂**), 4.003 (2H, q, CO-O-C**H₂**), 7.19-7.21 (6H, triplet, *p*-**H**), 7.23 (1H, m, N**H**), 7.20-7.28 (12H, m, *o*-**H**), 7.38, 7.42 (12H, m, *m*-**H**). ^{13}C-NMR (600 MHz, CD_2Cl_2, δ (ppm)): 14.8 (CO-O-CH_2-**C**H_3), 30.4 ((C6H5)$_3$C-S-**C**H_2), 32.2 (NH-CH_2-**C**), 38.0 (NH-**C**H_2), CH_2-NH-**C**O (172.7), O-**C**O (171.0), S-C-(**C**$_6$H$_5$)$_3$ (145.6), *m*-**C** (130.3), *O*-**C** (128.7), *p*-**C** (127.4), S-(C6H5)$_3$**C** (89.0), CO-O-**C**H_2 (61.0), - NH-CO-**C** (59.0), (CH_2)$_2$N-**C**H_2 (53.8), (CH_2)$_2$N-CH_2-**C** (50.7), S-CH_2-**C** (50.0). ESI-MS (*m/z*): 779 (779.33 calc'd for $[C_{49}H_{51}N_2O_3S_2]^+$ $[M+H]^+$) (**Figures 4.4 and 5.4**).

Ethyl 3-((2-mercaptoethyl)(2-((2-mercaptoethyl)amino)-2-oxoethyl)amino)propanoate (deprotection of trityl protected 222-MAMA(N-3-Ahx-OEt)) (4-4).

Compound **3-4** (81.21 mg, 0.104 mmol) was added to 2.23 mL of TFA and 0.13 mL of TES while stirring. The mixture was allowed to stir for

about 2 h and the solvent was evaporated under N_2(g) flow. The solids were extracted with ethyl acetate (4 × 10 mL). The extracts were combined and washed with hexanes (3 × 10 mL) to remove the impurities. The ethyl acetate portion was evaporated into dryness and characterized by LC-MS-MS, ^{1}H-NMR and HPLC (*m/z*): 293.6 (294.11 calc'd for $C_{11}H_{22}N_2O_3S_2$ $[M+H]^+$). Yield: 24 mg. 80%.

Scheme 4.2: Synthesis of ^{nat}ReO-222-MAMA(*N*-3-Ahx-OEt) (**5-4**).

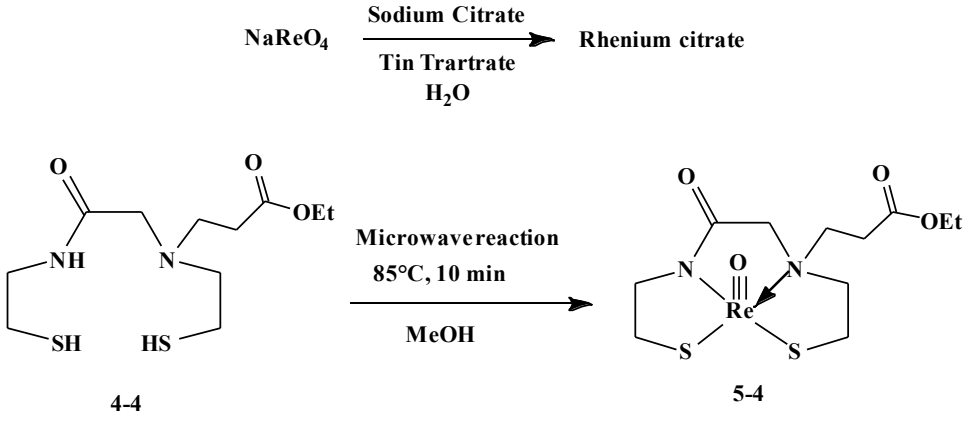

$ReO(Citrate)_2^-$ was synthesized by dissolving ammonium perrhenate (0.02 g, 0.08 mmol) and sodium citrate (0.03 g, 0.1 mmol) in DI water (2.5 mL). Deprotected ligand (compound **4-4**) was added into a 25 mL microwave vessel and dissolved in MeOH (12 mL). $ReO(Citrate)_2^-$ was also added into the microwave vessel. The reaction mixture was added to the microwave reaction vessel and purged. The solution was heated in a microwave reactor at 80 °C, 17 bar (max), and 150 W (max) for 30 min with stirring. The product mixture was rotary evaporated to dryness and dissolved in 20 mL of ethyl acetate and 20 mL of water. The aqueous layer was extracted with 20 mL of saturated sodium chloride. The organic layer was filtered through a medium porosity frit to remove yellowish brown solids. The organic layer was dried with anhydrous sodium sulfate and the solvent was removed *in vacuo*. The solids were dissolved in 2 mL of DCM and loaded on a silica gel column (30 cm long by 1 com diameter). The column was eluted with 200 mL of 100% DCM, 100 mL of 10% ethyl acetate in DCM, 50 mL of 50% ethyl acetate in DCM, and 100 mL ethyl acetate. The fractions were monitored by silica gel TLC using 5%:95% ethyl acetate: DCM (product R_f = 0.5, fractions 16-20). Five fractions were combined and rotary evaporated to dryness to give a magenta-brown solid. Yield: 25 mg. 50%. ^{1}H-NMR (600 MHz, CD_2Cl_2, δ (ppm)): 1.133 (q, 3H, C**H**$_3$), 2.947 (m, 2H, SC**H**$_2$CH$_2$N), 3.249 (m, 6H, **H**$_2$CNC**H**$_2$C**H**$_2$), 3.489 (m, 2H, O=CNC**H**$_2$CH$_2$), 3.950, 4.250 (m, 2H, O=CC**H**$_2$), 4.198 (m, 2H, OC**H**$_2$CH$_3$), 4.697 (m, 2H, O=CNCH$_2$C**H**$_2$S),

^{13}C-NMR (600 MHz, CD_2Cl_2, δ (ppm)): 29.51 (**C**H_3), 39.02 (S**C**H_2CH_2) , 48.16 (H_2**C**NCH_2CH_2), 58.25, 58.32 (O**C**H_2, O=C**C**H_2), 59.91 (O=CNCH_2**C**H_2S), 61.71 (H_2CN**C**H_2CH_2), 64.79 (O=CN**C**H_2CH_2), 66.36 (H_2CNCH_2**C**H_2), 169.70 (N**C**=O), 186.64 (O=**C**O). LC-ESI-MS (*m/z*): 495 (495.03 calc'd for $[C_{11}H_{20}N_2O_4ReS_2]^+$ $[M+H]^+$) (**Scheme 4.2, Figures 4.6, and 4.7**).

Scheme 4.3: Radiotracer synthesis of ^{186}ReO-222-MAMA(N-3-Ahx-OEt) (**6-4**).

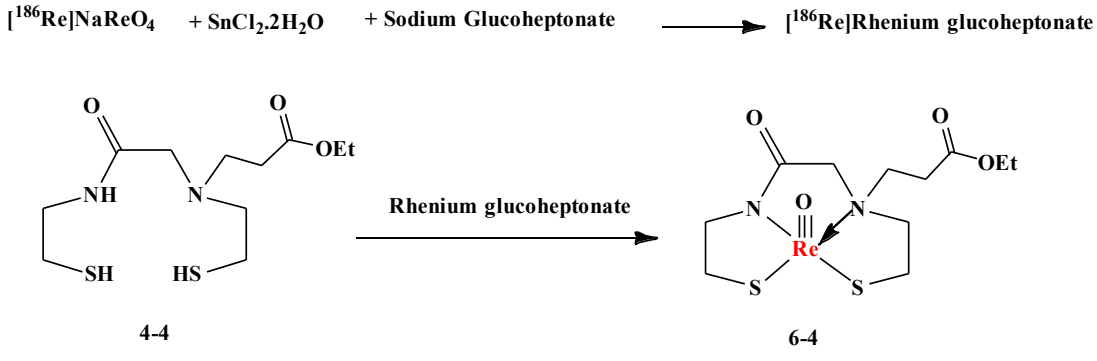

4-4 **6-4**

Yield at RT (room temperature): 75%
Yield at 55 °C : 55%

Radiotracer synthesis of ^{186}ReO-222-MAMA(N-3-Ahx-OEt) (6-4).

(50.0 mg, 0.064 mmol) of compound **3-4** was added to 2 mL of trifluoroacetic acid and 0.25 mL of triethylsilane while stirring. The mixture was allowed to stir for about 2 h and the solvent was evaporated under N_2(g) flow. The product was extracted with ethyl acetate (4 × 10 mL). The Extracts were combined and washed with hexanes (3 × 10 mL) to remove the impurities. The ethyl acetate portion was evaporated into dryness and characterized by LC-ESI-MS and HPLC. Without further purification or neutralization, the deprotected 222-MAMA(*N*-3-Ahx-OEt) ligand (compound **4-4**) was dissolved in 1 mL of ethyl acetate. Sodium glucoheptonate (30.9 mg, 0.142 mol) was dissolved in 1 mL of 18 MΩ water. Stannous chloride ($SnCl_2$**.**$2H_2O$) (6.37 mg, 2.82 mmol) was dissolved in 15.5 µL of 0.25 M HCl. 382 µL of sodium glucoheptonate solution, 9 µL of $SnCl_2$**.**$2H_2O$ solution, 387 µL of 18 MΩ water and low-specific-activity (LSA) $^{186}ReO_4^-$ solution (10 µL, 3 mCi, 111 MBq) were combined in an Eppendorf tube and stirred in a thermomixer for 40 min at 40 ºC. The reaction mixture was then centrifuged. The supernatant was monitored by RP HPLC and radio-TLC (2 TLC plates (saturated paper), acetone and saline as the mobile phases) to determine the formation of rhenium glucoheptonate ([^{186}Re]rhenium glucoheptonate, $R_f \approx 0$ in acetone and [^{186}Re]rhenium glucoheptonate, $R_f \approx 0.95$ (95%) in saline determined by Bioscan). Two batches of the reaction mixture (100 µL each) were transferred to Two separate Eppendorf tubes. The deprotected 222-

MAMA(*N*-3-Ahx-OEt) ligand solution (compound **4-4**) (200 µL), (300 µL, 20mM Na_2HPO_4, pH=8) were added to each reaction mixture in the Eppendorf tubes. One of the reaction mixtures was placed in a 70 º C thermomixer and stirred for 45 min and the second reaction mixture was placed in the thermomixer and stirred at room temperature for 45 min. The reaction mixtures were then centrifuged and the supernatants were monitored by RP HPLC and radio-TLC (silica gel; 50% ACN/H_2O as the mobile phase, ^{186}ReO-222-MAMA(*N*-3-Ahx-OEt), $R_f \approx 0.5$(55%) and free^{186}Re, $R_f \approx 1$ (45%) for reaction 1, and ^{186}ReO(222-MAMA(*N*-3-Ahx-OEt), $R_f \approx 0.5$ (75%) and free^{186}Re, $R_f \approx 1$ (25%) for reaction 2 determined by Bioscan). The supernatants of the two reactions were also monitored using RP-HPLC. A Phenomenex Jupiter C18 column was eluted with a linear gradient. Two methods were used as the linear gradient with acetonitrile (ACN) in water each containing 0.1% trifluoroacetic acid (TFA) as follows: Method 1) 30 to 80% ACN over 20 min, and then from 80 to 90% ACN over 5 min, followed by returning to 30% ACN over 3 min. Method 2) 40 to 80% ACN over 20 min, then from 80 ACN to 80% ACN over 5 min, followed by returning to 40% ACN over 5 min (flow rate 1 mL/min) (**Table 4.1, Scheme 4.3, Figures 4.9**).

Purification of *^{186}ReO-222-MAMA(N-3-Ahx-OEt) (6-4)*

The reaction mixture (^{186}ReO(222-MAMA(N-3-Ahx-OEt) was cooled to room temperature and purified with HPLC. A linear gradient of acetonitrile (ACN) in water (each containing 0.1% trifluoroacetic acid

(TFA)) was as follows: 30/80 for 20 min, then from 30/80 to 80/90 over 5 min, followed by returning to 30/80 in 10 min (flow rate 1 mL/min). The fractions containing ^{186}ReO(222-MAMA(*N*-3-Ahx-OEt were collected and the solvent was removed under a stream of N_2(g) at 40 °C and then reconstituted with 18 MΩ water (**Figures 4.12 and 4.13**).

Distribution coefficient (log $D_{7.4}$) determination of *^{186}ReO-222-MAMA(N-3-Ahx-OEt) (6-4)*

Phosphate buffered saline (PBS) buffer solution (2 mL, pH 7.4, 15 mM) was added to a centrifuge tube along with 2 mL of 1-octanol. ^{186}ReO(222-MAMA(*N*-3-Ahx-OEt) in DI water (200 µL, 7.4 MBq (200 µCi)) was added to the centrifuge tube and the resultant mixture stirred on a vortex mixer for 5 min, and then centrifuged (3200 rpm) for 2 min. The aqueous (1.5 mL) and the organic layers (1.5 mL) were separated and each counted on an HPGe detector. The experiment was carried out in triplicate.

Stability of *^{186}ReO(222-MAMA(N-3-Ahx-OEt) (6-4)*

The stability of ^{186}ReO-222-MAMA(*N*-3-Ahx-OEt) in saline solution, and containing ascorbic acid as prepared above, was assessed over 72 h by RP-HPLC (a linear gradient of acetonitrile (ACN) in water (each containing 0.1% trifluoroacetic acid (TFA)) was as follows: 30/80 for 20 min, then from 30/80 to 80/90 over 5 min, followed by returning to 30/80 in 10 min (flow rate 1 mL/min)) and radio-TLC (silica gel; 50% ACN/H_2O as the mobile phase. ^{186}ReO(222-MAMA(N-3-Ahx-OEt), R_f

≈0.60; free ^{186}Re, R_f≈1). [^{186}ReO(222-MAMA(N-3-Ahx-OEt) (11.6 MBq (300 μCi)) in sterile saline was set aside at room temperature and monitored.

Scheme 4.4: Radiotracer synthesis of ^{99m}TcO(222-MAMA(N-3-Ahx-OEt) (**7**-4).

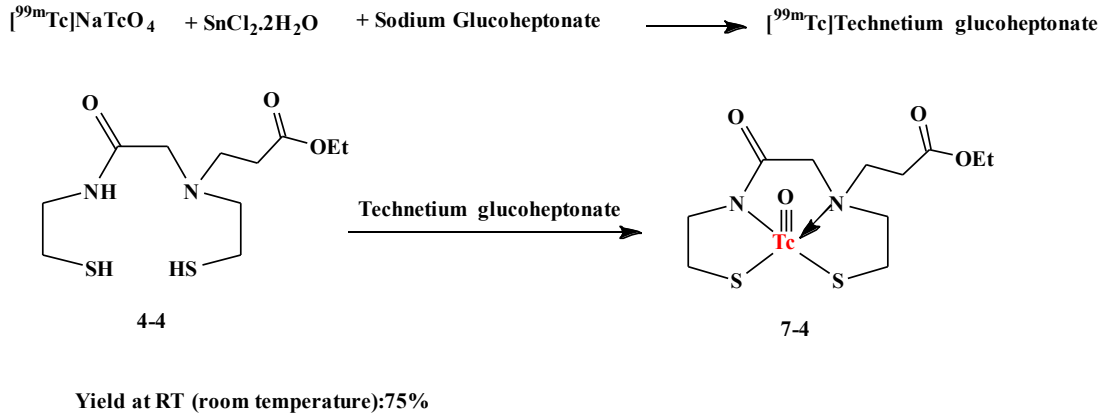

Radiotracer synthesis of *^{99m}TcO(222-MAMA(N-3-Ahx-OEt) (7-4).*

(50.0 mg, 0.064 mmol) of compound **3-4** was added to 2 mL of trifluoroacetic acid and 0.25 mL of triethylsilane while stirring. The mixture was allowed to stir for about 2 h and the solvent was evaporated under N_2(g) flow. The product was extracted with ethyl acetate (4 × 10 mL). The extracts were combined and washed with Hexanes (3 × 10 mL) to remove the impurities. The ethyl acetate portion was evaporated to dryness and characterized by LC-ESI-MS and HPLC. Without further purification or neutralization, the deprotected 222-MAMA(*N*-3-Ahx-OEt) ligand (compound **4-4**) was dissolved in 1 mL of ethyl acetate. Sodium

glucoheptonate (30.9 mg, 0.142 mol) was dissolved in 1 mL of 18 MΩ water. Stannous chloride ($SnCl_2.2H_2O$) (6.37 mg, 2.82 mmol) was dissolved in 15.5 µL of 0.25 M HCl. 382 µL of sodium glucoheptonate solution, 9 µL of $SnCl_2.2H_2O$ solution and [^{99m}Tc]TcO_4^- solution (50 µL, 1 mCi, 37 MBq) were combined in an Eppendorf tube and stirred in a thermomixer for 40 min at 40 ºC. The reaction mixture was then centrifuged. The supernatant was monitored by RP-HPLC and radio-TLC (2 TLC (saturated papers), eluted with acetone and saline separately as the mobile phases) to determine the formation of [^{186}Re]rhenium glucoheptonate ($R_f \approx 0$ in acetone and $R_f \approx 0$ 5%, $R_f \approx 0.95$, 95% in saline determined by Bioscan). The reaction mixture (100 µL) was transferred to two separate Eppendorf tubes. The deprotected 222-MAMA(*N*-3-Ahx-OEt) ligand solution (compound **4-4**), phosphate buffer (300 µL, 20mM Na_2HPO_4, pH=8) were added to each reaction mixture in the Eppendorf tubes. The reaction mixtures were placed in a thermomixer and stirred at room temperature for 45 min. The reaction mixtures were then centrifuged and the supernatants were monitored by RP HPLC and radio-TLC (silica gel; 50% ACN/H_2O as the mobile phase, ^{99m}TcO(222-MAMA(N-3-Ahx-OEt)), $R_f \approx 0.5$(75%) and free^{99m}Tc, $R_f \approx 1$ (25%)determined by Bioscan). The supernatant of the reaction was also monitored using RP-HPLC. A Phenomenex Jupiter C18 column was eluted with a linear gradient of acetonitrile (ACN) in water each containing 0.1% trifluoroacetic acid (TFA) was used as follows: Three methods were used as the linear

gradient: 40 to 80% ACN over 20 min, then from 80 to 90% ACN over 3 min, followed by returning to 40% ACN over 2 min (flow rate 1 mL/min). (flow rate 1 mL/min) **(Scheme 4.3, Figures 4.10**).

Results and Discussion

Previous N_2S_2 chelates synthesized for the purpose of theranostic $^{186/188}$Re radiopharmaceuticals showed high *in vivo* stability but were too lipophilic for in vivo applications based on biodistribution results**.** A less hydrophobic linkable MAMA ligand (trityl protected) was synthesized for the purpose of conjugation to the RM2 peptide for targeting prostate cancer.

Ligand synthesis

Synthesis of this 222-MAMA(*N*-3-Ahx-OEt) chelate (compound **3-4**) used commercially available reagents. **Scheme 4.1** shows the synthetic steps for preparation of 2-(tritylthio)ethan-1-amine hydrochloride (**1-4**) and *N*-(2-(tritylthio)ethyl)-2-((2-(tritylthio)ethyl)amino)acetamide (222-MAMA-Tr_2-free amine, compound **2-4**), which have been reported before. [7] 222-MAMA(*N*-3-Ahx-OEt) was synthesized from the reaction of 222-MAMA-Tr_2-free amine (**2-4**) and ethyl 3-bromopropionate in anhydrous ACN. The reaction was refluxed under a N_2 atmosphere at 85˚C. (**Figure 4.14**, **Scheme 4.1**). The product was purified by silica gel column chromatography and isolated in 38% yield and characterized by liquid chromatography electrospray ionization mass spectrometry (LC-ESI-MS),

HPLC, ^{1}H-NMR and ^{13}C-NMR spectroscopies. Trityl groups of compound **3-4** were removed by TFA in the presence of TES (as the scavenger for trityl groups) to afford compound **4-4**. Compound **4-4** was reacted with rhenium-citrate, or *in situ* with ^{186}Re or ^{99m}Tc on the radiotracer level in the presence of Sn^{2+} and low pH conditions to afford compounds **5-4**, **6-4** and **7-4,** respectively.

Rhenium complex

The ^{nat}ReO(222-MAMA(*N*-3-Ahx-OEt) (**5-4**) complex was synthesized from $ReO(citrate)_2^-$ and compound **4-4** in a microwave reactor at 80 °C. The product was purified by silica gel column chromatography and isolated in 50% yield and characterized by LC-ESI-MS, HPLC, ^{1}H-NMR and ^{13}C-NMR. All of the ^{13}C-NMR carbon signals showed downfield shift on complexation to the monooxorhenium(V) center. The rhenium complex was characterized by reversed phase HPLC, as standards for the ^{99m}Tc and carrier-added ^{186}Re analogues prepared at the radiotracer level using methods **1** and **2 (Figures 4.9 and 4.10)**. **Table 4.1** shows the retention times of the complexes based on methods **1**, **2** and **3**. The RP-HPLC chromatogram of ^{nat}ReO(222-MAMA(*N*-3-Ahx-OEt) showed two major peaks, which were 1.1 min apart. The peaks at 6.1 min and 7.2 were isolated using HPLC (method **2**) and characterized by LC-ESI-MS. Both compounds showed identical *m/z* values of 495.07, which corresponds with the molecular weight of ^{nat}ReO(222-MAMA(*N*-3-Ahx-OEt). Therefore, it could be suggested that the peaks at 6.1 min and 7.2 min

correspond to the *anti* and *syn* isomers of ^{nat}ReO(222-MAMA(*N*-3-Ahx-OEt).

Table 4.1: HPLC retention times of components.

	Method 1 **Betabasic-18, 30–80% ACN with 0.1% TFA over 20 min, 1 mL/min**	**Method 2** **Betabasic-18, 40–80% ACN with 0.1% TFA over 20 min, 1 mL/min**	**Method 3** **Betabasic-18, 10–50% ACN with 0.1% TFA over 30 min, 1 mL/min**
^{nat}ReO(222-MAMA(N-3-Ahx-OEt) (*syn*)	9.5 min	7.2 min	
^{nat}ReO(222-MAMA(N-3-Ahx-OEt) (*anti*)		6.1 min	
^{186}ReO(222-MAMA(N-3-Ahx-OEt)	9.8 min	7.9 min	25.8 min
^{99m}TcO(222-MAMA(N-3-Ahx-OEt)		7.1 min	

Radiolabeling of 4 with LSA ^{186}Re

The reduction of LSA$^{186}ReO_4^-$ and radiolabeling of **4-4** with ^{186}Re were optimized under a variety of reaction conditions. The concentration of stannous chloride and sodium glucoheptonate in reduction of $^{186}ReO_4^-$ (with oxidation state of +7) and formation of [^{186}Re]rhenium glucoheptonate (with oxidation state of +5) were optimized. Radiolabeling reaction with [^{186}Re]rhenium glucoheptonate was also optimized using different reaction conditions (pH, temperature, concentration). The highest reduction yield (95%) was observed with 142 mM sodium glucoheptonate at 40°C yielding [^{186}Re]rhenium glucoheptonate. The highest

radiolabeling yield of compound **4-4** with LSA ^{186}Re was 75% at pH of ~3, which was adjusted with 20 mM pH 8–9 phosphate buffer, and at room temperature yielding ^{186}ReO(222-MAMA(*N*-3-Ahx-OEt). ^{186}ReO(222-MAMA(*N*-3-Ahx-OEt) was analyzed by RP-HPLC (methods **1**, **2**) and results showed consistency between the retention time of ^{nat}ReO(222-MAMA(*N*-3-Ahx-OEt) (e.g., R_t=9.5 min , method **1**) and ^{186}ReO(222-MAMA(*N*-3-Ahx-OEt) (e.g., R_t=9.8 min , method **1**).

Radiolabeling of 4 with ^{99m}Tc

The reduction of $^{99m}TcO_4^-$ (generator eluted) and radiolabeling of **4-4** with ^{99m}Tc were optimized under a variety of reaction conditions. The concentration of stannous chloride and sodium glucoheptonate in reduction of $^{99m}TcO_4^-$ (with oxidation state of +7) and formation of [^{99m}Tc]technetium glucoheptonate (with oxidation state of +5) were optimized. Radiolabeling reaction with [^{99m}Tc]technetium glucoheptonate was also optimized using different reaction conditions (pH, temperature, concentration). The highest reduction yield (95%) was observed with 142 mM sodium glucoheptonate at 40°C yielding [^{99m}Tc]technetium glucoheptonate. The highest radiolabeling yield of compound **4-4** with ^{99m}Tc was 75% at pH of ~3, which was adjusted with 20 mM pH 8–9 phosphate buffer, and at room temperature yielding ^{99m}TcO(222-

MAMA(*N*-3-Ahx-OEt). ^{99m}TcO(222-MAMA(*N*-3-Ahx-OEt) was analyzed by RP-HPLC (methods **2**) and results showed that the retention time of ^{99m}TcO(222-MAMA(*N*-3-Ahx-OEt) (e.g., R_t=7.1 min , method **2**), ^{nat}ReO(222-MAMA(*N*-3-Ahx-OEt) (*syn or anti*) (e.g., R_t=7.2 min , method **2**) and^{186}ReO(222-MAMA(*N*-3-Ahx-OEt) (e.g., R_t=7.1 min , method **2**) are very close. (**Table 4.1, Figures 4.8-4.13**)

***In vitro* stability studies of ^{186}ReO(222-MAMA(N-3-Ahx-OEt)**

The *in vitro* stability of HPLC-purified RP-HPLC ^{186}ReO(222-MAMA(*N*-3-Ahx-OEt)) in saline solution with ascorbic acid added was assessed at 24, 48 and 72 h by RP-HPLC and radio-TLC. Only one radioactive peak at 9.8 min was observed over 72 h, which was consistent with the retention time of ^{186}ReO(222-MAMA(*N*-3-Ahx-OEt)). The formation of free ^{186}Re was not observed by RP-HPLC or radio-TLC.

***In vitro* lipophilicity (log $D_{7.4}$) studies of ^{186}ReO(222-MAMA(*N*-3-Ahx-OEt)**

The octanol-water partition coefficient was determined at pH 7.4 as an indicator of lipophilicity under biological pH. RP-HPLC purified ^{186}ReO(222-MAMA(*N*-3-Ahx-OEt), which had been reconstituted in pH 7.4 PBS was used for this determination. The log D_7 value was calculated from the following equation:

$$\log D = log \frac{Radioactivity\ in\ octanol}{Radioactivity\ in\ water}$$

The log $D_{7.4}$ value determined for this complex was = -0.30 ± 0.1. The negative log $D_{7.4}$ value is favorable since it shows that there is more activity in aqueous solution than organic solution and hence, ^{186}ReO(222-MAMA(*N*-3-Ahx-OEt) had less hydrophobic nature.

Conclusion and Future Studies

The 222-MAMA-based chelator 222-MAMA(*N*-3-Ahx-OEt) with improved hydrophilicity was synthesized for potential use in $^{186/188}$Re radiopharmaceuticals. Log $D_{7.4}$ value and RP-HPLC chromatogram of ^{186}ReO(222-MAMA(*N*-3-Ahx-OEt)) showed improvement in hydrophilicity compare with previously evaluated ^{186}ReO(222-MAMA(*N*-6-Ahx-OEt)). [7] The future work will focus on conjugation of 222-MAMA chelator to RM2 peptide and its non-radioactive Re, and carrier-added and no-carrier-added ^{186}Re complexation studies followed by *in vitro* cell binding studies and biodistribution evaluation.

Appendix

Table 2.4: Crystal data and structure refinement for tribromodimethylisophthalate (**1**).

Identification code	s1
Empirical formula	C15 H17 Br3 O5
Formula weight	517.02
Temperature	100.0 K
Wavelength	1.54178 Å
Crystal system	Monoclinic
Space group	P 1 21/c 1
Unit cell dimensions	a = 7.1298(2) Å
α= 90°.	
	b = 10.2428(2) Å
β= 93.9410(9)°.	
	c = 24.1482(5) Å
γ: = 90°.	
Volume	1759.35(7) $Å^3$
Z	4
Density (calculated)	1.952 Mg/m^3
Absorption coefficient	8.703 mm^{-1}
F(000)	1008
Crystal size	0.35 x 0.2 x 0.14 mm^3
Theta range for data collection	3.669 to 74.274°.
Index ranges	-8<=h<=8, -12<=k<=12, -28<=l<=29
Reflections collected	41396

Independent reflections	3565 [R(int) = 0.0318]
Completeness to theta = 67.679°	99.9 %
Absorption correction	Semi-empirical from equivalents
Max. and min. transmission	0.7538 and 0.4092
Refinement method	Full-matrix least-squares on F^2
Data / restraints / parameters	3565 / 0 / 210
Goodness-of-fit on F^2	1.159
Final R indices [I>2sigma(I)]	R1 = 0.0211, wR2 = 0.0528
R indices (all data)	R1 = 0.0214, wR2 = 0.0529
Extinction coefficient	n/a
Largest diff. peak and hole	0.716 and -0.444 e.$Å^{-3}$

Table 2.5: Atomic coordinates (x 10^4) and equivalent isotropic displacement parameters ($Å^2$x 10^3) for tribromodimethylisophthalate (**1**). U(eq) is defined as one third of the trace of the orthogonalized U^{ij} tensor.

	x	y	z	U(eq)
Br(1)	13307(1)	-1007(1)	2424(1)	19(1)
Br(2)	8205(1)	284(1)	2377(1)	21(1)
Br(3)	14721(1)	2182(1)	1273(1)	24(1)
C(8)	11504(3)	1161(2)	1833(1)	13(1)
C(10)	10424(3)	1396(2)	2354(1)	16(1)
C(9)	12025(3)	-266(2)	1753(1)	16(1)
C(7)	10293(3)	1577(2)	1316(1)	15(1)
O(1)	9960(2)	2942(1)	1378(1)	18(1)
O(3)	7509(2)	7804(1)	217(1)	24(1)
O(4)	6942(2)	1969(2)	-571(1)	26(1)
O(5)	6182(2)	3988(2)	-877(1)	21(1)
O(2)	8821(2)	7691(2)	1086(1)	29(1)
C(2)	9060(3)	4950(2)	1000(1)	16(1)
C(5)	7585(3)	3803(2)	25(1)	15(1)
C(3)	8254(3)	5720(2)	573(1)	16(1)
C(6)	8391(3)	3020(2)	450(1)	15(1)
C(1)	9132(3)	3604(2)	935(1)	15(1)
C(12)	8247(3)	7164(2)	662(1)	19(1)
C(14)	6874(3)	3133(2)	-498(1)	17(1)
C(4)	7512(3)	5155(2)	80(1)	16(1)
C(11)	13247(3)	2034(2)	1924(1)	16(1)
C(15)	5624(4)	3448(2)	-1415(1)	28(1)

C(13)	7459(4)	9209(2)	270(1)	30(1)

Table 2.6: Bond lengths [Å] and angles [°] for tribromodimethylisophthalate (**1**).

Br(1)-C(9)	1.9592(19)
Br(2)-C(10)	1.9538(19)
Br(3)-C(11)	1.956(2)
C(8)-C(10)	1.538(3)
C(8)-C(9)	1.524(3)
C(8)-C(7)	1.530(3)
C(8)-C(11)	1.534(3)
C(7)-O(1)	1.428(2)
O(1)-C(1)	1.365(2)
O(3)-C(12)	1.335(3)
O(3)-C(13)	1.446(2)
O(4)-C(14)	1.207(3)
O(5)-C(14)	1.337(3)
O(5)-C(15)	1.442(3)
O(2)-C(12)	1.205(3)
C(2)-C(3)	1.390(3)
C(2)-C(1)	1.388(3)
C(5)-C(6)	1.394(3)
C(5)-C(14)	1.493(3)
C(5)-C(4)	1.393(3)
C(3)-C(12)	1.494(3)
C(3)-C(4)	1.396(3)
C(6)-C(1)	1.389(3)

C(9)-C(8)-C(10)	113.23(15)
C(9)-C(8)-C(7)	106.94(15)
C(9)-C(8)-C(11)	112.01(16)
C(7)-C(8)-C(10)	109.80(15)
C(7)-C(8)-C(11)	111.11(16)
C(11)-C(8)-C(10)	103.80(15)
C(8)-C(10)-Br(2)	112.59(13)
C(8)-C(9)-Br(1)	111.72(13)
O(1)-C(7)-C(8)	106.00(15)
C(1)-O(1)-C(7)	118.12(15)
C(12)-O(3)-C(13)	115.36(18)
C(14)-O(5)-C(15)	115.61(17)
C(1)-C(2)-C(3)	119.81(19)
C(6)-C(5)-C(14)	117.16(17)
C(4)-C(5)-C(6)	121.16(19)
C(4)-C(5)-C(14)	121.64(18)
C(2)-C(3)-C(12)	117.46(18)
C(2)-C(3)-C(4)	120.70(18)
C(4)-C(3)-C(12)	121.84(18)
C(1)-C(6)-C(5)	119.19(18)
O(1)-C(1)-C(2)	115.06(18)
O(1)-C(1)-C(6)	124.45(18)
C(2)-C(1)-C(6)	120.49(18)
O(3)-C(12)-C(3)	112.08(18)
O(2)-C(12)-O(3)	123.81(19)
O(2)-C(12)-C(3)	124.1(2)
O(4)-C(14)-O(5)	124.27(19)

O(4)-C(14)-C(5)	124.24(19)
O(5)-C(14)-C(5)	111.48(17)
C(5)-C(4)-C(3)	118.64(18)
C(8)-C(11)-Br(3)	113.92(13)

Symmetry transformations used to generate equivalent atoms:

Table 2.7: Anisotropic displacement parameters ($Å^2 x\ 10^3$) for tribromodimethylisophthalate (**1**). The anisotropic displacement factor exponent takes the form: $-2\pi^2[\ h^2\ a^{*2}U^{11} + ...\ + 2\ h\ k\ a^*\ b^*\ U^{12}\ ]$.

	U^{11}	U^{22}	U^{33}	U^{23}	U^{13}	U^{12}
Br(1)	19(1)	13(1)	25(1)	3(1)	-5(1)	1(1)
Br(2)	17(1)	19(1)	29(1)	6(1)	7(1)	0(1)
Br(3)	17(1)	31(1)	26(1)	6(1)	5(1)	-3(1)
C(8)	13(1)	11(1)	16(1)	1(1)	1(1)	0(1)
C(10)	15(1)	14(1)	19(1)	1(1)	3(1)	-1(1)
C(9)	17(1)	14(1)	17(1)	1(1)	-2(1)	2(1)
C(7)	17(1)	10(1)	17(1)	0(1)	0(1)	0(1)
O(1)	23(1)	12(1)	18(1)	0(1)	-3(1)	3(1)
O(3)	33(1)	11(1)	28(1)	1(1)	0(1)	5(1)
O(4)	40(1)	16(1)	21(1)	-2(1)	-2(1)	1(1)
O(5)	26(1)	22(1)	15(1)	0(1)	-1(1)	5(1)
O(2)	37(1)	16(1)	33(1)	-4(1)	-5(1)	-4(1)

C(2)	16(1)	16(1)	18(1)	-1(1)	2(1)	-1(1)
C(5)	13(1)	15(1)	18(1)	0(1)	4(1)	1(1)
C(3)	13(1)	14(1)	22(1)	1(1)	4(1)	0(1)
C(6)	14(1)	12(1)	19(1)	1(1)	4(1)	1(1)
C(1)	12(1)	16(1)	18(1)	3(1)	2(1)	1(1)
C(12)	16(1)	15(1)	26(1)	2(1)	3(1)	0(1)
C(14)	16(1)	19(1)	18(1)	0(1)	3(1)	1(1)
C(4)	13(1)	15(1)	19(1)	4(1)	4(1)	2(1)
C(11)	16(1)	14(1)	20(1)	0(1)	2(1)	-2(1)
C(15)	36(1)	33(1)	14(1)	-2(1)	-1(1)	3(1)
C(13)	41(1)	10(1)	40(1)	2(1)	3(1)	4(1)

Table 2.8: Hydrogen coordinates (x 10^4) and isotropic displacement parameters ($Å^2$x 10^3) for tribromodimethylisophthalate (**1**).

	x	y	z	U(eq)
H(10A)	10031	2322	2364	19
H(10B)	11274	1228	2688	19
H(9A)	12855	-336	1442	19
H(9B)	10870	-775	1653	19
H(7A)	10961	1408	977	18
H(7B)	9091	1090	1289	18
H(2)	9559	5343	1335	20
H(6)	8433	2099	407	18
H(4)	6968	5682	-213	19
H(11A)	14063	1678	2236	20
H(11B)	12842	2917	2031	20
H(15A)	4990	4122	-1647	42
H(15B)	4764	2715	-1372	42
H(15C)	6740	3141	-1592	42
H(13A)	6995	9595	-85	46
H(13B)	8728	9535	373	46
H(13C)	6619	9450	558	46

Table 2.9: Torsion angles [°] for tribromodimethylisophthalate (**1**).

C(8)-C(7)-O(1)-C(1)	170.91(16)
C(10)-C(8)-C(9)-Br(1)	-51.54(19)
C(10)-C(8)-C(7)-O(1)	61.72(19)
C(10)-C(8)-C(11)-Br(3)	-170.35(12)
C(9)-C(8)-C(10)-Br(2)	-53.72(19)
C(9)-C(8)-C(7)-O(1)	-175.05(15)
C(9)-C(8)-C(11)-Br(3)	67.14(18)
C(7)-C(8)-C(10)-Br(2)	65.72(17)
C(7)-C(8)-C(9)-Br(1)	-172.61(13)
C(7)-C(8)-C(11)-Br(3)	-52.39(19)
C(7)-O(1)-C(1)-C(2)	-172.41(17)
C(7)-O(1)-C(1)-C(6)	7.8(3)
C(2)-C(3)-C(12)-O(3)	177.44(17)
C(2)-C(3)-C(12)-O(2)	-3.3(3)
C(2)-C(3)-C(4)-C(5)	0.4(3)
C(5)-C(6)-C(1)-O(1)	-179.74(18)
C(5)-C(6)-C(1)-C(2)	0.5(3)
C(3)-C(2)-C(1)-O(1)	179.66(17)
C(3)-C(2)-C(1)-C(6)	-0.5(3)
C(6)-C(5)-C(14)-O(4)	0.6(3)
C(6)-C(5)-C(14)-O(5)	-178.37(17)
C(6)-C(5)-C(4)-C(3)	-0.4(3)
C(1)-C(2)-C(3)-C(12)	-178.93(18)
C(1)-C(2)-C(3)-C(4)	0.1(3)

C(12)-C(3)-C(4)-C(5)	179.36(18)
C(14)-C(5)-C(6)-C(1)	177.73(17)
C(14)-C(5)-C(4)-C(3)	-178.05(17)
C(4)-C(5)-C(6)-C(1)	0.0(3)
C(4)-C(5)-C(14)-O(4)	178.3(2)
C(4)-C(5)-C(14)-O(5)	-0.7(3)
C(4)-C(3)-C(12)-O(3)	-1.6(3)
C(4)-C(3)-C(12)-O(2)	177.7(2)
C(11)-C(8)-C(10)-Br(2)	-175.42(12)
C(11)-C(8)-C(9)-Br(1)	65.43(18)
C(11)-C(8)-C(7)-O(1)	-52.5(2)
C(15)-O(5)-C(14)-O(4)	-4.7(3)
C(15)-O(5)-C(14)-C(5)	174.31(17)
C(13)-O(3)-C(12)-O(2)	0.9(3)
C(13)-O(3)-C(12)-C(3)	-179.80(18)

Symmetry transformations used to generate equivalent atoms.

Figure 2.9: ^{1}H NMR spectrum of Dimethyl 5-(3-bromo-2,2-bis(bromomethyl)propoxy)isophthalate [$C_{15}H_{17}Br_3O_5$],) in $CDCl_3$ (600 MHz, calibrated at 7.26 ppm) **1.**

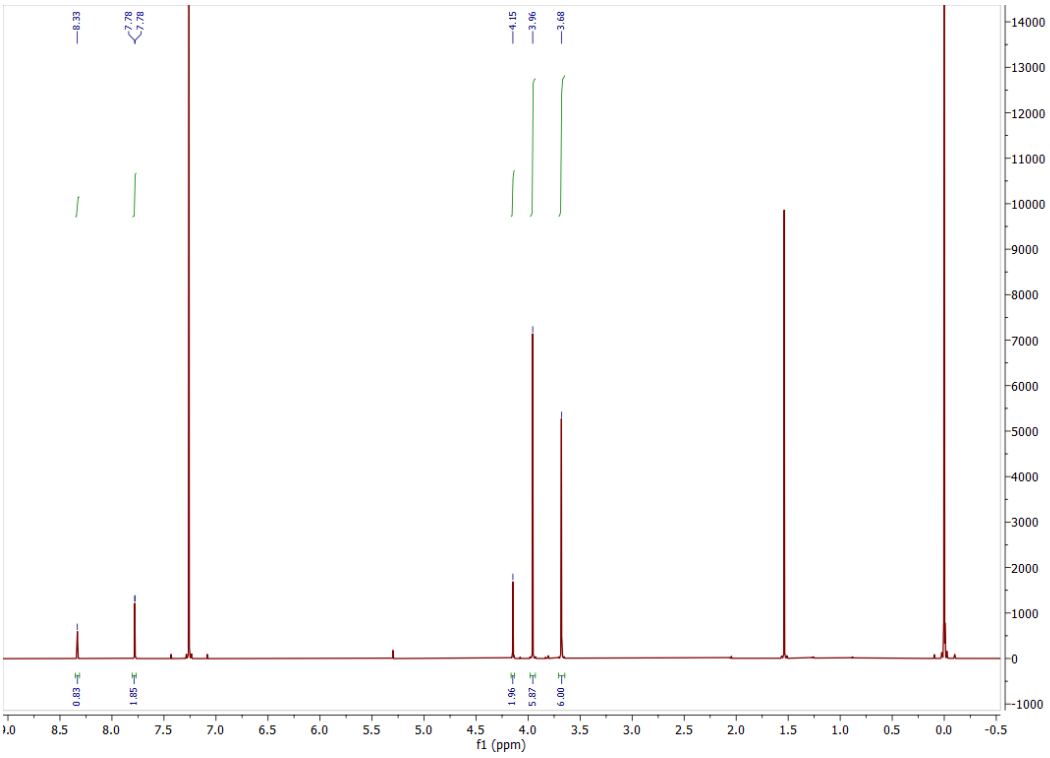

Figure 2.10: ^{13}C NMR spectrum of Dimethyl 5-(3-bromo-2,2-bis(bromomethyl)propoxy)isophthalate [$C_{15}H_{17}Br_3O_5$],) in $CDCl_3$ (600 MHz, at 77.36 ppm) **1.**

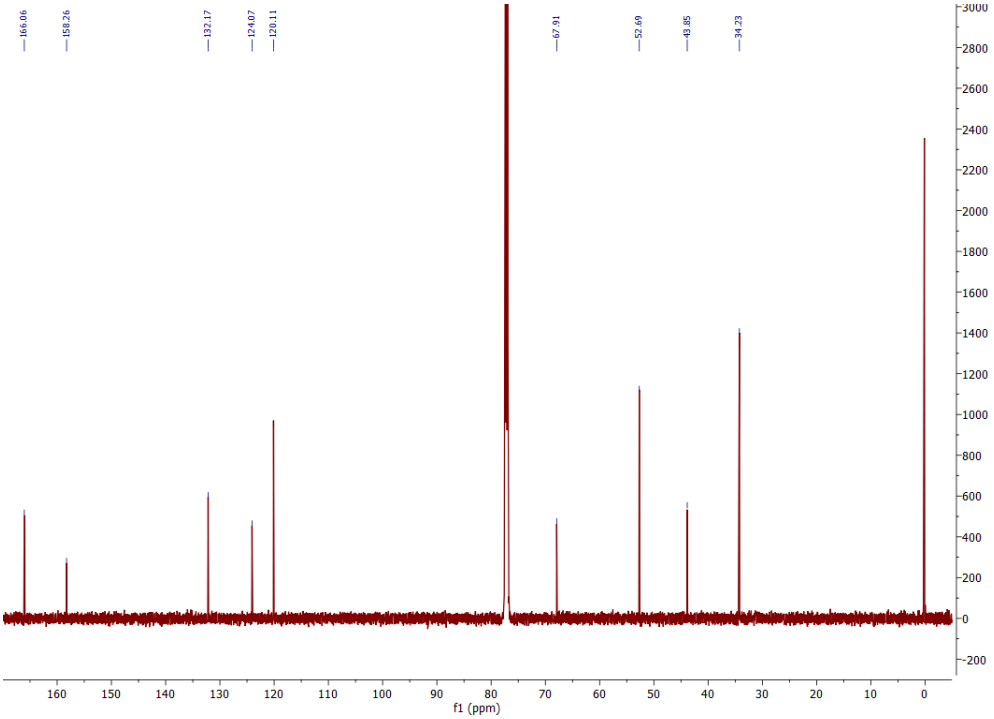

Figure 2.11: Mass Spectrum of Dimethyl 5-(3-bromo-2,2-bis(bromomethyl)propoxy)isophthalate [$C_{15}H_{17}Br_3O_5$], **1**.

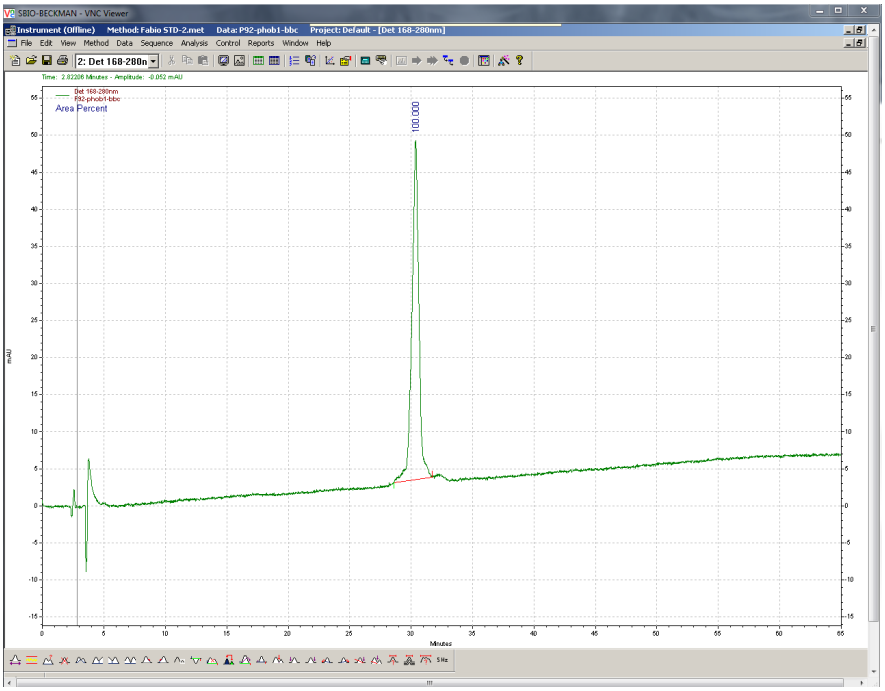

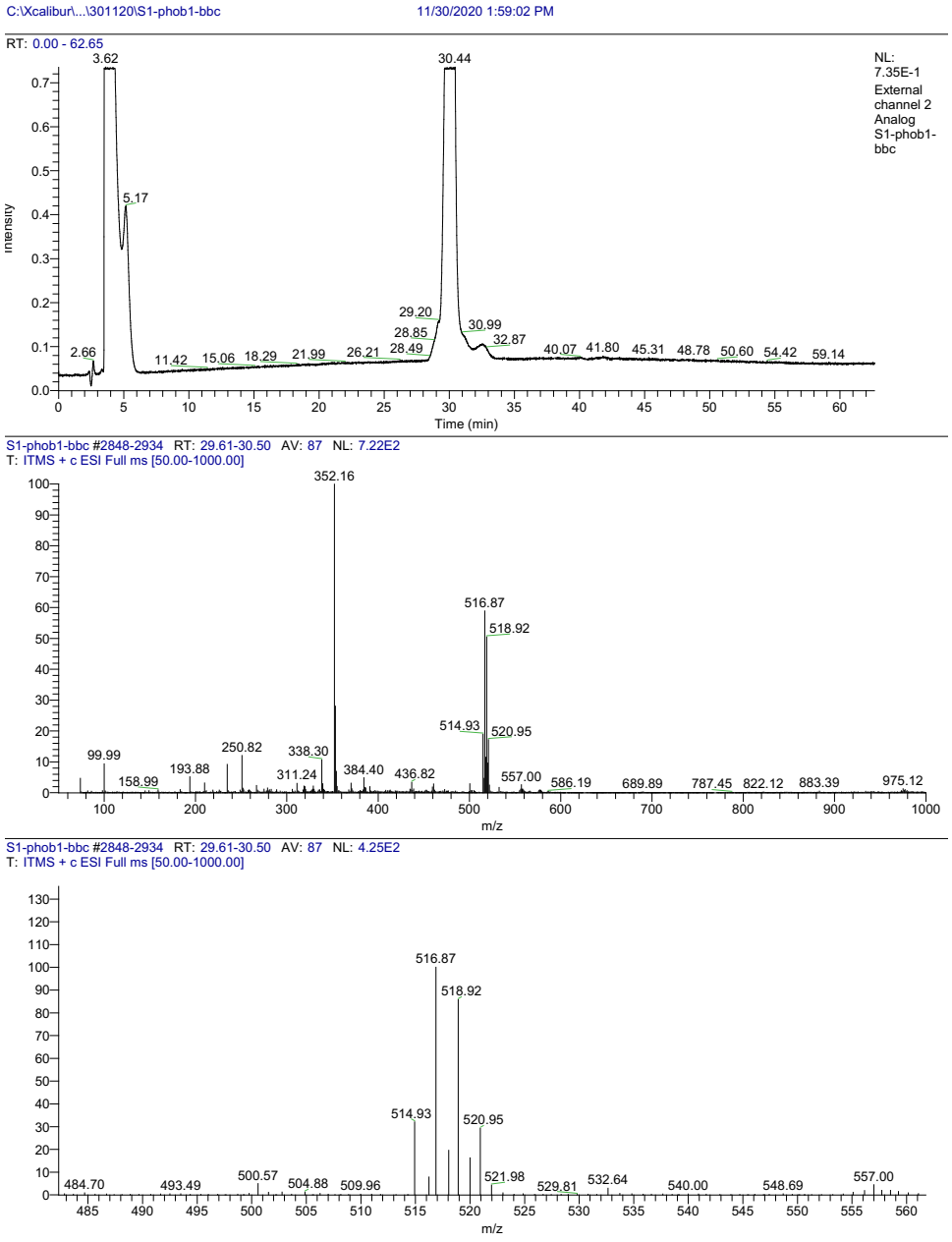
C:\Xcalibur\...\301120\S1-phob1-bbc 11/30/2020 1:59:02 PM
RT: 0.00 - 62.65
NL: 7.35E-1
External channel 2 Analog S1-phob1-bbc
Intensity
Time (min)
S1-phob1-bbc #2848-2934 RT: 29.61-30.50 AV: 87 NL: 7.22E2
T: ITMS + c ESI Full ms [50.00-1000.00]
m/z
S1-phob1-bbc #2848-2934 RT: 29.61-30.50 AV: 87 NL: 4.25E2
T: ITMS + c ESI Full ms [50.00-1000.00]
m/z

Figure 2.12: ^{1}H-NMR spectrum of 3-(methoxycarbonyl)-5-(3-(tritylthio)-2,2- bis((tritylthio)methyl)propoxy)benzoic acid, [$C_{71}H_{60}O_5S_3$]) in $CDCl_3$ (600 MHz, calibrated at 7.26 ppm) **2.**

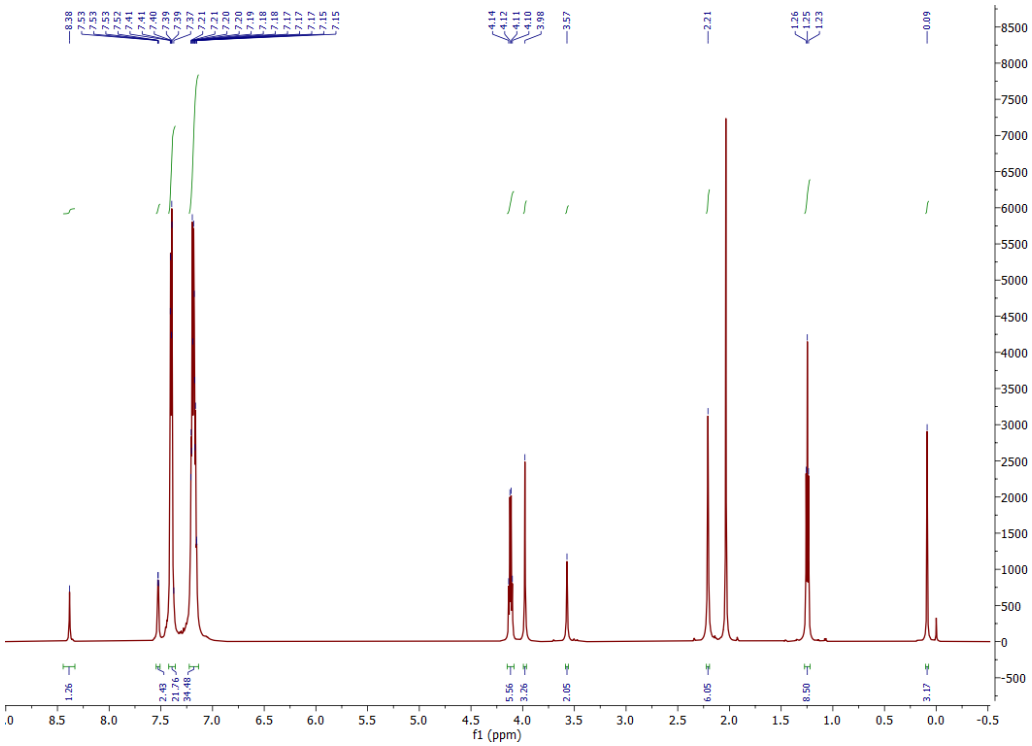

Figure 2.13: ^{13}C-NMR spectrum of 3-(methoxycarbonyl)-5-(3-(tritylthio)-2,2- bis((tritylthio)methyl)propoxy)benzoic acid, [$C_{71}H_{60}O_5S_3$]) in $CDCl_3$ (600 MHz, calibrated at 77.36 ppm) **2.**

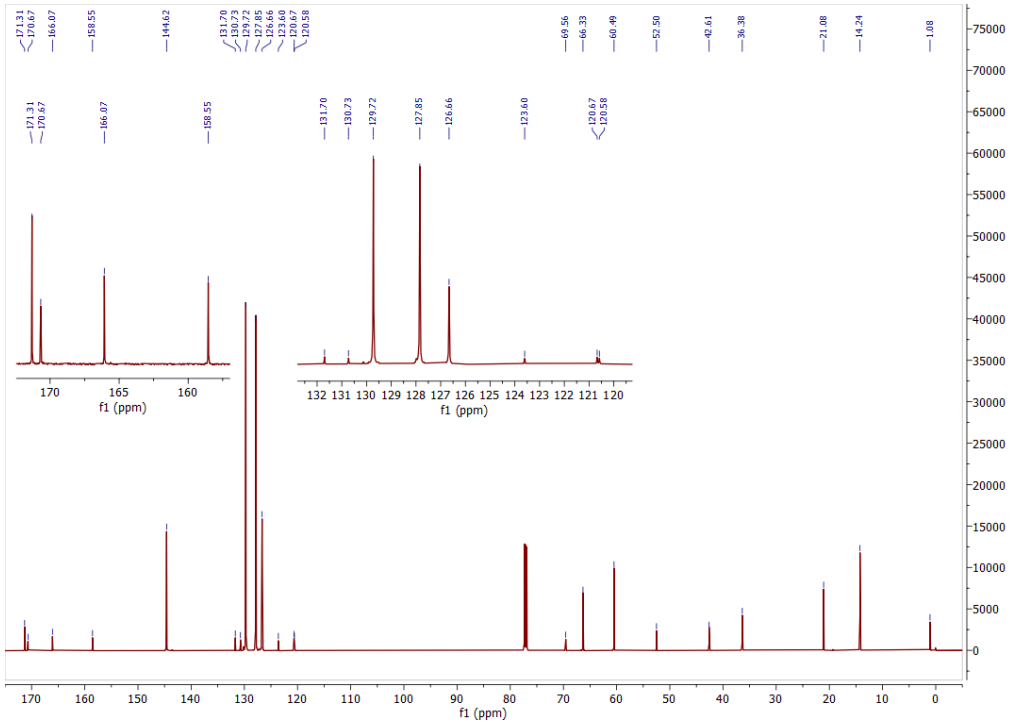

Figure 2.14: Mass spectrum of 3-(methoxycarbonyl)-5-(3-(tritylthio)-2,2-bis((tritylthio)methyl)propoxy)benzoic acid, [$C_{71}H_{60}O_5S_3$] **2.**

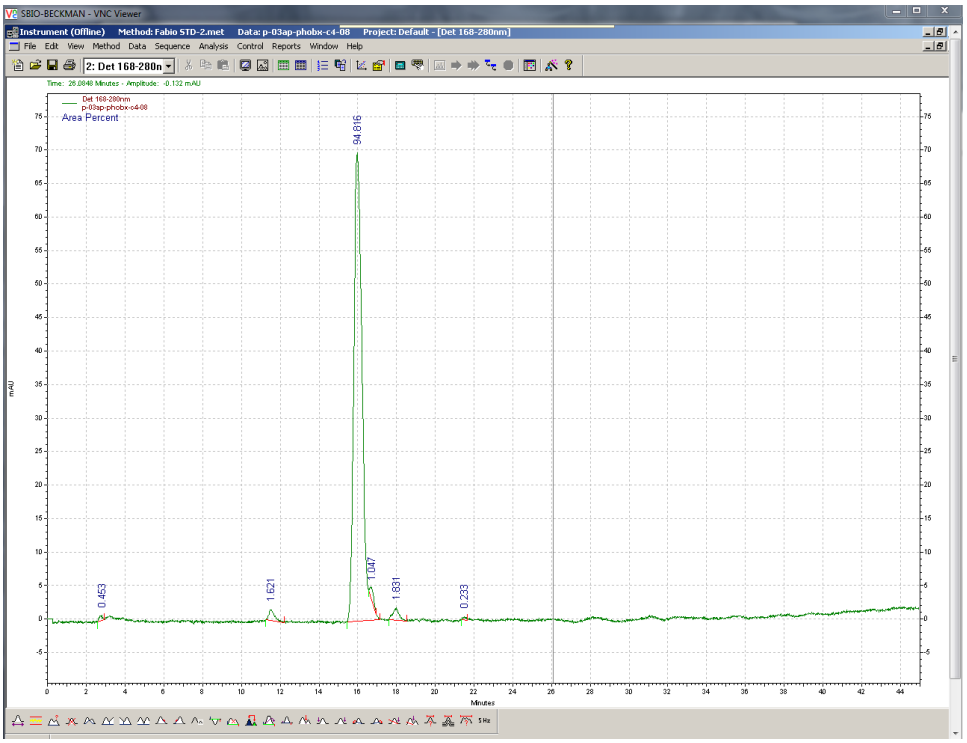

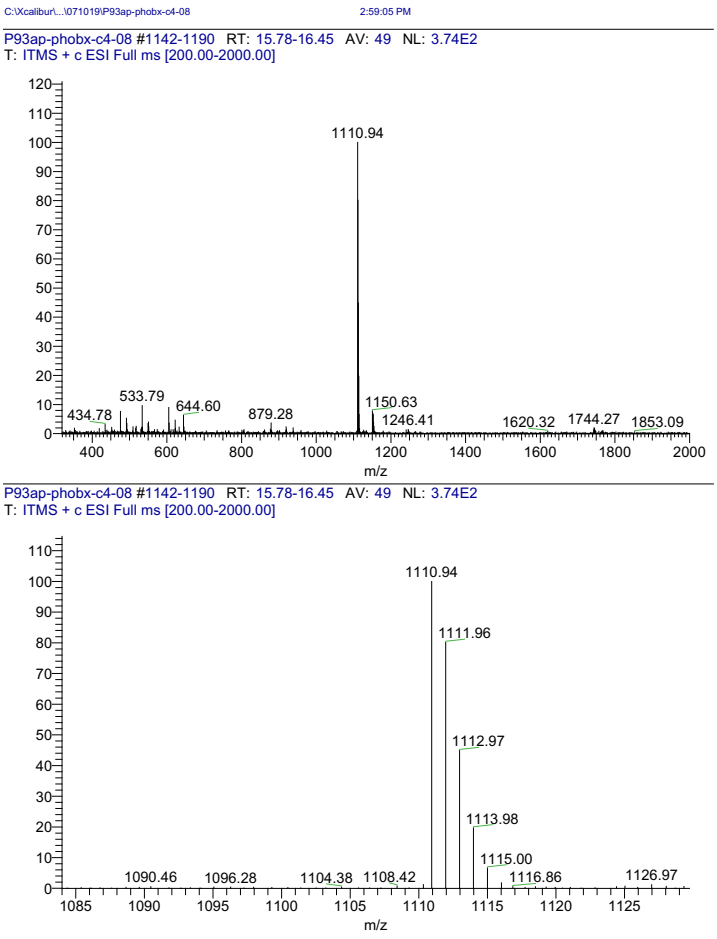
C:\Xcalibur\...\071019\P93ap-phobx-c4-08 2:59:05 PM
P93ap-phobx-c4-08 #1142-1190 RT: 15.78-16.45 AV: 49 NL: 3.74E2
T: ITMS + c ESI Full ms [200.00-2000.00]
1110.94
533.79
644.60
434.78
879.28
1150.63
1246.41
1620.32
1744.27
1853.09
m/z
P93ap-phobx-c4-08 #1142-1190 RT: 15.78-16.45 AV: 49 NL: 3.74E2
T: ITMS + c ESI Full ms [200.00-2000.00]
1110.94
1111.96
1112.97
1113.98
1115.00
1090.46
1096.28
1104.38
1108.42
1116.86
1126.97
m/z

Figure 2.15: LC-ESI-MS data of Trithiol(b)-(Ser)$_2$-RM2 (**3**). 'Trithiol(b)'-SS-dPhe-QWAVGH-Sta-L-CONH$_2$. Calc MW: 1631 Da. 47 mg >90 % purity.

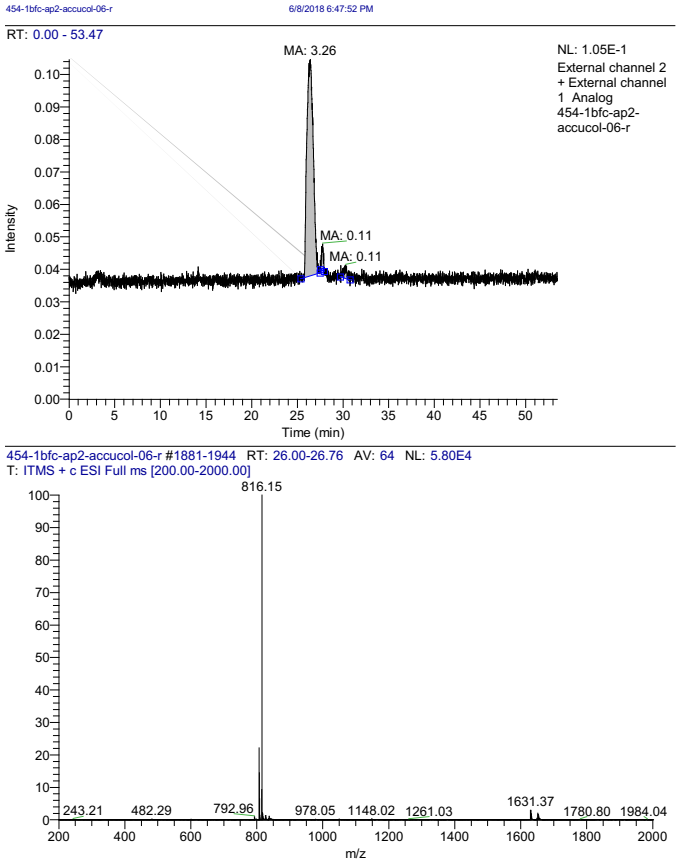

Figure 2.16: LC-ESI-MS data of non-radioactive As-trithiol(b)-$(Ser)_2$-RM2, **5**. Calc MW: 1703 Da. >95 % purity.

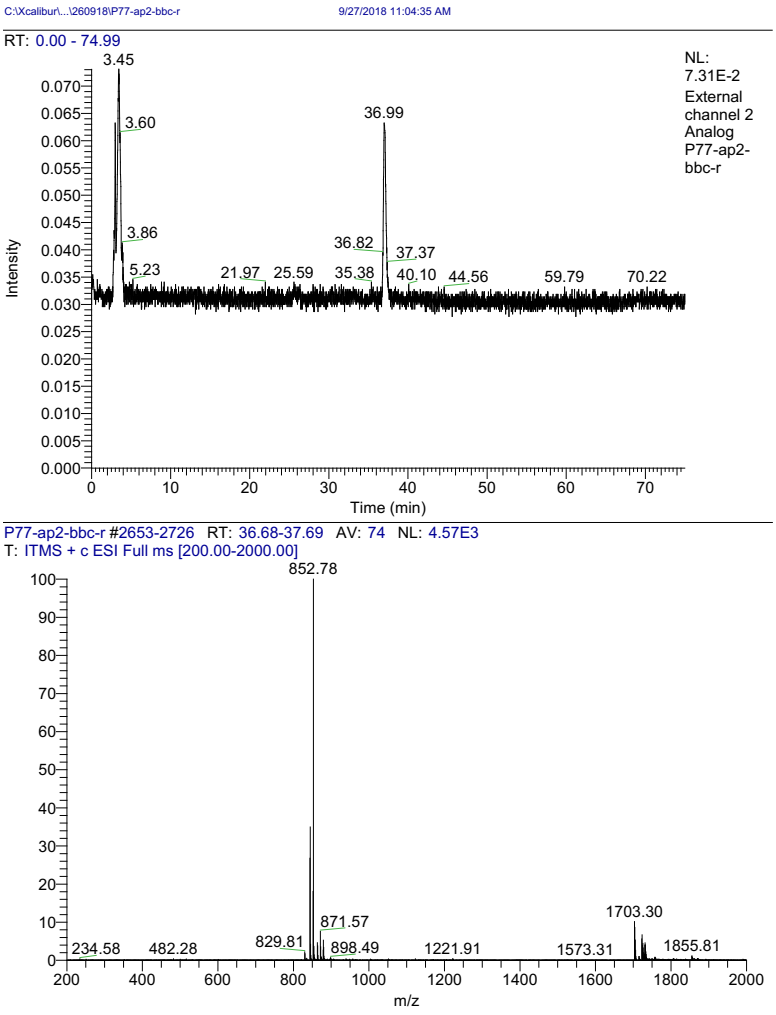

Figure 2.17: RP HPLC chromatogram of non-radioactive As-trithiol(b)-$(Ser)_2$-RM2, **5 (**Wavelength 280 nm).

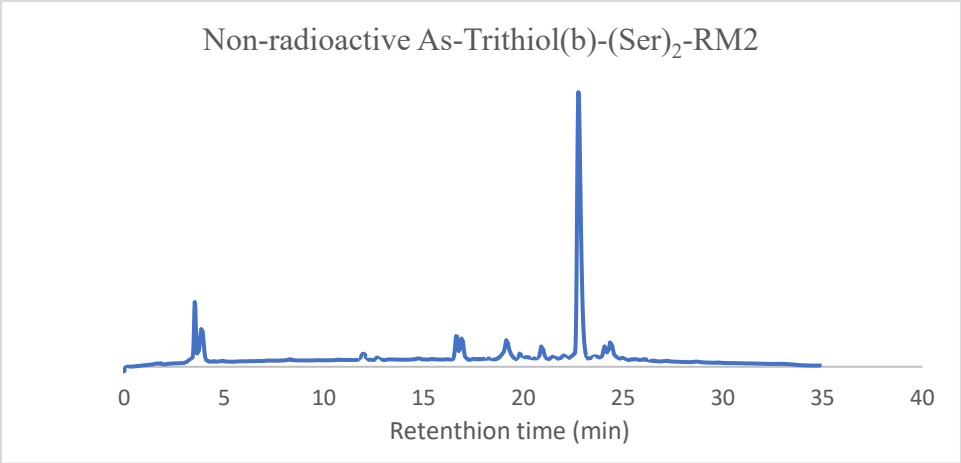

Figure 3.2: ^{1}H NMR spectrum of 5-(3-(tritylthio)-2,2-bis((tritylthio)methyl)propoxy)isophthalic acid, (**2-3**) in CD_2Cl_2 (600 MHz, calibrated to residual $CHDCl_2$ at 5.32 ppm).

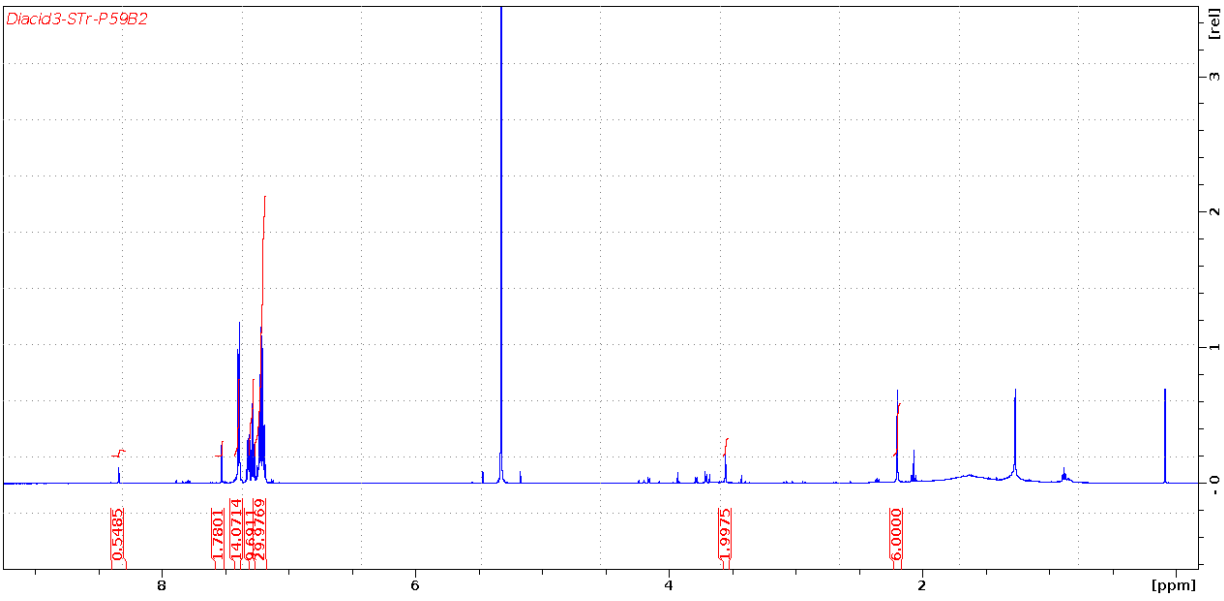

Figure 3.3: ^{13}C NMR spectrum of 5-(3-(tritylthio)-2,2-bis((tritylthio)methyl)propoxy)isophthalic acid, (**2-3**) in CD_2Cl_2 (600 MHz, calibrated at 53.5 ppm).

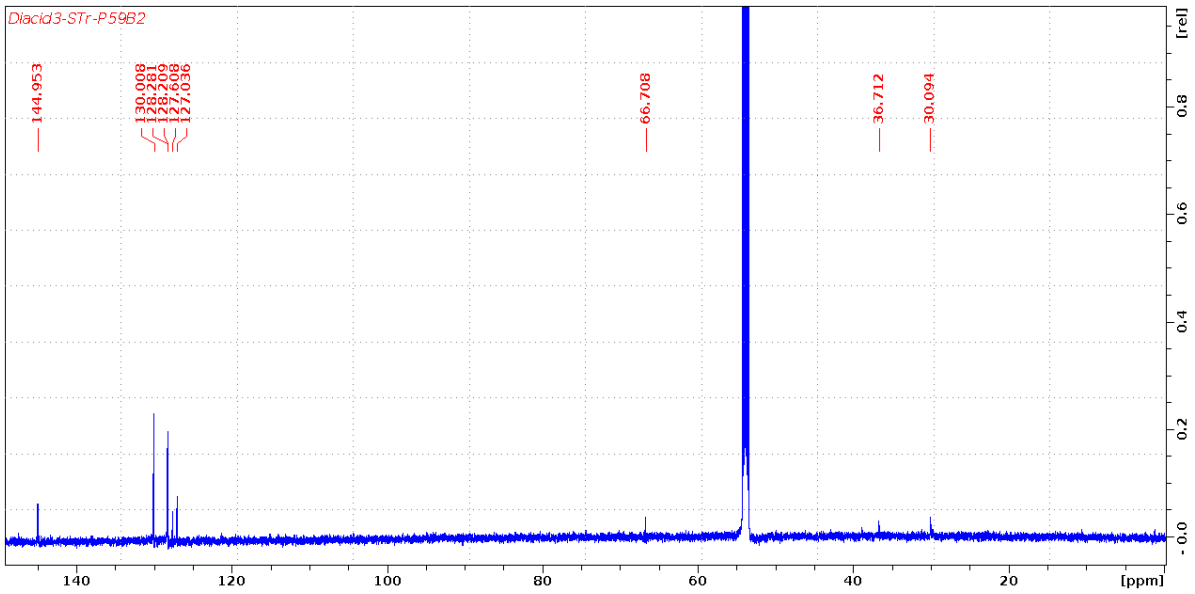
Diacid3-STr-P59B2
144.953
130.008
128.281
127.609
127.208
127.036
66.708
36.712
30.094
[rel]
0.8
0.6
0.4
0.2
0.0
140
120
100
80
60
40
20
[ppm]

Figure 3.4: ^{1}H NMR spectrum of 3-(((2,5-dioxopyrrolidin-1-yl)oxy)carbonyl)-5-(3-(tritylthio)-2,2-bis((tritylthio)methyl)propoxy)benzoic acid (**4-3**) in CD_2Cl_2 (500 MHz, calibrated to residual $CHDCl_2$ at 5.32 ppm).

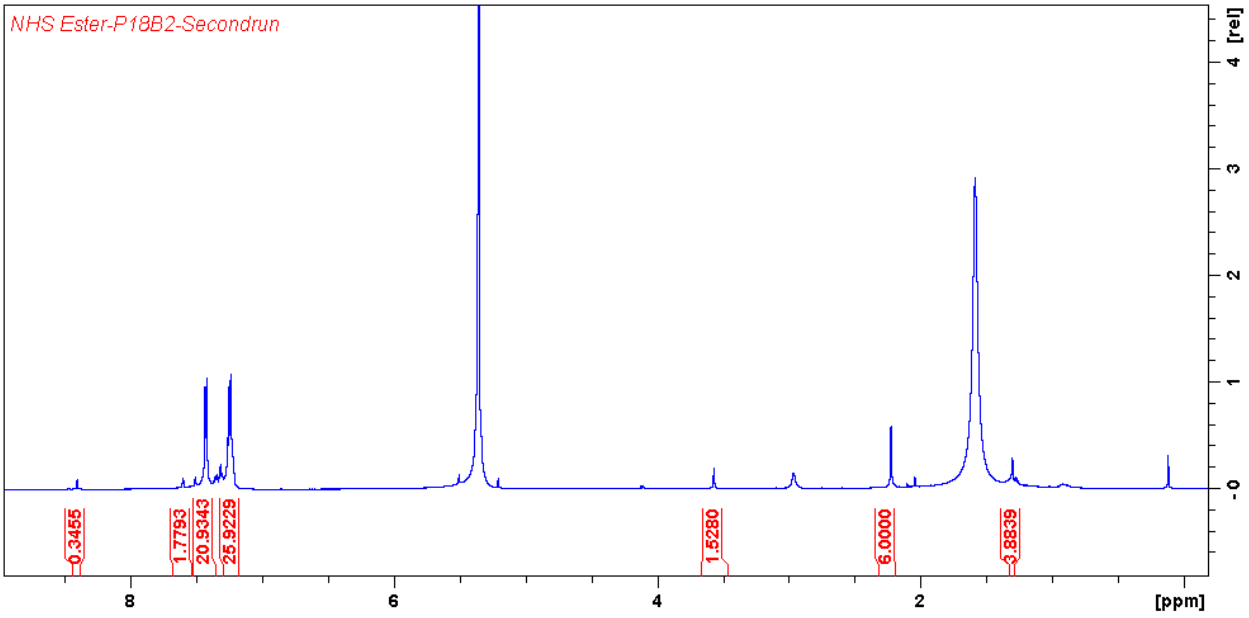

Figure 3.5: ^{13}C NMR spectrum of 3-(((2,5-dioxopyrrolidin-1-yl)oxy)carbonyl)-5-(3-(tritylthio)-2,2-bis((tritylthio)methyl)propoxy)benzoic acid (**4-3**) in CD_2Cl_2 (500 MHz, calibrated at 53.5 ppm).

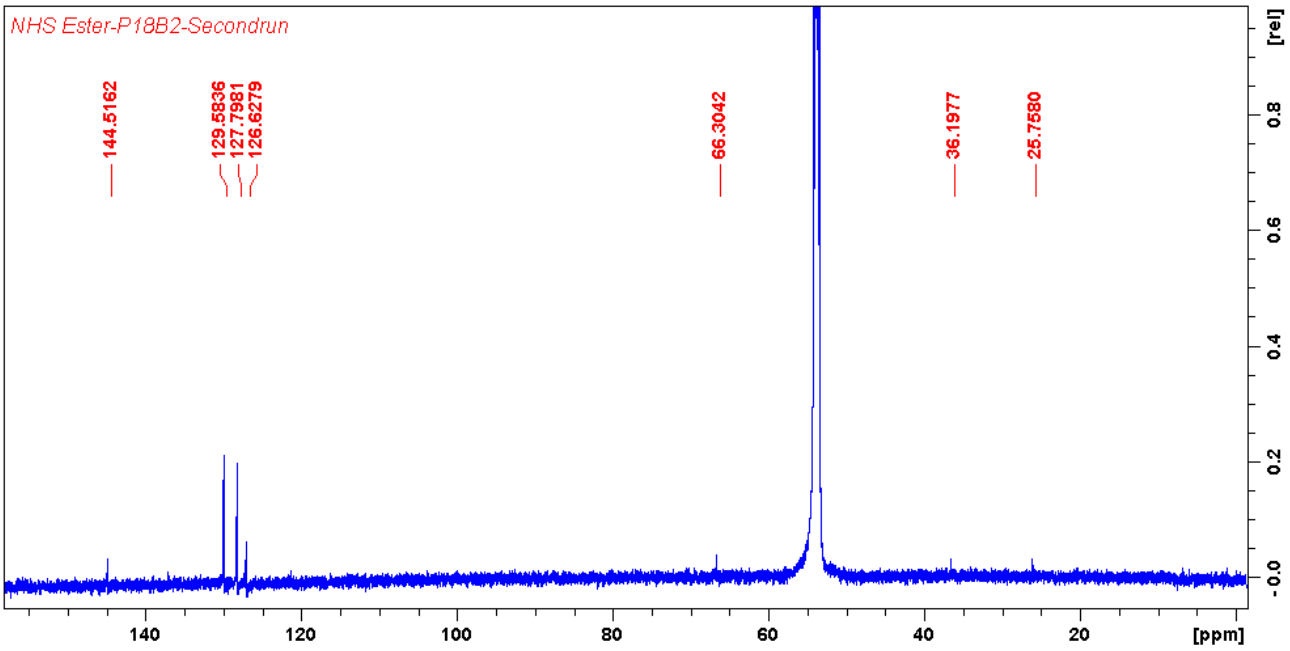

Figure 3.6: LC-ESI-MS of 3-(((2,5-dioxopyrrolidin-1-yl)oxy)carbonyl)-5-(3-(tritylthio)-2,2-bis((tritylthio)methyl)propoxy)benzoic acid (**4-3**).

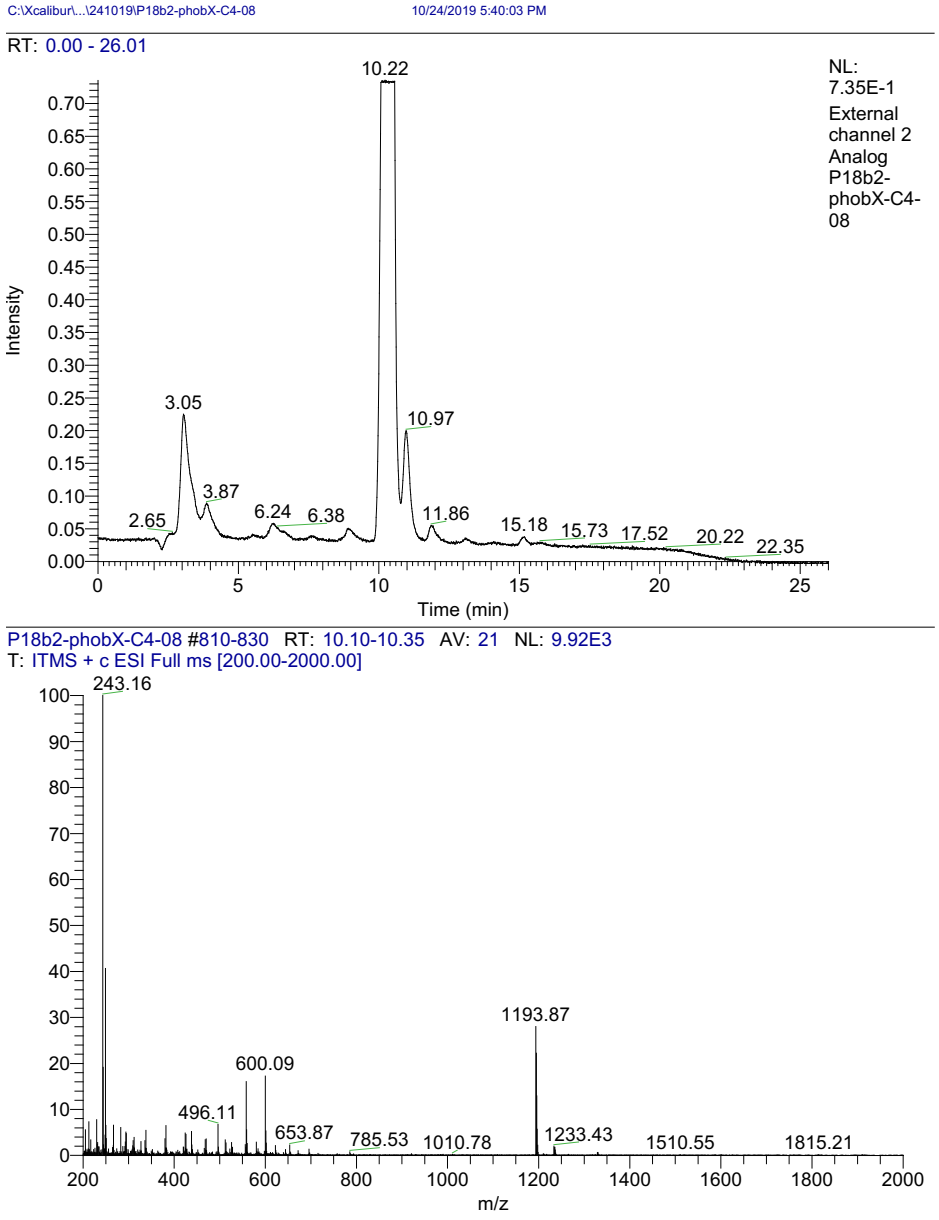

Figure 3.7: LC-ESI-MS of 3-(((2,5-dioxopyrrolidin-1-yl)oxy)carbonyl)-5-(3-mercapto-2,2-bis(mercaptomethyl)propoxy)benzoic acid, $C_{17}H_{19}NO_7S_3$ (**5-3**).

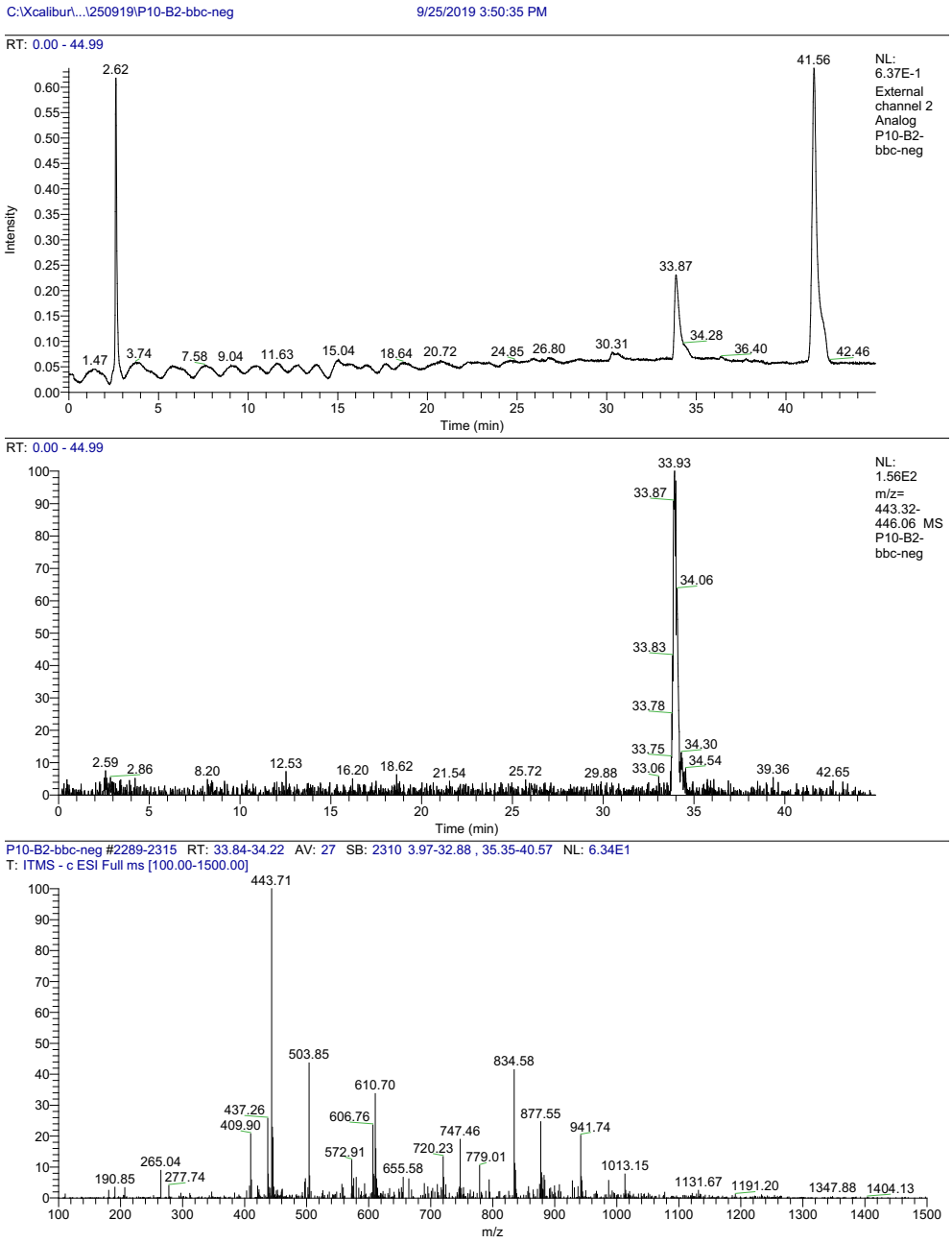

Figure 3.8: HPLC chromatogram of protein standard: thyroglobulin (at 6.37 min), γ-globulin (at 8.95 min), Ovalbumin (at 10.7 min), ribonuclease A (at 11.87 min), *p*-aminobenzoic acid (at 14.49 min).

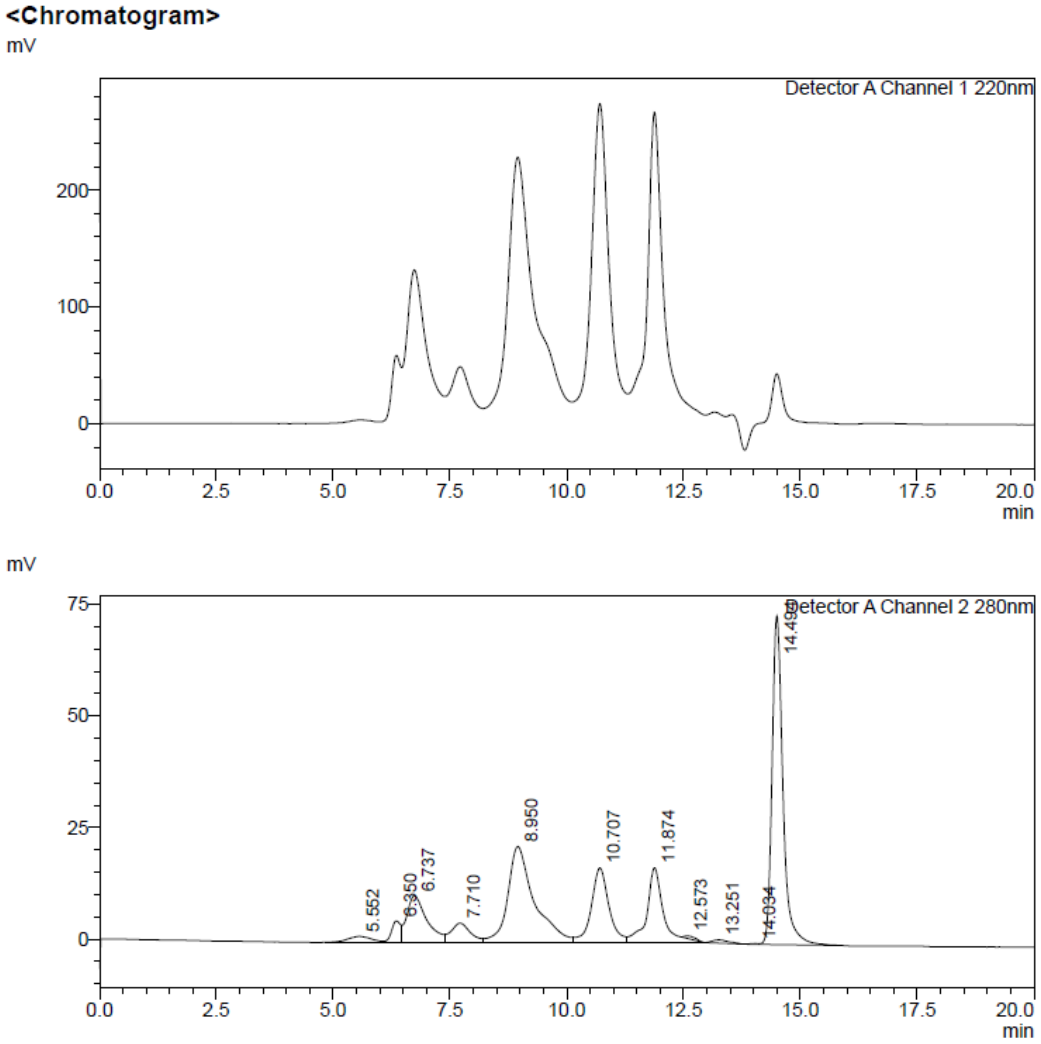

Figure 3.9: HPLC chromatogram of Native Antibody (Herceptin).

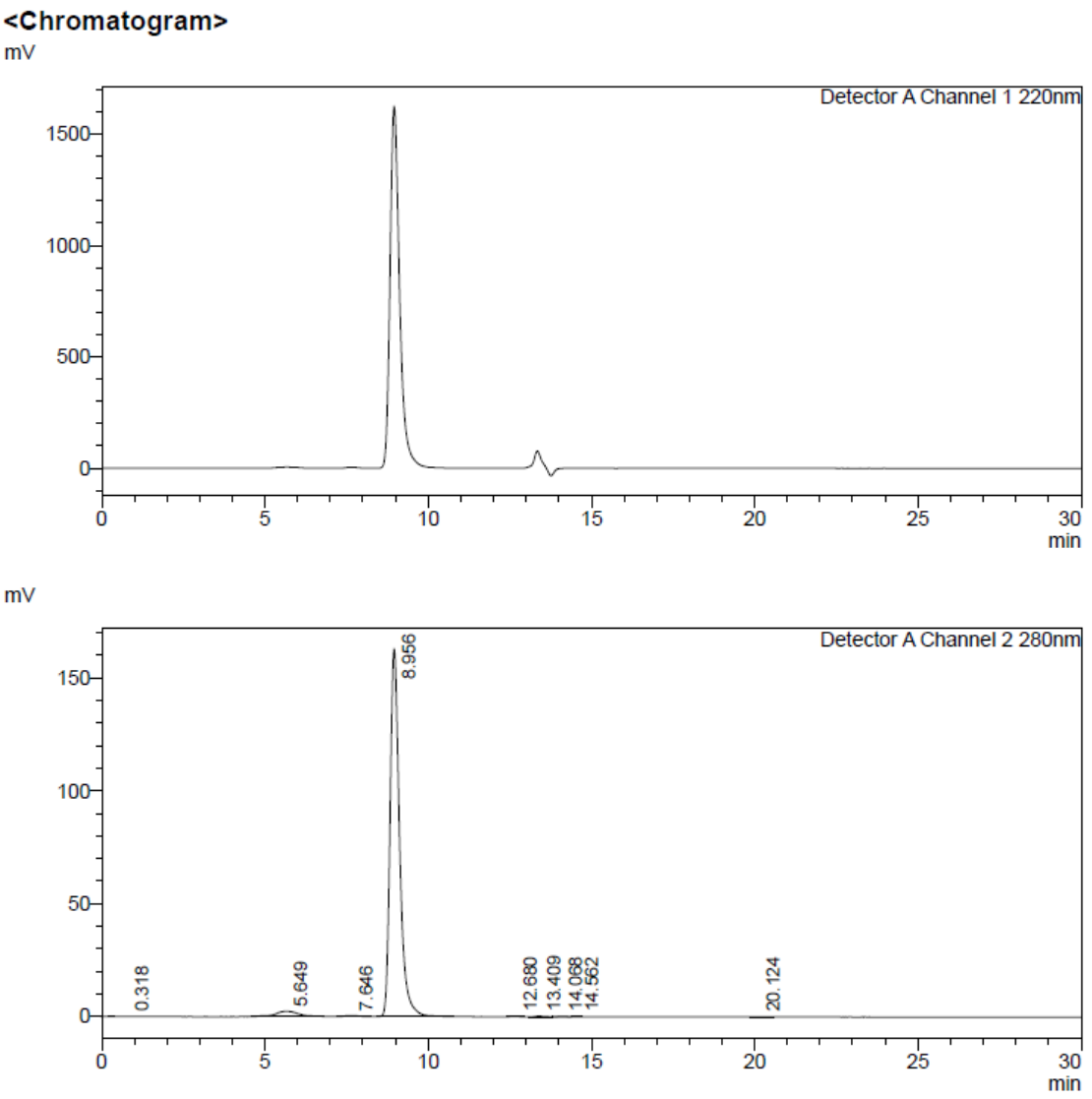

Figure 3.10: HPLC chromatogram of crude conjugated Herceptin-trithiol (eluted at 9.03 min) (top); purified Herceptin-trithiol (bottom). The peak at 13.51 min is free unreacted NHS active ester-trithiol and the peak at 18.23 min is excess EDC.

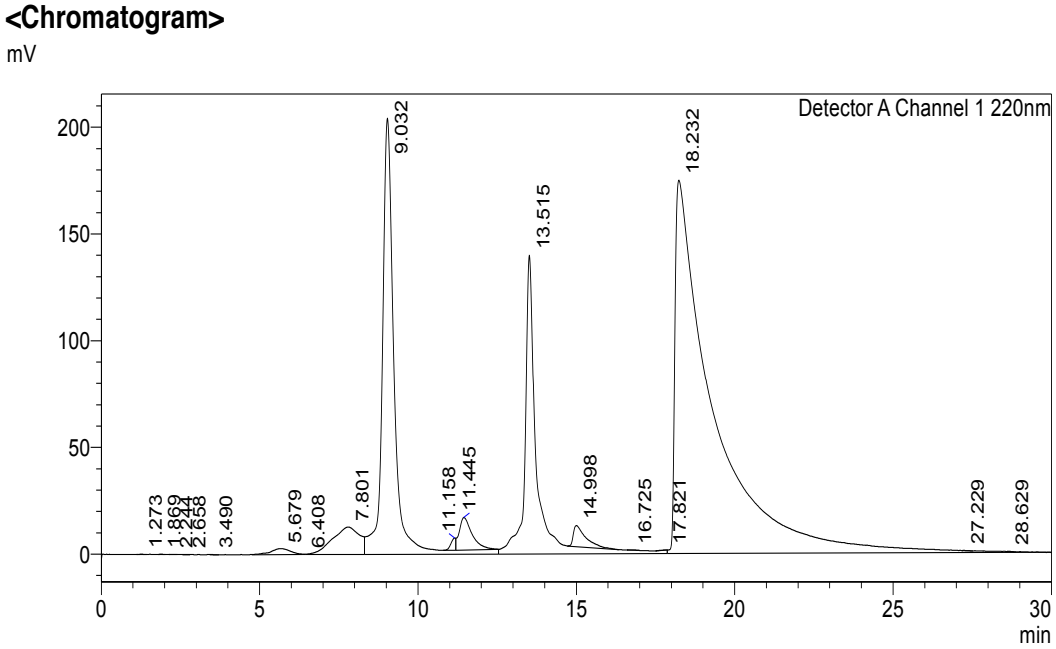

<Chromatogram>

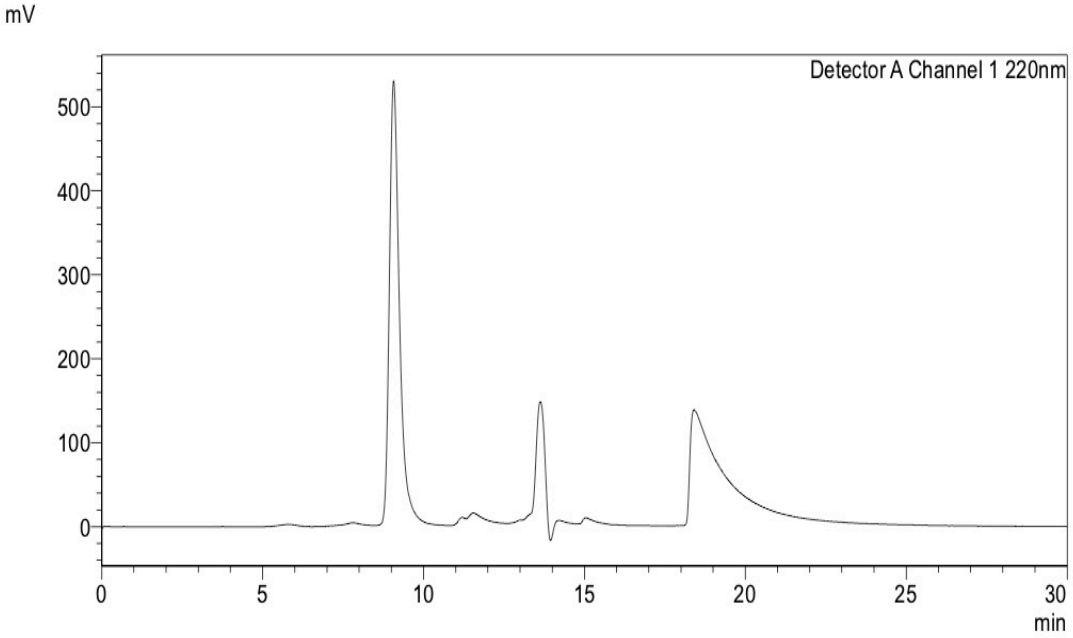

Figure 3.11: High resolution mass spectrum on Herceptin-Trithiol conjugation.

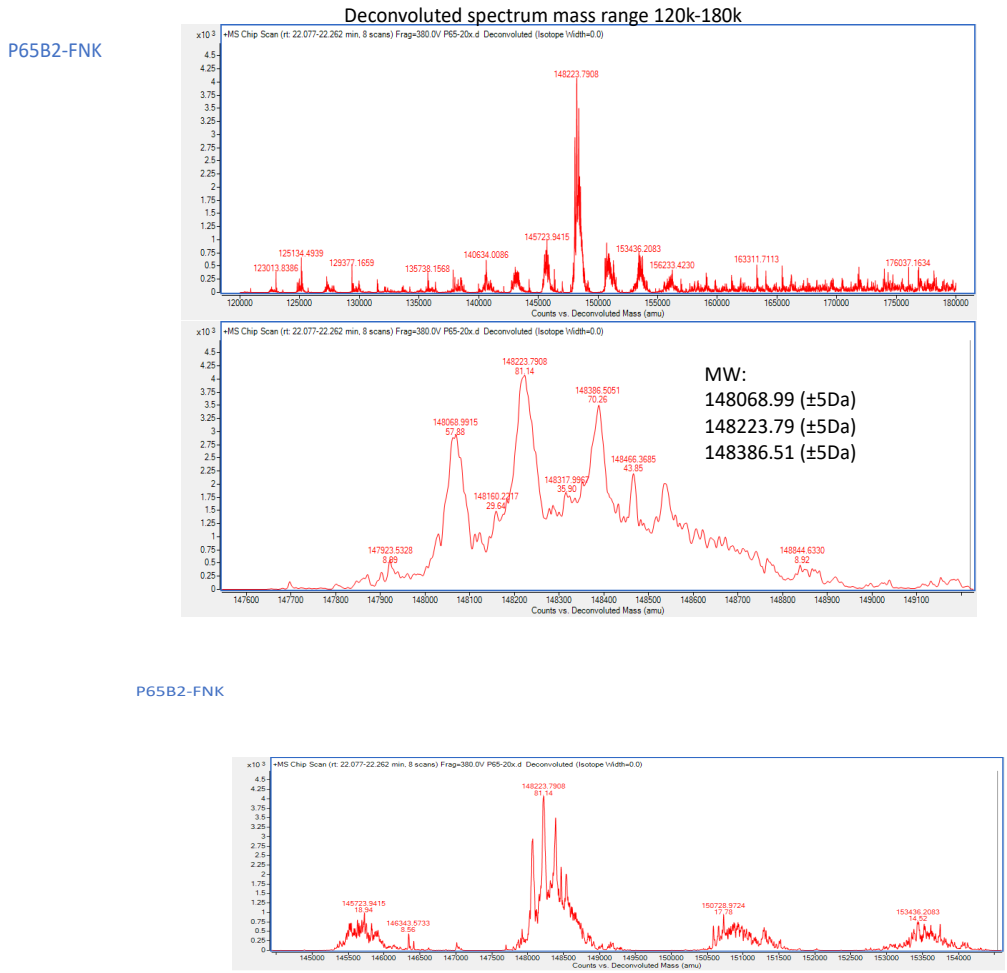

Smaller MW Species

P65B2-FNK

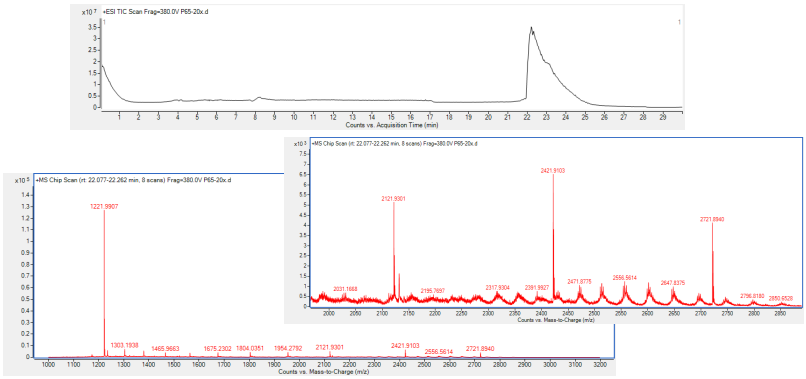

Figure 3.13: a) HPLC chromatogram of Compound **5-3** (at 13.4 min) **b)** Radiolabeling chromatogram of Herceptin-Trithiol conjugate (6-3) with $^{77}As(SR)_3$. The chromatogram indicates radiolabeling of a species with a lower molecular weight (maybe free trithiol) after denaturing of Herceptin-Trithiol conjugate.

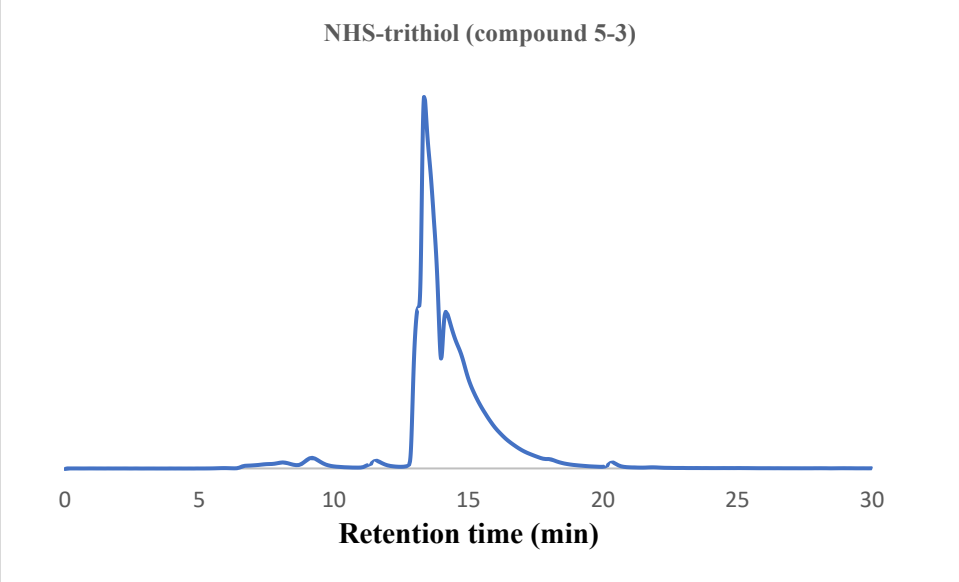

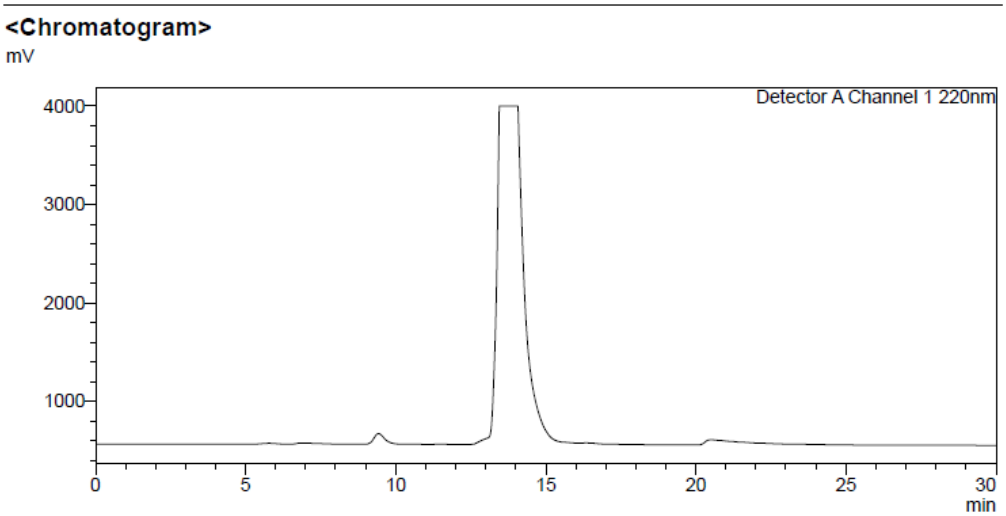

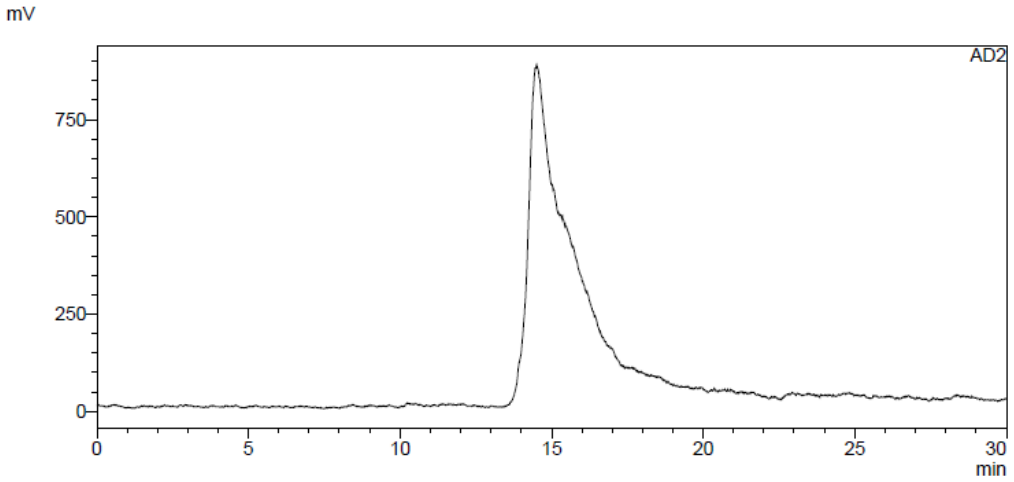
mV
AD2
750
500
250
0
0
5
10
15
20
25
30
min

Table 3.1: Crystal data and structure refinement for 5-(3-mercapto-2,2-bis(mercaptomethyl)propoxy)isophthalic acid (**3-3**).

Identification code	s1
Empirical formula	C30 H38 O12 S6
Formula weight	782.96
Temperature	100.0 K
Wavelength	0.71073 Å
Crystal system	Monoclinic
Space group	C 1 2/c 1
Unit cell dimensions	a = 8.5559(10) Å
α=90°.	
	b = 9.6839(12) Å
β=93.930(4)°.	
	c = 41.059(5) Å
γ=90°.	
Volume	3393.9(7) $Å^3$
Z	4
Density (calculated)	1.532 Mg/m^3
Absorption coefficient	0.466 mm^{-1}
F(000)	1640
Crystal size	0.42 x 0.1 x 0.1 mm^3

Theta range for data collection	2.984 to 26.424°.
Index ranges.	-10<=h<=10, -11<=k<=12, - 51<=l<=51
Reflections collected	31111
Independent reflections	3467 [R(int) = 0.0968]
Completeness to theta = 25.242°	99.9 %
Absorption correction	Semi-empirical from equivalents
Max. and min. transmission	0.7454 and 0.6238
Refinement method	Full-matrix least-squares on F^2
Data / restraints / parameters	3467 / 2 / 227
Goodness-of-fit on F^2	1.204
Final R indices [I>2sigma(I)]	R1 = 0.0840, wR2 = 0.1597
R indices (all data)	R1 = 0.1073, wR2 = 0.1676
Extinction coefficient	n/a
Largest diff. peak and hole	1.017 and -0.468 e.Å

Table 3.2: Atomic coordinates (x 10^4) and equivalent isotropic displacement parameters (Å^{2}x 10^3) for 5-(3-mercapto-2,2-bis(mercaptomethyl)propoxy)isophthalic acid (**3-3**). U(eq) is defined as one third of the trace of the orthogonalized U^{ij} tensor.

	x	y	z	U(eq)
S(2)	10890(2)	1375(2)	3060(1)	22(1)
S(1)	10872(2)	3454(1)	3149(1)	22(1)
S(3)	6122(2)	3048(2)	2430(1)	20(1)
O(1)	5890(4)	1678(4)	3369(1)	16(1)
O(5)	3739(5)	5661(4)	3979(1)	23(1)
O(3)	1994(4)	-398(4)	4410(1)	21(1)
O(4)	2195(5)	4746(4)	4343(1)	24(1)
O(2)	3257(4)	-1680(4)	4057(1)	19(1)
C(13)	3061(6)	4611(6)	4121(1)	18(1)
C(3)	3364(6)	778(5)	4014(1)	14(1)
C(1)	4919(5)	1873(5)	3621(1)	14(1)
C(10)	8913(6)	1227(5)	3186(1)	15(1)
C(8)	7885(5)	2377(5)	3020(1)	12(1)
C(11)	7104(6)	1795(5)	2702(1)	16(1)
C(5)	3484(6)	3243(5)	3988(1)	16(1)

C(6)	4491(5)	3156(5)	3733(1)	15(1)
C(12)	2875(6)	-546(5)	4159(1)	15(1)
C(4)	2903(6)	2053(5)	4124(1)	16(1)
C(2)	4379(5)	676(5)	3761(1)	13(1)
C(9)	8934(6)	3645(6)	2945(1)	18(1)
C(7)	6691(6)	2858(5)	3258(1)	13(1)
O(1S)	1232(5)	7196(4)	4618(1)	26(1)
C(1S)	316(7)	6812(7)	4884(1)	28(1)
C(2S)	-276(8)	8089(8)	5033(2)	45(2)

Table 3.3: Bond lengths [Å] and angles [°] for 5-(3-mercapto-2,2-bis(mercaptomethyl)propoxy)isophthalic acid (**3-3**).

S(2)-S(1)	2.046(2)
S(2)-C(10)	1.809(5)
S(1)-C(9)	1.814(5)
S(3)-S(3)#1	2.042(3)
S(3)-C(11)	1.817(5)
O(1)-C(1)	1.382(6)
O(1)-C(7)	1.424(6)
O(5)-C(13)	1.325(7)
O(3)-C(12)	1.326(6)
O(4)-C(13)	1.222(6)
O(2)-C(12)	1.228(6)
C(13)-C(5)	1.487(7)
C(3)-C(12)	1.486(7)
C(3)-C(4)	1.383(7)
C(3)-C(2)	1.401(7)
C(1)-C(6)	1.383(7)
C(1)-C(2)	1.388(7)

C(10)-C(8)	1.548(7)
C(8)-C(11)	1.532(7)
C(8)-C(9)	1.563(7)
C(8)-C(7)	1.532(6)
C(5)-C(6)	1.403(7)
C(5)-C(4)	1.389(7)
O(1S)-C(1S)	1.437(6)
C(1S)-C(2S)	1.483(9)

C(10)-S(2)-S(1)	90.46(18)
C(9)-S(1)-S(2)	92.07(19)
C(11)-S(3)-S(3)#1	103.32(17)
C(1)-O(1)-C(7)	117.2(4)
O(5)-C(13)-C(5)	113.5(4)
O(4)-C(13)-O(5)	123.5(5)
O(4)-C(13)-C(5)	123.0(5)
C(4)-C(3)-C(12)	123.0(4)
C(4)-C(3)-C(2)	120.7(5)
C(2)-C(3)-C(12)	116.2(5)
O(1)-C(1)-C(6)	123.9(5)

O(1)-C(1)-C(2)	115.5(4)
C(6)-C(1)-C(2)	120.6(4)
C(8)-C(10)-S(2)	109.3(3)
C(10)-C(8)-C(9)	109.5(4)
C(11)-C(8)-C(10)	108.1(4)
C(11)-C(8)-C(9)	110.1(4)
C(11)-C(8)-C(7)	112.5(4)
C(7)-C(8)-C(10)	108.8(4)
C(7)-C(8)-C(9)	107.7(4)
C(8)-C(11)-S(3)	115.8(4)
C(6)-C(5)-C(13)	120.3(5)
C(4)-C(5)-C(13)	119.2(4)
C(4)-C(5)-C(6)	120.4(5)
C(1)-C(6)-C(5)	119.5(5)
O(3)-C(12)-C(3)	114.1(4)
O(2)-C(12)-O(3)	122.7(5)
O(2)-C(12)-C(3)	123.1(5)
C(3)-C(4)-C(5)	119.4(5)
C(1)-C(2)-C(3)	119.4(5)
C(8)-C(9)-S(1)	110.4(4)

O(1)-C(7)-C(8)	108.5(4)
O(1S)-C(1S)-C(2S)	108.5(5)

–

Symmetry transformations used to generate equivalent atoms:

#1 -x+1,y,-z+1/2

Table 3.4: Anisotropic displacement parameters ($Å^2 x\ 10^3$) for 5-(3-mercapto-2,2-bis(mercaptomethyl)propoxy)isophthalic acid (**3-3**). The anisotropic displacement factor exponent takes the form: $-2Л^2[h^2 a^{*2} U^{11} + ... + 2 h k a^* b^* U^{12}]$

	U^{11}	U^{22}	U^{33}	U^{23}	U^{13}	U^{12}
S(2)	14(1)	17(1)	35(1)	1(1)	7(1)	3(1)
S(1)	11(1)	16(1)	38(1)	-1(1)	2(1)	-1(1)
S(3)	13(1)	29(1)	18(1)	6(1)	0(1)	-3(1)
O(1)	19(2)	12(2)	19(2)	0(2)	10(1)	-3(2)
O(5)	36(2)	11(2)	24(2)	0(2)	12(2)	2(2)
O(3)	27(2)	19(2)	19(2)	-2(2)	13(2)	-1(2)
O(4)	32(2)	19(2)	22(2)	0(2)	14(2)	2(2)
O(2)	27(2)	10(2)	23(2)	-1(2)	9(2)	-2(2)
C(13)	20(3)	18(3)	16(3)	3(2)	-1(2)	1(2)
C(3)	13(2)	16(3)	13(2)	-1(2)	0(2)	-1(2)
C(1)	12(2)	16(3)	15(2)	-4(2)	-2(2)	1(2)
C(10)	14(2)	12(3)	21(3)	2(2)	5(2)	-3(2)
C(8)	12(2)	6(2)	17(3)	2(2)	5(2)	0(2)

C(11)	14(2)	15(3)	19(3)	2(2)	3(2)	-1(2)
C(5)	11(2)	18(3)	17(3)	-1(2)	-1(2)	1(2)
C(6)	11(2)	17(3)	16(2)	5(2)	2(2)	-3(2)
C(12)	12(2)	18(3)	15(3)	-1(2)	-3(2)	-1(2)
C(4)	14(2)	18(3)	16(3)	0(2)	2(2)	0(2)
C(2)	12(2)	8(2)	19(3)	-4(2)	2(2)	0(2)
C(9)	13(2)	22(3)	21(3)	2(2)	3(2)	-5(2)
C(7)	13(2)	12(3)	16(2)	2(2)	4(2)	-1(2)
O(1S)	33(2)	20(2)	28(2)	1(2)	17(2)	-3(2)
C(1S)	27(3)	31(3)	27(3)	2(3)	8(2)	-8(3)
C(2S)	44(4)	54(5)	40(4)	-11(4)	20(3)	-3(4)

Table 3.5: Hydrogen coordinates ($x10^4$) and isotropic displacement parameters ($Å^2 x\ 10^3$) for 5-(3-mercapto-2,2-bis(mercaptomethyl)propoxy)isophthalic acid (**3-3**).

	x	y	z	U(eq)
H(10A)	8478	310	3123	18
H(10B)	8917	1316	3426	18
H(11A)	6328	1091	2759	19
H(11B)	7914	1320	2583	19
H(6)	4875	3972	3638	18
H(4)	2195	2115	4292	19
H(2)	4696	-203	3687	16
H(9A)	8443	4502	3021	22
H(9B)	9021	3720	2707	22
H(7A)	7234	3344	3445	16
H(7B)	5935	3506	3147	16
H(1SA)	970	6284	5049	34
H(1SB)	-573	6222	4804	34

H(2SA)	-924	8603	4869	68
H(2SB)	612	8663	5114	68
H(2SC)	-905	7843	5215	68
H(5)	3380(90)	6500(40)	4040(19)	68
H(3)	1730(90)	-1240(40)	4487(19)	68
H(1S)	1530(90)	6310(90)	4503(19)	68

Table 3.6: Torsion angles [°] for 5-(3-mercapto-2,2-bis(mercaptomethyl)propoxy)isophthalic acid (**3-3**).

S(2)-S(1)-C(9)-C(8)	38.0(3)
S(2)-C(10)-C(8)-C(11)	92.8(4)
S(2)-C(10)-C(8)-C(9)	-27.3(5)
S(2)-C(10)-C(8)-C(7)	-144.7(4)
S(1)-S(2)-C(10)-C(8)	47.0(3)
S(3)#1-S(3)-C(11)-C(8)	-91.5(3)
O(1)-C(1)-C(6)-C(5)	179.3(4)
O(1)-C(1)-C(2)-C(3)	-178.8(4)
O(5)-C(13)-C(5)-C(6)	-1.0(7)
O(5)-C(13)-C(5)-C(4)	177.4(5)
O(4)-C(13)-C(5)-C(6)	-179.7(5)
O(4)-C(13)-C(5)-C(4)	-1.4(8)
C(13)-C(5)-C(6)-C(1)	177.5(5)
C(13)-C(5)-C(4)-C(3)	-176.3(5)
C(1)-O(1)-C(7)-C(8)	171.1(4)
C(10)-C(8)-C(11)-S(3)	-169.3(3)
C(10)-C(8)-C(9)-S(1)	-11.2(5)

C(10)-C(8)-C(7)-O(1)	-52.3(5)
C(11)-C(8)-C(9)-S(1)	-130.0(4)
C(11)-C(8)-C(7)-O(1)	67.5(5)
C(6)-C(1)-C(2)-C(3)	1.5(7)
C(6)-C(5)-C(4)-C(3)	2.0(7)
C(12)-C(3)-C(4)-C(5)	176.4(5)
C(12)-C(3)-C(2)-C(1)	-178.3(4)
C(4)-C(3)-C(12)-O(3)	-1.9(7)
C(4)-C(3)-C(12)-O(2)	178.5(5)
C(4)-C(3)-C(2)-C(1)	-0.3(7)
C(4)-C(5)-C(6)-C(1)	-0.8(7)
C(2)-C(3)-C(12)-O(3)	176.0(4)
C(2)-C(3)-C(12)-O(2)	-3.5(7)
C(2)-C(3)-C(4)-C(5)	-1.5(7)
C(2)-C(1)-C(6)-C(5)	-1.0(7)
C(9)-C(8)-C(11)-S(3)	-49.6(5)
C(9)-C(8)-C(7)-O(1)	-170.9(4)
C(7)-O(1)-C(1)-C(6)	10.7(7)
C(7)-O(1)-C(1)-C(2)	-169.0(4)
C(7)-C(8)-C(11)-S(3)	70.5(5)

C(7)-C(8)-C(9)-S(1)	106.9(4)

Symmetry transformations used to generate equivalent atoms:

#1 -x+1,y,-z+1/2

Figure 4.1: ^{1}H NMR spectrum of 2-(tritylthio)ethan-1-amine hydrochloride (**1-4**) in CD_2Cl_2 (500 MHz, calibrated to residual $CHDCl_2$ at 5.32 ppm).

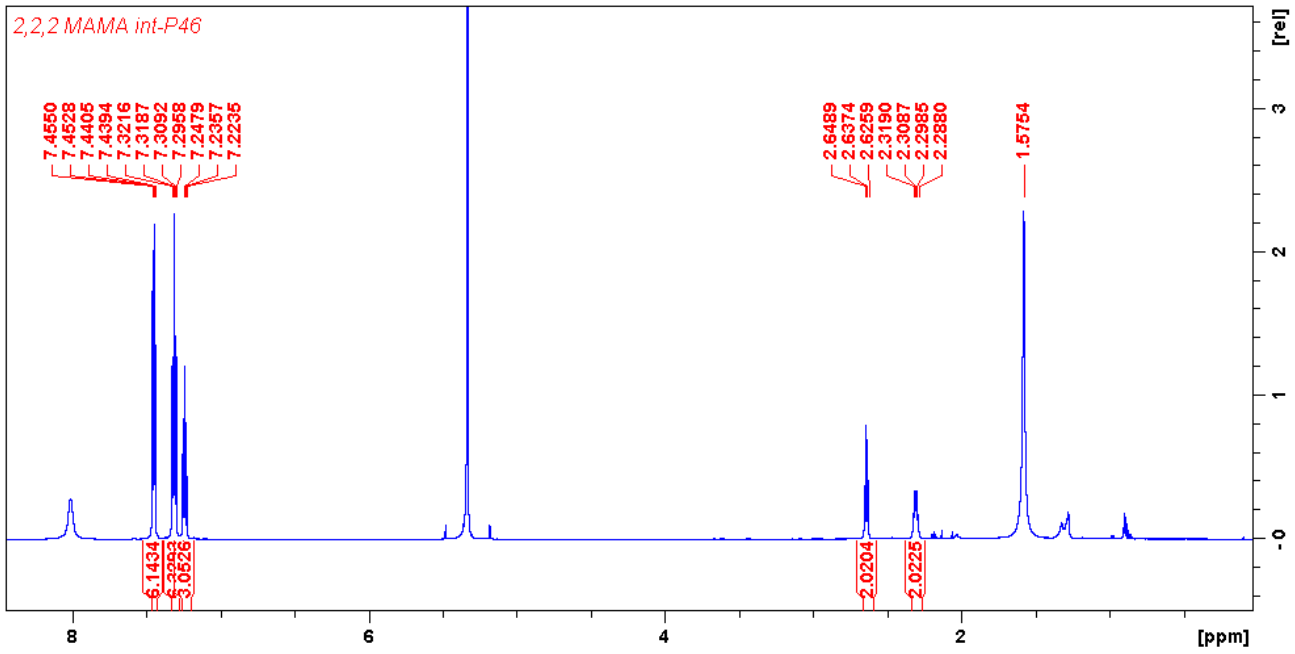

Figure 4.2: ^{1}H NMR spectrum of *N*-(2-(tritylthio)ethyl)-2-((2-(tritylthio)ethyl)amino)acetamide **(2-4)**) in CD_2Cl_2 (500 MHz, calibrated at 7.26 ppm).

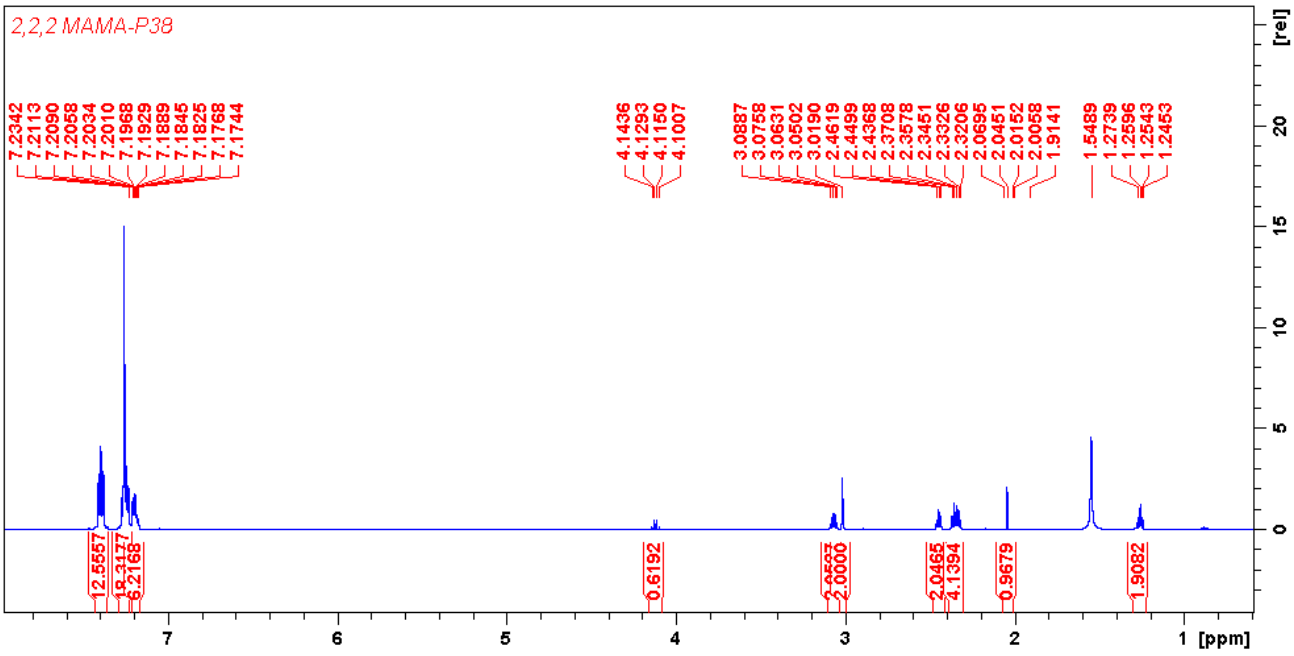

Figure 4.3: ^{13}C NMR spectrum of *N*-(2-(tritylthio)ethyl)-2-((2-(tritylthio)ethyl)amino)acetamide **(2-4)** in CD_2Cl_2 (500 MHz, calibrated at 77.36 ppm).

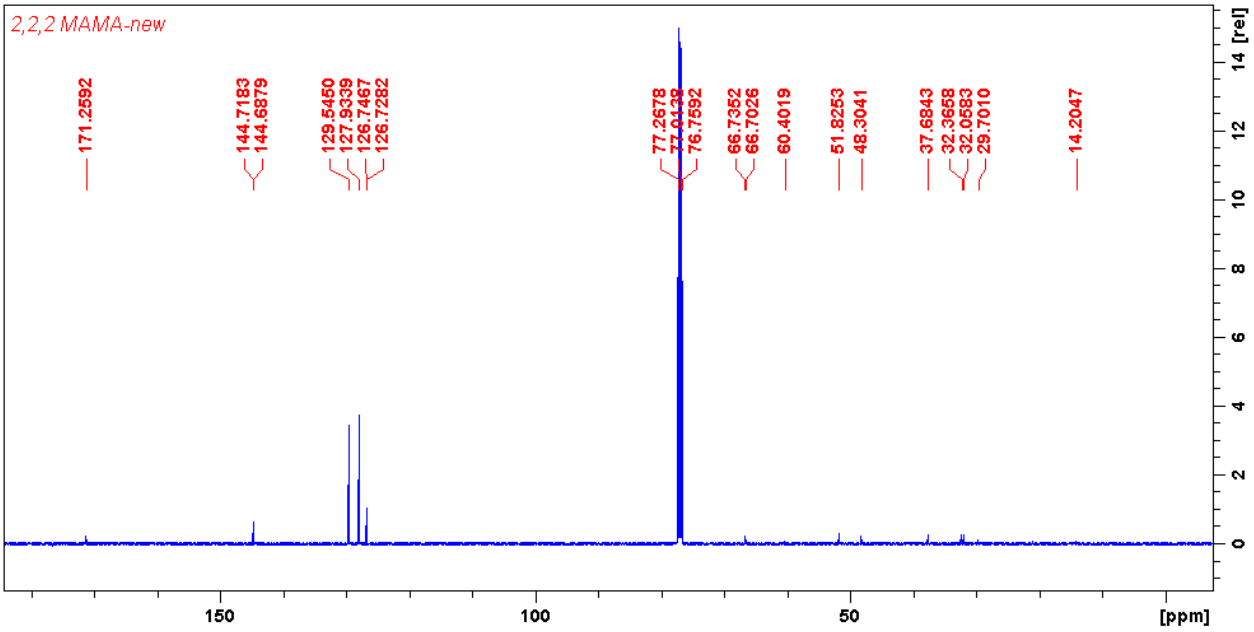

Figure 4.4: ^{1}H NMR spectrum of ethyl 3-((2-oxo-2-((2-(tritylthio)ethyl)amino)ethyl)(2-(tritylthio)ethyl)amino)propionate [trityl protected 222-MAMA(*N*-3-Ahx-OEt)] **(3-4) (**500 MHz calibrated at 5.35 ppm).

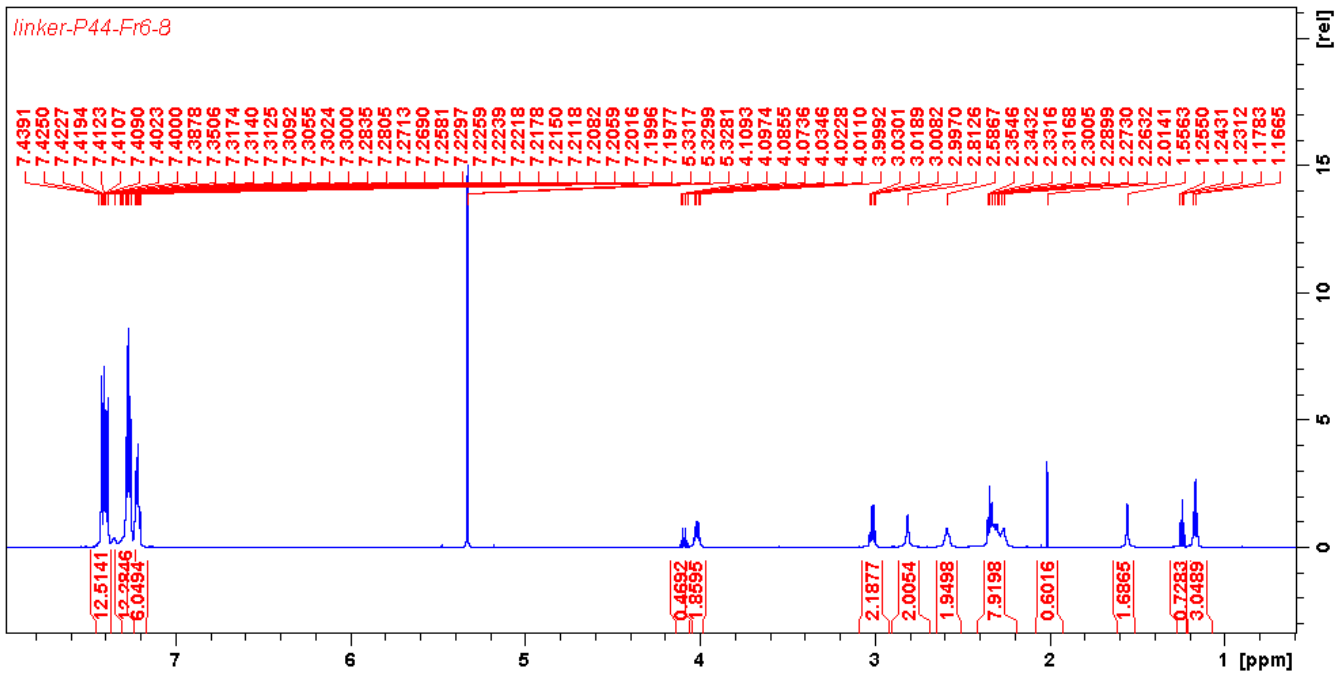

Figure 4.5: ^{13}C NMR spectrum of ethyl 3-((2-oxo-2-((2-(tritylthio)ethyl)amino)ethyl)(2-(tritylthio)ethyl)amino)propionate [trityl protected 222-MAMA(*N*-3-Ahx-OEt)] **(3-4)** (500 MHz calibrated at 53.5 ppm).

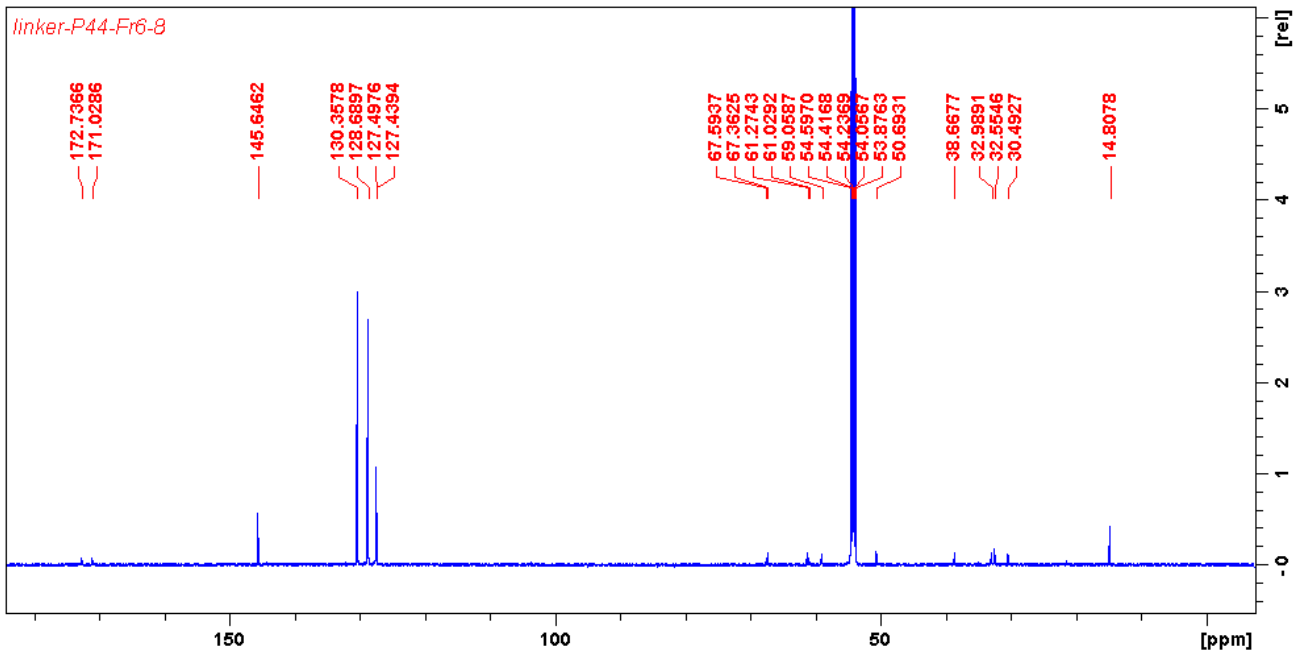

Figure 4.6: ^{1}H NMR spectrum of ^{nat}ReO(222-MAMA(*N*-3-Ahx-OEt) (**5-4**) (600 MHz calibrated at 5.32 ppm).

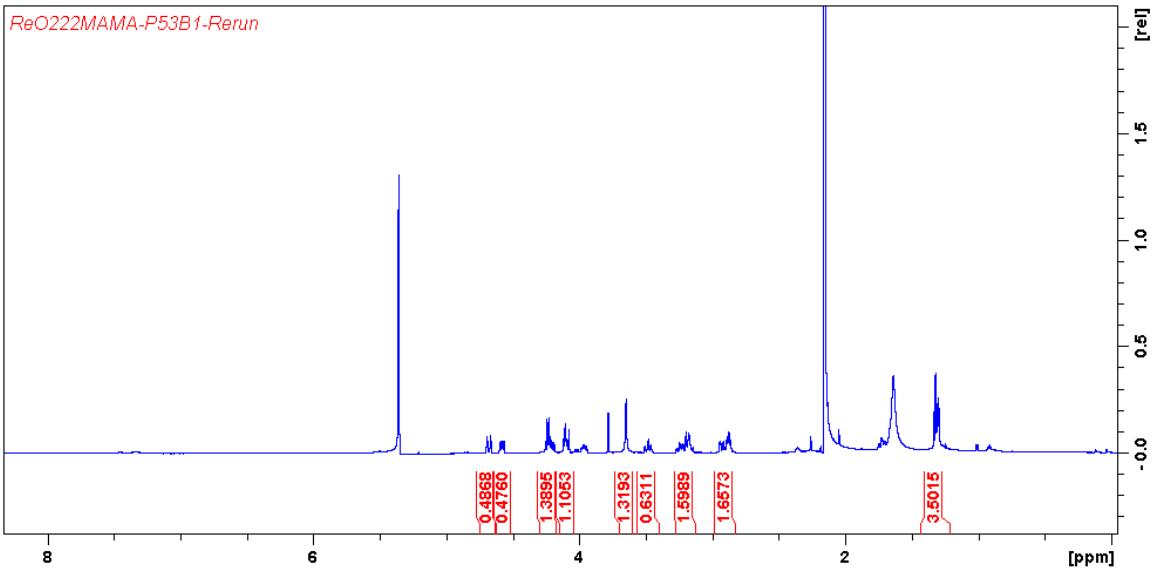

Figure 4.7: ^{13}C NMR spectrum of ^{nat}ReO(222-MAMA(*N*-3-Ahx-OEt) (**5-4**) (600 MHz calibrated at 53.5 ppm).

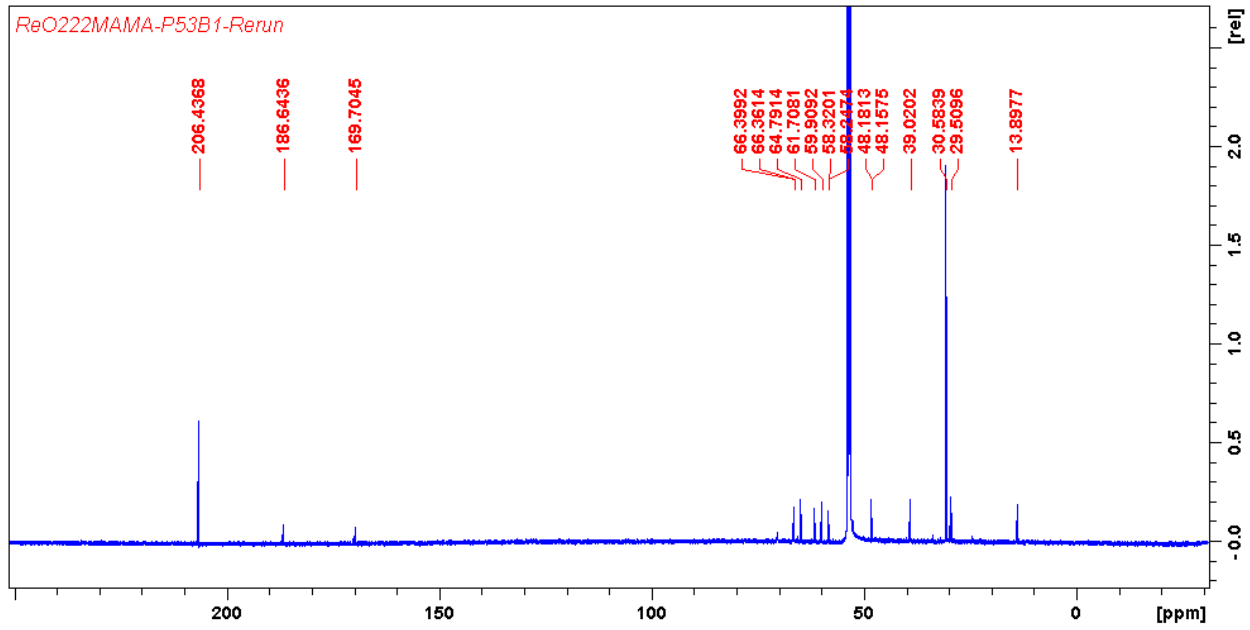

Figure 4.8: RP-HPLC chromatogram of ^{nat}ReO(222-MAMA(*N*-3-Ahx-OEt) (**5-4**) (method **2)**

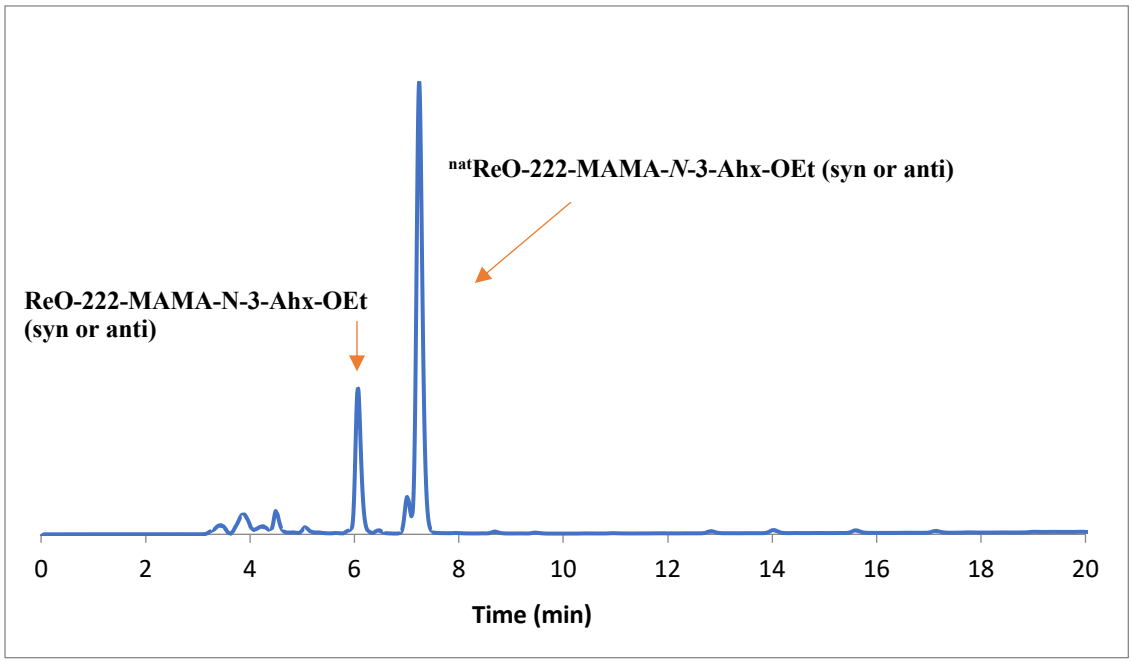

Figure 4.9: RP-HPLC chromatogram of ^{186}ReO(222-MAMA(*N*-3-Ahx-OEt) (**5-4**) (method **2**)

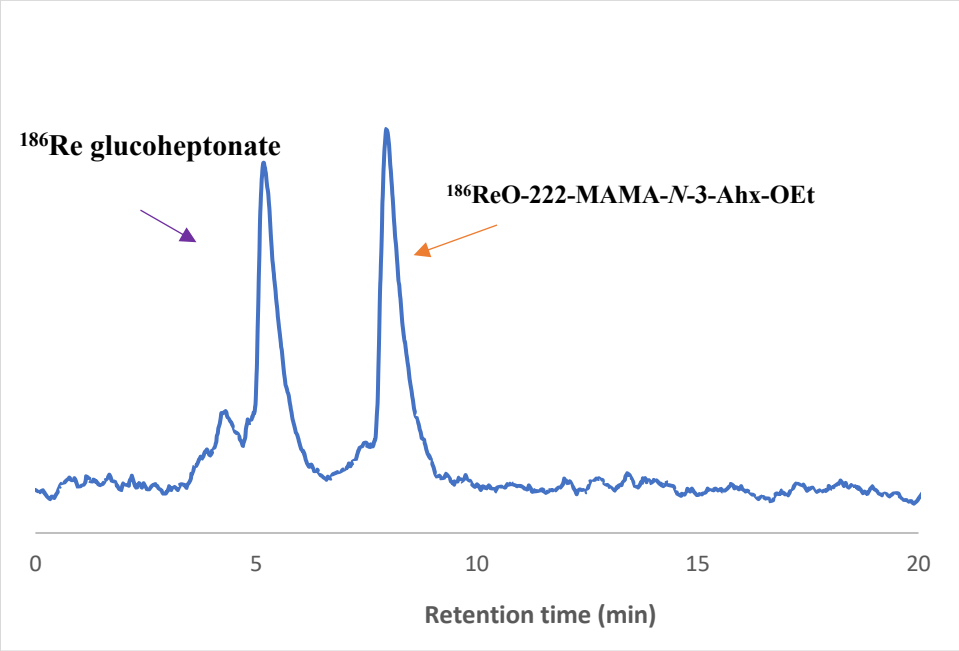

Figure 4.10: RP-HPLC chromatogram of ^{99m}TcO(222-MAMA(N-3-Ahx-OEt) (**5-4**) (method **2**)

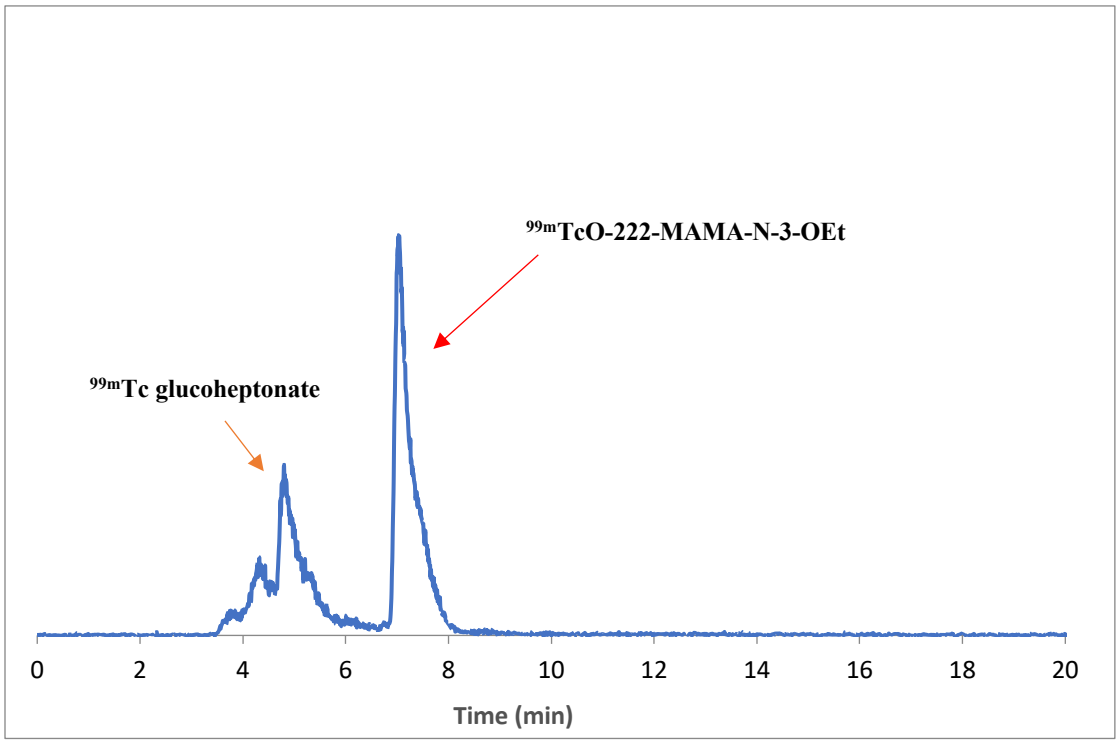

Figure 4.11: RP-HPLC chromatogram of purified ^{nat}ReO(222-MAMA(N-3-Ahx-OEt) (**5-4**) (method **1**)

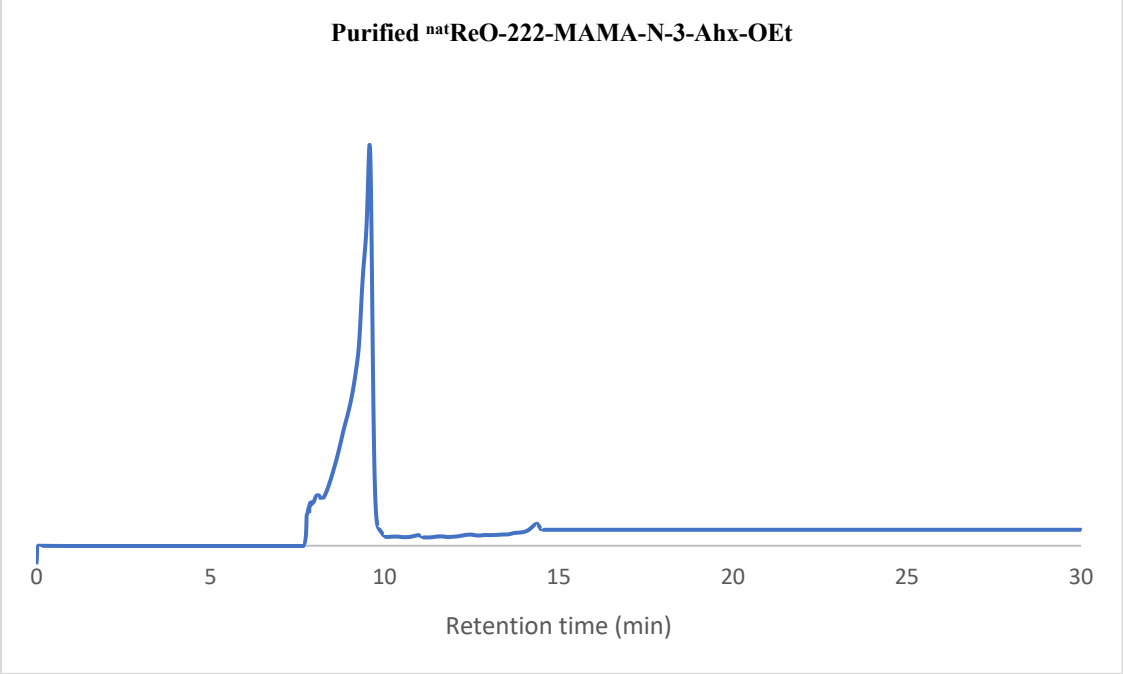

Figure 4.12: RP-HPLC chromatogram of purified ^{186}ReO(222-MAMA(N-3-Ahx-OEt) (**5-4**) (method **1**)

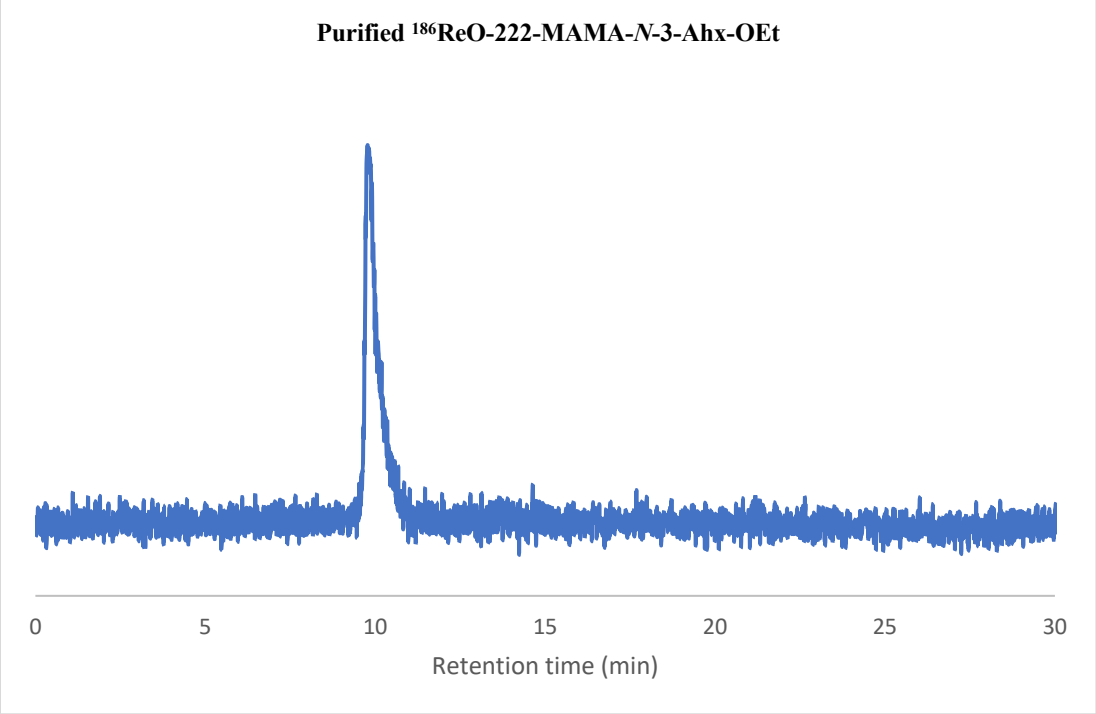

Figure 4.13: RP-HPLC chromatogram of purified ^{186}ReO(222-MAMA(*N*-3-Ahx-OEt) (**5-4**) (method **3**)

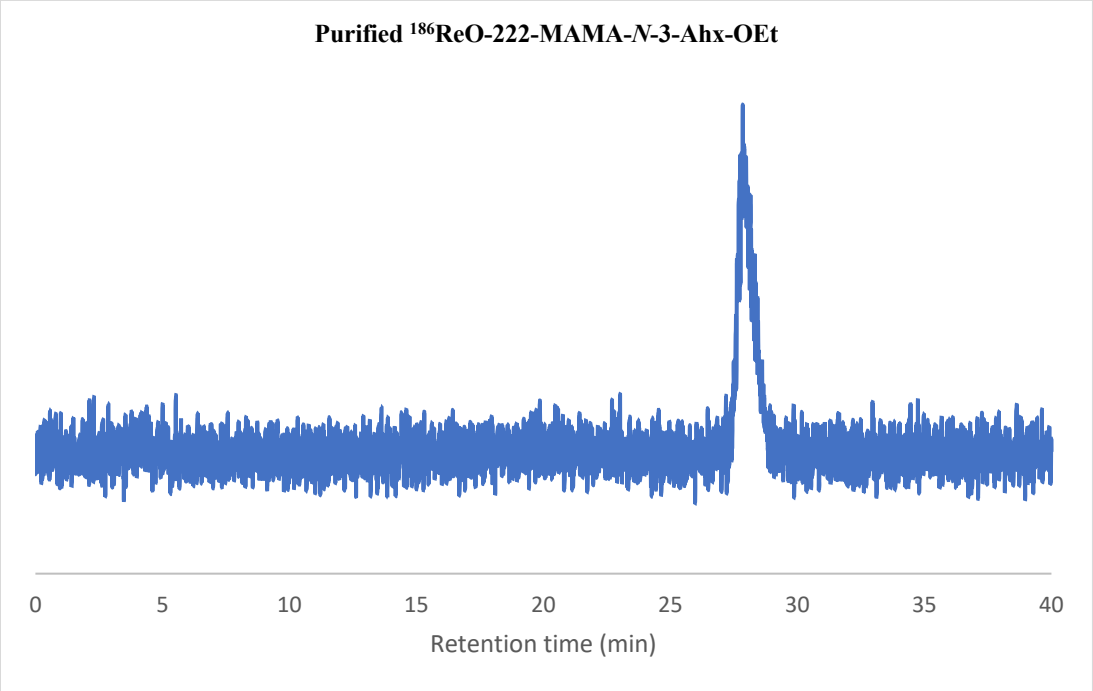

Figure 4.14: LC-ESI-MS of ^{nat}ReO(222-MAMA(*N*-3-Ahx-OEt) (**5-4**).

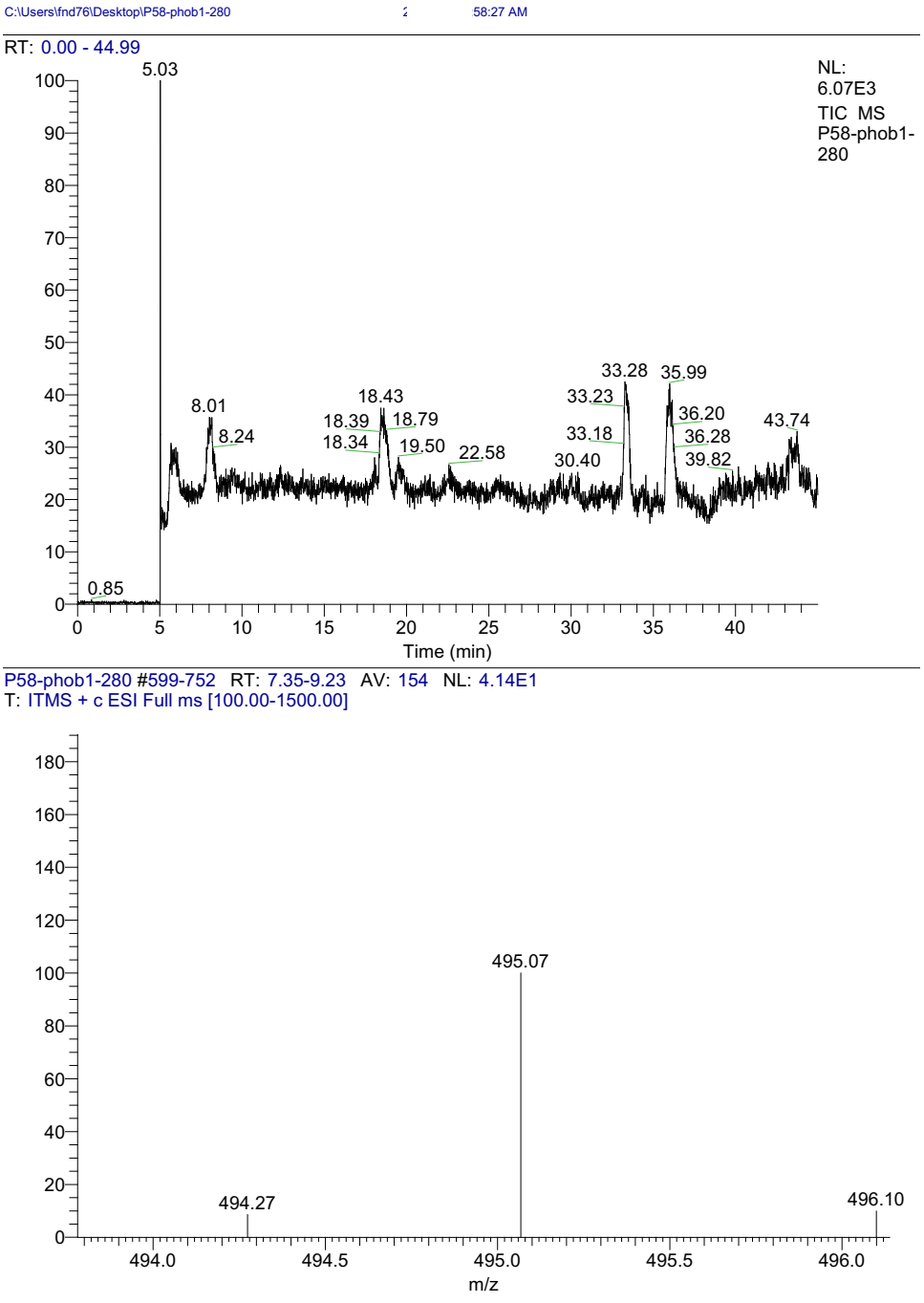

References

1. Lewis, M. R.; Kao, J. Y.; Anderson, A.-L. J.; Shively, J. E.; Raubitschek, A., *An improved method for conjugating monoclonal antibodies with N-hydroxysulfosuccinimidyl DOTA.* Bioconjug. Chem. **2001,** *12* (2), 320-324.

2. Staros, J. V.; Wright, R. W.; Swingle, D. M., *Enhancement by N-hydroxysulfosuccinimide of water-soluble carbodiimide-mediated coupling reactions.* Anal. Biochem. **1986,** *156* (1), 220-222.

3. Duncan, R. J. S.; Weston, P. D.; Wrigglesworth, R., *A new reagent which may be used to introduce sulfhydryl groups into proteins, and its use in the preparation of conjugates for immunoassay.* Anal. Biochem. **1983,** *132* (1), 68-73.

4. Meares, C. F., *Chelating agents for the binding of metal ions to antibodies.* Int. J. Rad. Appl. Instrum [B] **1986,** *13* (4), 311-318.

5. Gansow, O. A., *Newer approaches to the radiolabeling of monoclonal antibodies by use of metal chelates.* Nucl. Med. Biol. **1991,** *18* (4), 369-381.

6. Liu, Y.-F.; Wu, C.-C. *Radiolabeling of monoclonal antibodies with metal chelates.* Pure & Appl. Chem. **1991,** *63* (3), 427-463.

7. Demoin, D. W.; Dame, A. N.; Minard, W. D.; Gallazzi, F.; Seickman, G. L.; Rold, T. L.; Bernskoetter, N.; Fassbender, M. E.; Hoffman, T. J.; Deakyne, C. A., M*onooxorhenium (V) complexes with 222-N_2S_2 MAMA ligands for bifunctional chelator agents: Syntheses and preliminary in vivo evaluation.* Nucl. Med. Biol. **2016,** *43* (12), 802-811.

8. Loveland, W. D.; Morrissey, D. J.; Seaborg, G. T., *Modern nuclear chemistry*. John Wiley & Sons: **2017**.

9. Hevesy, G. J., *Application of isotopes in biology.* J.A.C.S. **1939**, 1213-1223.

10. Qaim, S. M., T*herapeutic radionuclides and nuclear data.* Radiochim. Acta **2001,** *89* (4-5), 297-304.

11. Howell, R. W., *Radiobiological effects of Auger electrons in the decay of platinum-195m.* **1989**.

12. Ehmann, W. D.; Vance, D. E., *Radiochemistry and nuclear methods of analysis*. Wiley New York: **1991**.

13. Falzone, N.; Lee, B. Q.; Fernández-Varea, J. M.; Kartsonaki, C.; Stuchbery, A. E.; Kibédi, T.; Vallis, K. A., Biology, Absorbed dose evaluation of Auger electron-emitting radionuclides: impact of input decay spectra on dose point kernels and S-values. Phys. Med. biol. **2017,** *62* (6), 2239.

14. Chopin, G. J.; Rydberg,. *Nuclear Chemistry* (**1980**).".

15. Cutler, C. S.; Hennkens, H. M.; Sisay, N.; Huclier-Markai, S.; Jurisson, S. S., *Radiometals for combined imaging and therapy.* Chem. Rev. **2013,** *113* (2), 858-883.

16. Burke, B. P.; Seemann, J.; Archibald, S. J., *Advanced chelator design for metal complexes in imaging applications: radiopharmaceuticals, protein targeting, and conjugation.* Adv. Inorg. Chem. **2016**; Vol. 68, 301-339.

17. Solnes, L.; Werner, R.; Jones, K. M.; Sadaghiani, M. S.; Bailey, C. R.; Lapa, C.; Pomper, M. G.; Rowe, S. P., *Theranostics: Leveraging Molecular Imaging and Therapy to Impact Patient Management and Secure the Future of Nuclear Medicine.* J. Nucl. Med. **2020**, 118.220665.

18. Saptiama, I.; Lestari, E.; Sarmini, E.; Lubis, H.; Marlina, M.; Mutalib, A., *Development of ^{99}Mo/^{99m}Tc Generator System for Production of Medical Radionuclide ^{99m}Tc using a Neutron-activated ^{99}Mo and Zirconium Based Material (ZBM) as its Adsorbent.* Atom Indonesia. **2016,** *42* (3), 115-121.

19. Greenwood, N. N.; Earnshaw, A., *Chemistry of the Elements*. Elsevier: **2012**.

20. Herth, M. M.; Barz, M.; Jahn, M.; Zentel, R.; Rösch, F., $^{72/74}$As-labeling of HPMA based polymers for long-term in vivo PET imaging. Bioorganic Med. Chem. Lett. **2010,** *20* (18), 5454-5458.

21. Okoye, N. C.; Baumeister, J. E.; Khosroshahi, F. N.; Hennkens, H. M.; Jurisson, S. S., C*helators and metal complex stability for radiopharmaceutical applications.* Radiochim. Acta **2019,** *107* (9-11), 1087-1120.

22. Oláh, Z.; Vogg, A. T.; Kremmer, T.; Szűcs, Z.; Varga, Z.; Dóczi, R., *Optimization of the reduction of ^{74}As (V) to ^{74}As (III) and of the labelling of dithiol dihydrolipoic acid.* Appl. Radiat. Isot. **2019,** *149*, 75-82.

23. Gott, M. D.; DeGraffenreid, A. J.; Feng, Y.; Phipps, M. D.; Wycoff, D. E.; Embree, M. F.; Cutler, C. S.; Ketring, A. R.; Jurisson, S. S., *Chromatographic separation of germanium and arsenic for the production of high purity ^{77}As.* J. Chromatogr. A. **2016,** *1441*, 68-74.

24. Feng, Y.; Phipps, M. D.; Phelps, T. E.; Okoye, N. C.; Baumeister, J. E.; Wycoff, D. E.; Dorman, E. F.; Wooten, A. L.; Vlasenko, V.; Berendzen, A. F., *Evaluation of ^{72}Se/^{72}As generator and production of ^{72}Se for supplying 72As as a potential PET imaging radionuclide.* Radiochim. Acta. **2019,** *143*, 113-122.

25. Jennewein, M.; Schmidt, A.; Novgorodov, A.; Qaim, S. M.; Rösch, F., *A no-carrier-added ^{72}Se/^{72}As radionuclide generator based on distillation.* Radiochim. Acta. **2004,** *92* (4-6), 245-249.

26. Jennewein, M.; Qaim, S. M.; Kulkarni, P.; Mason, R.; Hermanne, A.; Rösch, F., *A no-carrier-added ^{72}Se/^{72}As radionuclide generator based on solid phase extraction.* Radiochim. Acta. **2005,** *93* (9-10), 579-583.

27. Sanders, V.; Cutler, C. S., Radioarsenic: *A promising theragnostic candidate for nuclear medicine.* Nucl. Med. Biol. **2020**.

28. DeGraffenreid, A. J.; Feng, Y.; Barnes, C. L.; Ketring, A. R.; Cutler, C. S.; Jurisson, S. S., *Trithiols and their arsenic compounds for potential use in diagnostic and therapeutic radiopharmaceuticals. Nucl. Med. Biol.* **2016,** *43* (5), 288-295.

29. DeGraffenreid, A. J.; Feng, Y.; Wycoff, D. E.; Morrow, R.; Phipps, M. D.; Cutler, C. S.; Ketring, A. R.; Barnes, C. L.; Jurisson, S. S., D*ithiol aryl arsenic compounds as potential diagnostic and therapeutic radiopharmaceuticals.* Inorg. Chem. **2016,** *55* (16), 8091-8098.

30. Jennewein, M.; Hermanne, A.; Mason, R.; Thorpe, P.; Rösch, F., *Methods in Physics Research Section A: Accelerators, S., Detectors; Equipment, A., A new method for the labelling of proteins with radioactive arsenic isotopes.* Nucl. Instrum. Methods Phy. Res. **2006,** *569* (2), 512-517.

31. Jennewein, M.; Lewis, M. A.; Zhao, D.; Tsyganov, E.; Slavine, N.; He, J.; Watkins, L.; Kodibagkar, V. D.; O'Kelly, S.; Kulkarni, P., *Vascular imaging of solid tumors in rats with a radioactive arsenic-labeled antibody that binds exposed phosphatidylserine*. Clin. Cancer. Res. **2008,** *14* (5), 1377-1385.

32. Wycoff, D. E.; Gott, M. D.; DeGraffenreid, A. J.; Morrow, R. P.; Sisay, N.; Embree, M. F.; Ballard, B.; Fassbender, M. E.; Cutler, C. S.; Ketring, A. R., C*hromatographic separation of selenium and arsenic: A potential $^{72}Se/^{72}As$ generator.* J. Chromatogr. A. **2014,** *1340*, 109-114.

33. Ballard, B.; M Nortier, F.; R Birnbaum, E.; D John, K.; R Phillips, D.; E Fassbender, M., *Radioarsenic from a portable $^{72}Se/^{72}As$ generator: a current perspective.* Curr. Radiopharm. **2012,** *5* (3), 264-270.

34. Chajduk, E.; Doner, K.; Polkowska-Motrenko, H.; Bilewicz, A., N*ovel radiochemical separation of arsenic from selenium for $^{72}Se/^{72}As$ generator.*Appl. Radiat. Isot. **2012,** *70* (5), 819-822.

35. Jennewein, M.; Schmidt, A.; Novgorodov, A.; Qaim, S. M.; Rosch, F., *A no-carrier-added $^{72}Se/^{72}As$ radionuclide generator based on distillation.* Int. J. Dev. Biol. **2004,** *92* (4-6), 245-250.

36. Mudrova, B.; Kopecký, P.; Svoboda, K., *The separation of carrier-free ^{72}Se from a germanium oxide target.* Int. J. Appl. Radiat. Isot. **1973,** *24* (10), 610-612.

37. Feng, Y.; DeGraffenreid, A. J.; Phipps, M. D.; Rold, T. L.; Okoye, N. C.; Gallazzi, F. A.; Barnes, C. L.; Cutler, C. S.; Ketring, A. R.; Hoffman, T. J., *A trithiol bifunctional chelate for $^{72, 77}As$: A matched pair theranostic complex with high in vivo stability.*Nucl. Med. Biol. **2018,** *61*, 1-10.

38. Reubi, J. C. J., *Neuropeptide receptors in health and disease: the molecular basis for in vivo imaging.* J. Nucl. Med. **1995,** *36* (10), 1825-1835.

39. Ohki-Hamazaki, H.; Iwabuchi, M.; Maekawa, F. J., *Development and function of bombesin-like peptides and their receptors.* Int. J. Dev. Biol. **2003,** *49* (2-3), 293-300.

40. Abd-Elgaliel, W. R.; Gallazzi, F.; Garrison, J. C.; Rold, T. L.; Sieckman, G. L.; Figueroa, S. D.; Hoffman, T. J.; Lever, S. Z., *Design, Synthesis, and Biological Evaluation of an Antagonist− Bombesin Analogue as Targeting Vector.* Bioconjug. Chem. **2008,** *19* (10), 2040-2048.

41. Hoffman, T. J.; Smith, C., *True radiotracers: Cu-64 targeting vectors based upon bombesin peptide.* Nucl. Med. Biol. **2009,** *6* (36), 579-585.

42. Lane, S. R.; Nanda, P.; Rold, T. L.; Sieckman, G. L.; Figueroa, S. D.; Hoffman, T. J.; Jurisson, S. S.; Smith, C. J., *Optimization, biological evaluation and microPET imaging of copper-64-labeled bombesin agonists,[64Cu-NO2A-(X)-BBN (7–14) NH_2], in a prostate tumor xenografted mouse model.* Nucl. Med. Biol. **2010,** *37* (7), 751-761.

43. Hou, Y.-L.; Yee, K.-K.; Wong, Y.-L.; Zha, M.; He, J.; Zeller, M.; Hunter, A. D.; Yang, K.; Xu, Z., M*etalation triggers single crystalline order in a porous solid.* J.A.C.S. **2016,** *138* (45), 14852-14855.

44. Garrison, J. C.; Rold, T. L.; Sieckman, G. L.; Figueroa, S. D.; Volkert, W. A.; Jurisson, S. S.; Hoffman, T. J., *In vivo evaluation and small-animal PET/CT of a prostate cancer mouse model using ^{64}Cu bombesin analogs: side-by-side comparison of the CB-TE2A and DOTA chelation systems.* J. Nucl. Med. **2007,** *48* (8), 1327-1337.

45. Sheldrick, G. M., *Crystal structure refinement with SHELXL*.Acta Crystallogr. Sec. C.:Struct. Chem. **2015,** *71* (1), 3-8.

46. Dolomanov, O. V.; Bourhis, L. J.; Gildea, R.; Howard J. A. K.; Puschmann. H., *OLEX2: A complete structure solution, refinement and analysis program.* J. appl. Cryst. **2009,** *42*, 339-341.

47. Feng, Y. *Arsenic-72, 77 as a matched pair radiopharmaceutical for imaging and radiotherapy.* **2018**.

48. *Iagaru, A.; Minamimoto, R.; Hancock, S. L.; Mittra, E.; Loening, A.; Vasanawala, S., ^{68}Ga-DOTA-Bombesin (^{68}Ga-RM2 or ^{68}Ga-Bombesin) PET versus ^{68}Ga-PSMA PET: A pilot prospective evaluation in patients with biochemical recurrence of prostate cancer.* American Society of Clinical Oncology: **2016**.

49. Makris, G.; Bandari, R. P.; Kuchuk, M.; Jurisson, S. S.; Smith, C. J.; Hennkens, H. M., *Development and Preclinical Evaluation of ^{99m}Tc-and ^{186}Re-Labeled NOTA and NODAGA Bioconjugates Demonstrating Matched Pair Targeting of GRPR-Expressing Tumors.* Mol. Imaging. **2020**, 1-10.

50. Smith, C. J.; Gali, H.; Sieckman, G. L.; Hayes, D. L.; Owen, N. K.; Mazuru, D. G.; Volkert, W. A.; Hoffman, T. J., R*adiochemical investigations of ^{177}Lu-DOTA-8-Aoc-BBN [7-14] NH_2: an in vitro/in vivo assessment of the targeting ability of this new radiopharmaceutical for PC-3 human prostate cancer cells.*Nucl. Med. Biol. **2003,** *30* (2), 101-109.

51. Chadwick, D.; Millen, D. J., *Microwave spectrum of dibromomethane. Part 1.—Molecular structure.* J. Chem. Soc. Faraday Trans. **1971,** *67*, 1539-1550.

52. Demaison, J.; Margules, L.; Boggs, *The equilibrium C–Cl, C–Br, and C–I bond lengths from ab initio calculations, microwave and infrared spectroscopies, and empirical correlations.* Struct. Chem. **2003,** *14* (2), 159-174.

53. Pyrka, G.; Fernando, Q.; Inoue, M.; Inoue, M.; Velazquez. E. M., *Structure of 3, 3, 5'-tribromo-2, 2'-bithiophene.* Acta Cryst. **1988,** *44* (10), 1800-1803.

54. Yao, Y.; Yu, L.; Su, X.; Wang, Y.; Li, W.; Wu, Y.; Cheng, X.; Zhang, H.; Wei, X.; Chen, H., *Synthesis, characterization and targeting chemotherapy for ovarian cancer of trastuzumab-SN-38 conjugates.* J.C.R. **2015,** *220*, 5-17.

55. Nahta, R.; Esteva, F. J., *Herceptin: mechanisms of action and resistance.* Cancer Lett. **2006,** *232* (2), 123-138.

56. Izumi, Y.; Xu, L.; Di Tomaso, E.; Fukumura, D.; Jain, R. K., *Herceptin acts as an anti-angiogenic cocktail*. Nature. **2002,** *416* (6878), 279-280.

57. Cuatrecasas, P.; Parikh, I., *Adsorbents for affinity chromatography. Use of N-hydroxysuccinimide esters of agarose.* J. Biochem. **1972,** *11* (12), 2291-2299.

58. Grabarek, Z.; Gergely, J., *Zero-length crosslinking procedure with the use of active esters.* Anal. Biochem. **1990,** *185* (1), 131-135.

59. Apex3, AXScale, and SAINT, version 2017.3-0, Bruker AXS, Inc., Madison, WI, *2017*.

60. Sheldrick, G. M. *SHELXS* version 2017/1, Göttingen, Germany **2017**.

Vita

Firouzeh Najafi Khosroshahi immigrated to the US in 2014 to study Master of Chemistry at Southern Illinois University Edwardsville (SIUE). She graduated from SIUE in 2016 and moved to Columbia, Missouri, to enter a Ph.D. program in Radiochemistry at the University of Missouri in Dr. Silvia Jurisson's group to pursue my childhood dream to become a radiochemist. Her goal is joining a radiochemistry group as a post-doctoral scholar after graduation and expand her knowledge in the exciting world of radiochemistry and radiopharmaceuticals.